THE INTERNATIONAL SCIENTIFIC JOURNAL

PROBLEMS
OF
TRIBOLOGY

Volume 27   *No 1/103-2022*

МІЖНАРОДНИЙ НАУКОВИЙ ЖУРНАЛ

ПРОБЛЕМИ ТРИБОЛОГІЇ

PROBLEMS OF TRIBOLOGY

INTERNATIONAL SCIENTIFIC JOURNAL

Published since 1996, four time a year

Volume 27 No 1/103-2022

CONTENTS

Problems of Tribology

ЗМІСТ

Wear resistance of composite electrolytic coatings

M.Ye. Skyba, M.S. Stechyshyn, V.P. Oleksandrenko, N.S. Mashovets*, Y.M. Bilyk

Khmelnytsky National University, Ukraine
*E-mail: mashovetsns@ukr.net

Abstract

The article analyzes the influence of composite electrolytic coatings (CEC) on the wear resistance of structural steels. The issues of matrix selection and various combinations in composite coatings of different chemical elements and compounds are considered. Coatings based on chromium, nickel, iron, copper, cobalt and others are widely used in industry, but nickel-based composite coatings are the most widely used. Nickel is widely used as a matrix for CEC, because it has an affinity for most particles used as the second phase and easily forms a coating with them. These coatings are used for corrosion protection, increase of physical and mechanical and chemical parameters, increase of hardness and wear resistance, restoration of the sizes, giving to a surface of self-lubricating properties.

Nickel-based coatings with SiC filler of various fractions from size 100/80 μm to nanoparticles smaller than 50 nm were investigated on the basis of the established installation for CEC application. Thus, SiC powders with the following sizes were used in the works: less than 50 nm - nanoparticles; M5; 28/20; 50/40; 100/80 μm.

In the studies performed, 0.01… 0.02 g/l sodium lauryl sulfate was additionally introduced into the electrolyte, which promotes the incorporation of SiC particles into the coating and improves the conditions for building the Nickel matrix.

Amorphous boron powders of about 1 μm size were also added to the silicon carbides as a filler, which is explained by the possibility of boron and nickel interaction during the subsequent heat treatment of the coating and obtaining new structures (solid solutions, eutectic, dispersion-hard alloys).

It is of practical interest to study the possibility of improving the physical and mechanical properties of nickel-based CEC by introducing metals capable of heat treatment, interact with the metal matrix to form solid substitution solutions and chemical compounds (solid phases of implementation) and determine tribotechnical characteristics of these coatings.

Keywords: composite electrolytic coatings (CEC), wear resistance.

Introduction

A significant contribution to the theory and practice of electrodeposition of composite electrolytic coatings (CEC) is the work of R.S. Saifulina, Sh.Kh. Yar-Mukhamedova, V.F. Molchanova, G.V. Guryanova, Д.К. Romanauskene, G. Brown, N. Guglielmi, I.Z. Pribish, I.G. Khabibulina, R.S. Kuramshina, V. Metzegra, L.I. Lozytskoho, Yu.O. Guslienko, MV Luchki and others. Various combinations of different chemical elements and compounds in composite coatings have been studied, but the main attention is paid to the technology of application, the study of structures and the formation of various complexes of physical and mechanical properties. Studies of CEC from the standpoint of tribotechnics are very few, or they are presented in the form of single results, which can not give a general picture of the possible prospects for the use of CEC to increase the wear resistance of machine parts.

The industry widely uses coatings in which the metal base is chromium, nickel, iron, copper, cobalt and others. But the most widely used are composite coatings based on nickel. Nickel is widely used as a matrix for CEC, because it has an affinity for most particles used as the second phase and easily forms a coating with them. In addition, electrolytic nickel has sufficient mechanical properties, high corrosion resistance, ductility [1, 2].

Nickel-based CEC is used in ship, automobile, tractor, aircraft, aircraft, rocket, mechanical engineering, chemical industry, for parts and assemblies operating in particularly severe friction conditions, elevated temperatures, in conditions of friction without lubrication, heavy loads. These coatings are used for corrosion protection, increase of physical and mechanical and chemical parameters, increase of hardness and wear resistance, restoration of the sizes, giving to a surface of self-lubricating properties.

CEC application technologies

In comparison with other methods of obtaining protective coatings, the technology of applying CEC is relatively simple and is reduced to the introduction into the known electrolytes of dispersed particles of chemical compounds maintained in suspended state by periodic or continuous stirring of the electrolyte suspension. Being in static or dynamic contact with the cathode surface during electrolysis, the filler particles are overgrown with the base metal. A number of works are devoted to the development of the technology of obtaining composite electrolytic coatings (CEC) [1, 3, 4, 5]. In these works the theoretical bases of joint deposition of metal and dispersed particles are stated, a large number of CEC of various properties and appointments is offered.

The type of dispersed materials for obtaining CEC is selected depending on the operating conditions of the part, physico-mechanical and chemical properties of the filler and the main effect it has on the composition.

As a filler in the creation of CEC, use dispersed particles of the following materials: diamond, amorphous carbon, boron, graphite, silicon, solid refractory compounds: oxides (Al_2O_3, SiO_2, TiO_2, ZrO_2, CrO_2, MoO_2, $BeO_2$2), carbides (SiC, B_4C, TiC, ZrC, HfC, TaC, VC, WC), borides (TiB_2, ZrB_2, VB_2, CrB_2), nitrides (TiN, BN, AlN, $Si_3N_4$3N4), silicides ($MoSi_2$, $NbSi_2$, $TaSi_2$, $HfSi_2$, WSi_2), powders various metals (Ti, Mo, W), low-melting powders (Sn, In, Pl) and other particles [1-5].

The properties of CEC with different types of filler are mostly determined by the physical and mechanical properties of the inclusions. Thus, borides have high heat resistance, hardness and pronounced metallic properties, however, they can interact with electrolytes, and are not sufficiently stable in acids; carbides of many metals have high hardness, heat resistance and chemical resistance; nitrides, in contrast to borides and carbides, have lower hardness, greater plasticity, sufficiently heat-resistant; oxides are more resistant to aggressive environments, heat resistant; silicides are promising as heat-resistant compounds, have magnetic properties and conductivity. Substances with a layered crystalline structure are of special interest for obtaining CEC. Such materials are the basis for self-lubricating coatings and coatings with improved antifriction properties.

The volume content of particles that can be introduced into the electrolyte depends on their shape, nature, dispersion, electrolyte acidity, cathodic current density, location of the cathode surface (horizontal or vertical), mixing conditions. Theoretically, when modeling the dense packaging of the dispersed phase in the form of powders of the same size, the maximum filling of the space, provided that the spherical particles touch, is 74%. The data presented in the monograph [65] indicate the possibility of obtaining a volume fraction of the dispersed phase in the CEC up to 50%. Theoretical calculations and experimental data show that when real dispersed powder particles have different shapes and sizes, when smaller particles can be located between large ones, then the maximum volume content in the coating can reach 60%. However, in the absence of contact between the filler particles, when a solid or frame structure of the matrix is formed, their volume fraction in the coating reaches only 30% [6]. Therefore, this volume content of the dispersed phase can be considered the limit, at which the particles are completely cemented by a metal matrix. The use of CEC filler powders of various nature and dispersion can have an effect on their volume content in the coating, but usually in the direction of its reduction.

It is established [1,3] that when using electrically conductive particles in the process of forming CEC, their volume content in the coating is always greater than those that do not conduct current. This allows a lower content of particles in the electrolyte-suspension to obtain a higher content in the coating compared to the use of non-conductive powders.

Of practical and theoretical interest is the method of calculating the maximum possible production of the dispersed phase in the CEC depending on the bulk density of the powder fraction and the deposition parameters, which is presented in [4].

As for the dispersion of particles, many researchers believe that the optimal fraction -2 + 0.1 μm, which provides the maximum number of particles in the coating when deposited in continuous stirring on a vertical cathode and a fraction of -50 + 40 μm and above when deposited on a horizontal cathode [3,5,7].

The volume content of particles in the CEC during its production is significantly influenced by the nature of the electrolyte, the presence of a sufficient number of particles, the cathode current density, the process temperature and so on. The ionic composition of the electrolyte, its electrical conductivity, density, acidity, deposition modes in different ways can affect the quality of CEC. The complexity of the deposition process, the large number of factors that affect it, does not allow to accurately predict the optimal modes of formation of CEC [1, 3, 4].

The basis for the installation for the formation of CEC, created at the Khmelnitsky National University (KhNU), the task of control and regulation of the rate of deposition of electrically conductive and sedimentation

of non-conductive particles of filler powders. This task is achieved due to the fact that in the process of electrolysis the delivery rate of the filler particles is controlled and regulated by changing the electric field strength using a potentiostat. [8].

Influence of filler content and electrolyte composition

The greatest influence on the content of inclusions in the coating, and, accordingly, on the physical and mechanical properties of the coating, has the number of powder particles in the electrolyte. From the literature data it follows [3] that with increasing concentration of both large and small particles in the electrolyte, the number of inclusions in the coating increases. The number of particles in the CEC increases both with increasing size of the fractions of the powders used and with increasing their concentration in the electrolyte. Moreover, with increasing the concentration of particles to 50 kg/m^3 there is a significant increase in their content in the coating. The maximum mass fraction of inclusions in the CEC is achieved at a concentration of particles in the electrolyte of 100 kg/m^3, so it can be considered optimal for all fractions of powders used.

The composition and parameters of the electrolyte affect the filler content in the coating in different ways. Thus, it was found that the formation of particles and their overgrowth with metal easily proceeds from the nickel electrolyte [3,5], and most difficult from the chromium electrolytes. The acidity of the electrolyte is a determining factor in the formation of CEC, for example, on the basis of chromium and does not have a significant effect on the production of CEC on Nickel basis. Thus, during the deposition of CEC based on Nickel using particles up to 10 μm, the change in electrolyte acidity in the range from 2 to 5 pH units does not affect the deposition of particles, including pH = 4-5 if the particles are larger than 20 μm [1].

Cathodic current density and electrolyte temperature

Increasing the cathode current density has a positive effect on the overgrowth of particles. In most cases, increasing the cathode current density leads to an increase in particle content and increase the thickness of the coating, but there is a critical value of the cathode current density exceeding which disrupts the electrolysis process and leads to deterioration of CEC [1,5].

The current density determines the rate of increase of the galvanic coating, but at a density of more than 2 kA/m^2 the surface of the coating has many defects, poor quality overgrown particles of silicon carbide of large fractions. In addition, the possible release of hydrogen ions and the coating is then loose, spongy and with a dendrotic structure. At a density of more than 1 kA/m^2 the surface has an uneven relief and high roughness. Studies have also shown that increasing the current density for non-conductive particles of boron and silicon carbide has virtually no effect on the bulk filling of the Nickel matrix with filler. Therefore, in our work, electrolysis was performed at a current density in the range of 0.4… 1 kA/m^2 [8].

It is noted [1] that the temperature regime of electrolytes in obtaining CEC has a certain effect on the deposition rate. This effect is especially noticeable when obtaining CEC based on metals of the iron family, although a certain pattern of the effect of temperature on the retention of particles in the coating is not observed.

The presence of two cooling circuits on the installation developed at KhNU allows to stabilize the electrolysis temperature in the cathode zone within ± 2 ^{0}C, which also helps to stabilize the electrolysis process in the formation of the metal matrix and in the formation of coatings with filler particles. It also allows to obtain a coating of uniform thickness and with a lower surface roughness [8].

Electrolyte mixing rate

The mixing rate of the electrolyte-suspension has a particularly large influence on the formation of CEC [1, 4]. Stirring of the electrolyte in the electrolysis process accelerates the process of electrochemical deposition of metals. Stirring is also necessary to ensure that the particles of the dispersed phase (even less than 1 μm), which are in the electrolyte, are always suspended. This is especially important when using particles larger than 5 microns. It is difficult to establish the explicit regularity of the influence of the stirring speed on the production of particles in the CEC, because it is not possible to accurately determine the rate of exit of particles in the current. In the general case, with increasing speed of rotation of the stirrer, the content of particles in the coating first increases, and then, when a certain limit is reached, decreases. The fraction of the filler powder has a determining influence [1, 5].

Influence of filler type for formation of nickel CEC

The study of the influence of dispersed filler particles of various natures introduced into the electrolyte on the process of formation of nickel CECs and their properties is devoted to works [1, 3, 4,5]. They present data on the effect of different filler particles on the microhardness, wear resistance and internal stresses of the CEC, determine their optimal concentrations in the electrolyte - suspension. Composite electrolytic coatings with

inclusions of titanium, tungsten and silicon carbides have the greatest wear resistance. Zirconium and aluminum oxides increase wear resistance to a lesser extent. In addition, carbides significantly (5-8 times) reduce the internal stresses of CEC [2].

In [6] the influence of electrical conductivity of dispersed particles on their distribution in the nickel matrix, structure and quality of precipitation was studied. For non-conductive particles (silicon carbide), their uniform distribution in the matrix is characteristic, while for electrically conductive materials (chromium carbide), this was not observed. The roughness of coatings filled with chromium carbide particles is higher than in CEC Nickel-silicon carbide. The wear resistance of CEC increases with increasing number of particles in the matrix [8].

Silicon carbide is recommended for the creation of compositions to increase hardness and wear resistance under friction without lubrication and at elevated temperatures [10, 11], corrosion resistance [8]. Silicon carbide in the nickel matrix improves the properties of the coating: microhardness increases by 1… 2.5 GPa, internal stresses decrease by 3… 8 times, and corrosion resistance increases by 4… 50 times [6]. Silicon carbide coatings have the best adhesion to steel compared to other fillers. The strength of adhesion to the base has the following range, kg/cm^2: 487-SiC; 213-TiC; 216-Cr7C3 [5].

In addition, silicon carbide has high mechanical properties: microhardness 29… 35 GPa, modulus of elasticity E = 394 GPa, tensile strength -180 MPa, flexural strength -173… 225 MPa, compressive strength -800 MPa [8, 12].

Silicon carbide has a low cost and is produced in large quantities in the form of powders packaged in fractions. Based on the above, in our work we investigated the CEC on a nickel basis with SiC filler of different fractions from 100/80 μm to nanoparticles smaller than 50 nm. Thus, SiC powders with the following sizes were used in the works: less than 50 nm - nanoparticles; M5; 28/20; 50/40; 100/80 μm. According to the sizes of SiC particles the following designations are accepted: $Ni-SiC_{nano}$; $Ni-SiC_5$; $Ni-SiC_{28}$; $Ni-SiC_{50}$; $Ni-SiC_{100}$.

Additives of surfactants

To intensify the process of deposition of CEC and improve the quality of sediments in the electrolyte is introduced various organic and inorganic additives and surfactants (surfactants), which contribute to the receipt of uniform and dense sediments with fine crystalline structure. It is known that the addition of soluble organic and some inorganic substances changes the cathodic polarization and the equalizing ability of the electrolyte [9]. It can be assumed that these substances will significantly affect the process of formation of CEC. Thus, when studying the effect of surfactants on the coprecipitation of Nickel with silicon carbide particles, it was found that the introduction of cationic surfactants reduces the rate of SiC at low concentrations of substances in the electrolyte and increases sharply at high, and the introduction of anionic surfactants at a certain concentration completely stops particle deposition. The effect of anionic surfactants is associated with the agglomeration of particles as the concentration increases and their deposition in the electrolyte; influence of cationic surfactants - with positive charging of particles and their sedimentation with the formation of a dense layer at the cathode.

In our studies, the electrolyte was additionally injected with sodium surfactant in the amount of 0.01… 0.02 g/l, which according to [12] promotes the inclusion of SiC particles in the coating and improves the conditions for building a nickel matrix.

Amorphous boron powders with a size of about 1 μm were also added to the silicon carbides as a filler, which is explained by the possibility of boron and nickel interaction during the subsequent heat treatment of the coating and obtaining new structures (solid solutions, eutectic, dispersion-hard alloys).

Intensification of CEC formation processes

Among the modern innovations in the technology of electrolytic coatings are the use of non-stationary electrical modes (reversible or pulsed currents, the application of alternating current to direct current) [11] and the application of ultrasound in the application of electrolytic coatings [10, 11]. The use of reverse current (current with periodic change of polarity) has a positive effect on electrode processes and increases the productivity of electrolysis. During the anode period, the microprojections on the cathode dissolve and as a result the unevenness of the coating and its porosity decreases. Also, the use of such modes allows to obtain a more dispersed structure of the sludge with lower internal stresses. The use of pulsed current (current pulses with a very short duration (<1 ms) and an amplitude that is an order of magnitude higher than the limiting current of the process) allows to increase the deposition rate to obtain more uniform and fine crystalline sediments, but slightly reduced (5-10%) cathode current output. The application of ultrasonic waves allows to precipitate metal at high current densities with high current output, electrodeposition of pure metals in the presence of impurities in the electrolyte, precipitate smooth, compact, fine with high corrosion resistance and lower internal coating stresses. Thus, these methods can improve the structure of the coating, increase microhardness, increase wear resistance and anti-corrosion properties.

Combined CEC

Analysis of the results of [1-5] shows that combined electrolytic coatings based on Nickel with inclusions of dispersed particles have a significantly higher wear resistance than coatings without particles. In the general case, the increase in wear resistance of CEC in comparison with pure galvanic coatings is 2.5-5.0 times [2]. Comparative tests for friction and wear show a clear advantage of nickel-based CEC with inclusions of oxides, borides, carbides, in comparison with hardened steels 45, 40X, 30HGT. It is noted that the inclusion of carbides in nickel CEC more significantly increases the wear resistance than the inclusion of oxides, and the lowest wear was observed for coatings containing particles of TiC, WC, Cr_3C_2 [3]. The authors explain the increase in wear resistance of Nickel coatings when particles are introduced into them by the fact that solid particles carry the main load and contribute to better distribution of lubricants. Coatings with inclusions of WC particles have a high microhardness (up to 500 kg/cm^2) and, accordingly, less wear than Nickel. The wear resistance of combined layers with SiC is almost 70% higher than for nickel without carbide. Data on the wear rate of composite coatings after heat treatment with nickel borides and chrome coatings are also given. It is noted that CEM with borides have the same wear resistance as chrome coatings, and sometimes exceed it.

In the absence of lubricant, galvanic coatings effectively reduce the coefficient of friction only when applied to a solid substrate. Coating steel with copper, zinc, tin, nickel, lead can reduce the coefficient of friction. Applying such coatings on a soft base is not acceptable for friction joints [3].

Wear and degree of destruction of CEC depend on friction conditions. At high specific loads (200 N/cm^2) plastic deformation precedes the formation of microcracks, which due to insufficient strength of adhesion of the coating to the matrix develops mainly at the interface. For reliable operation of the friction unit, the mechanical properties of the CEC matrix must be consistent with the external operating conditions.

The mechanical and antifriction properties of CEC have a significant effect on the crystal structure of the particles. Borides and carbides increase the hardness of CEC most effectively. Particles with a cubic crystal structure significantly increase the hardness of nickel coatings. This is due to a more even distribution of local stresses in the volume of coverage and a significant improvement in the elastic properties of the matrix.

In [2,3,4,12] the hardness, wear resistance and structure of CEC on a nickel basis with microparticles of boron carbide, chromium, silicon, titanium, industrial micropowders of carborundum and electrocorundum, synthetic diamonds when reaching their maximum content in coverage. Increasing the concentration of micropowder M1 from 50 to 300 g/l leads to an increase in the number of inclusions from 4 to 10% and microhardness from 3.25 to 4.5 GPa. Increasing the volume fraction of silicon carbide particles from 3.8 to 18.9% increases the microhardness from 2.9 to 5.5 GPa and, accordingly, increases the wear resistance by 3 times [12,13].

According to the authors of [6], the increase in the microhardness of coatings during the introduction of dispersed particles is associated with a change in the substructure of the deposited metals (reducing the size of crystal blocks and increasing the density of dislocations). Thus, the existence of optimal concentrations of particles of titanium carbide, zirconium dioxide and kaolin (30-50 g/l) in the nickel electrolyte, which correspond to the minimum block size and maximum micro-distortion size and dislocation density. The change in the size of the blocks in Nickel coatings is due to the different effects of particles introduced into the electrolyte on the ratio of growth rates and passivation of crystals. According to the author, the grinding of the blocks is facilitated by submicroscopic particles that are included in the sediment and prevent the growth of crystals by shielding their surface. The content of particles in the electrolyte has only an indirect effect on the substructure of the matrix. The decrease in mosaic blocks with increasing concentration of particles in the suspension can be explained by the depassive effect of not all particles in the electrolyte, but only by the action of particles deposited on the growth front of the matrix.

Self-lubricating CEC

Self-lubricating coatings are also used to reduce friction steam wear [2,5]. These are CECs, which contain solid lubricant particles and have a better ability to run and reduced friction. As the second phase in such coatings are particles of molybdenum disulfide, graphite, boron nitride and other substances. The introduction of such particles into the matrix usually increases its plasticity and the tendency of coatings to deformation hardening. Coatings with solid lubricants are suitable for use in vacuum conditions, and their use for air friction units is limited by the temperature regime and the tendency to oxidation of particles and as a result the coefficient of friction increases sharply. However, at moderate loads and sliding speeds, solid lubricants significantly reduced the wear of CEC [14].

Thus, the dispersed particles to obtain CEC must be selected taking into account their properties, nature and crystal structure, properties of the matrix, its crystal structure and friction conditions.

Heat treatment of CEC

The analysis of CEC on a nickel basis testifies to wide technological possibilities of their reception and a variety of the received structures and their properties. Electrochemically deposited metals in most cases do not require further heat treatment and are in a state typical of metals that are subjected to low-temperature hardening. However, due to the lack of coherent connection of particles with the matrix, it is possible to chip particles in the process. At the same time, the level of wear resistance of CEC is low in comparison with hard chrome coverings. In addition, electrolytic coatings, including CEC, in comparison with others have a number of disadvantages, namely: low adhesion to the substrate, the presence of pores and microdefects, internal stresses, sludge flooding. Therefore, many researchers [3, 4, 8,9] have studied the effect of annealing on the hardness and wear resistance of CEC, in order to improve the strength of adhesion to the metal substrate, increase the density of sediments by overgrowing pores, cracks and other defects inherent in electrolytic coatings. Thus, in the process of heat treatment there is a recrystallization of the metal and a change in properties, namely the improvement of ductility and wear resistance. In [9] studies on the effect of annealing modes on the bond strength of CEC Nickel-silicon carbide, Nickel-carborundum with aluminum alloys AK-18, AL-7, AD-25. The maximum bond strength of these coatings with the substrate was achieved after annealing at a temperature of 200 ° C for 2 hours. Studies [3,16,17] aimed at increasing the hardness of nickel-based CEC with the inclusion of oxides of chromium, titanium, thorium, aluminum, as well as chromium and silicon carbides due to their annealing did not give positive results. Annealing carried out in the temperature range from 200 to 700^0C, led to a loss of hardness, apparently due to the removal of internal stresses and weakening of the Nickel matrix. The microhardness of coatings with increasing annealing temperature decreased from 3.2-4.8 GPa to 2.0-3.2 GPa.

In some cases, combined electrolytic coatings are subjected to heat treatment to improve mechanical properties (high temperature resistance) or to detect the tendency to oxidation at high temperatures. For example, coatings of Ni + Al_2O_3, Ni + Ti and others. show increased durability at high temperatures. This type of heat treatment does not lead to the creation of qualitatively new structures and does not change the phase composition of the coatings.

It is possible to significantly increase the operational properties of CEC by heat treatment by conducting filler particles in them, which tend to interact with the metal matrix and form solid solutions and chemical compounds with high hardness and wear resistance. Thus, in [3, 4] data on heat treatment of combined electrolytic coatings based on Nickel, which aims to qualitatively change the phase composition and structure of the coating. The authors of these works received coatings containing powders of tungsten and molybdenum, which were subjected to subsequent annealing. Annealing of other electrolytic compositions, such as Ni+Cr (powder) and Fe+Cr (powder), leads to coatings such as stainless steel [5]. The process of heat treatment of composite coatings can be considered as a kind of chemical-heat treatment, in which the diffusion element is inside the metal matrix. In addition, the heat treatment of CEC can be carried out using concentrated energy sources such as lasers, high frequency currents, solar energy. The main advantages of such processing are locality, possibility of receiving high temperatures at insignificant duration of processing, high speeds of heating and cooling. The prospects for the use of these energy sources in heat treatment are noted in [3, 17, 18]. But in them the main attention is paid to studying of the structures formed at such processing. Based on this, it is of practical interest to study the possibility of improving the physical and mechanical properties of nickel-based CEC by introducing into their composition metals capable of heat treatment, interact with the metal matrix to form solid substitution solutions and chemical compounds (solid implementation phases) and determine tribotechnical characteristics of these coatings [8, 19].

Based on the analysis, thermal annealing in a muffle furnace was performed at a temperature of 400ºC for 1… 2 h, which increased the cavitation-erosion resistance of the Ni-SiC$_{nano}$ composition by approximately 20% in hard water and about 30% in 3% NaCl solution [8]. The latter is due to the reduction and equalization of internal stresses in the coating, reducing the heterogeneity of the structure. The annealing temperature was chosen on the grounds that irreversible transformations and eutectic formations take place in the temperature range 120… 220; 300… 350 and 370… 450ºC.

Vacuum annealing with melting of the coating surface was performed on the installation OKB 8086 at temperatures of 1085… 1090ºC. After holding in the furnace, the samples were cooled together with the furnace. After heat treatment, the microstructure forms a framework consisting of Ni-Ni$_3$B eutectic and Ni$_3$B borides with hardness H_μ = 6.6 ... 7.4 GPa. Cavitation-erosion tests of Ni-SiC$_{28}$-B CEC after vacuum annealing in hard water showed that the wear resistance in 2 hours of testing increases, compared to CEC without vacuum annealing, 2 times.

Therefore, vacuum annealing at the temperature of eutectic formation allows to obtain dense, smooth coatings with high cavitation and erosion wear resistance.

Conclusions

1. When forming CEC, depending on the physical and mechanical requirements for the surface of the part, it is necessary to choose the type of matrix, the nature of the particles and their fractionality, to find the optimal technological modes of electrolysis and so on.

2. CEC based on nickel matrix filled with silicon carbide (SiC) particles are promising coatings to improve the tribological characteristics of structural steels.

3. In order to improve the physico-chemical characteristics of the nickel-based CEC, it is necessary to introduce chemical compounds into the electrolyte, which as a result of heat treatment form solid substitution solutions and solid phases of introduction.

References

1. Antropov L.I., Lebedinsky Yu.N. Composite electrochemical coatings and materials. - K .: Technique, 1986. - 200 p.

2. Borodin I.N. Powder electroplating - M .: Mashinostroenie, 1990. - 240 p.

3. Guslienko Yu.A. Research on the processes of obtaining wear-resistant composite coatings based on nickel and iron and the study of their properties: Dis. ...cand. tech. Sciences: 05.16.01. - K., 1975. - 155p.

4. Luchka M.V., Kindrachuk M.V., Melnik P.I. Wear-resistant diffusion-alloyed composite coatings. - K .: Technique, 1993. - 143 p.

5. Saifullin R.S. Composite coatings and materials.– M. Chemistry, 1977.–272 p.

6. Samsonov G.V., Zhunkovsky G.L., Luchka M.V. Study of the process of formation of composite coatings based on titanium carbide // Powder metallurgy.– 1976.– No. 7.– P.53–56.

7. Kovalenko V.S., Golovko L.F., Chernenko V.S. Hardening and alloying of machine parts with a laser beam. - K .: Technika, 1990. -192 p.

8. Bilyk Yu.M. Increasing cavitation-erosion wear resistance of carbon structural steels by composite electrolytic coatings Dis. Cand. tech. Science: 05.02.04. - Khmelnytsky., 2014. - 169 p.

9. Frolova F.P., Zhitkevich I.I., Mikhailenets E.S. Causes of adhesion of nickel–silicon carbide coatings to aluminum alloy. AN Lit.SSR, 1975.– No. 5 (114). – P.21–28.

10. Yavorsky V.T., Kuntiy O.I., Khoma M.S. Electrochemical application of metal, conversion and composite coatings / Lviv Polytechnic State University. - L., 2000. - 216 p

11. Kuntiy OI Electroplating: Textbook for students majoring in 7.091603 "Technical Electrochemistry" / National University "Lviv Polytechnic". - L .: Lviv Polytechnic Publishing House, 2004. - 236 p.

12. Perene N.S., Taitsas L.I. Wear resistance of composite coatings // Tr.ANLit.SSR.– 1977.– No. 1 (98). – P.27–31.

13. Bykova M.I., Antropov L.I. Combined nickel coatings with increased hardness and wear resistance // Obtaining hard wear-resistant galvanic coatings.– M.: MDNTP, 1970. – P. 106–110.

14. Molchanov V.F., Ayupov F.A., Vandyshev V.A. Combined electrolytic coatings. - K.: Tehnika, 1976 - 176p.

15. Borodin I.N. Powder electroplating - M.: Mashinostroenie, 1990. - 240 p.

16. Pletnev D.V., Brusentsova V.N. Fundamentals of technology of wear-resistant and anti-friction coatings. – M.: Mashinostroenie, 1968. – 272 p.

17. Wagner E., Broszeit E. An electrochemical investigation of corrosive wear of as-plated and heat-treated Ni and Ni-SiC coatings // Wear. - 1979. - Vol. 55, No. 2. - P. 235-244.

18. Tikhonovich T.N. Structure formation, properties and technology for obtaining protective composite electrolytic boride coatings based on metals of the iron family: dissertation cand. tech. Sciences: 05.16.01. - K., 1989. - 145p.

19. Obtaining composite boride coatings by surface heating with concentrated energy sources // Yu.A. Guslienko, T.N. Tikhonovich, V.P. Stetsenko, V.S. Dvernyakov // Protective coatings on metals. - 1993. - Issue. 27. – P. 35–39.

Скиба М.Є., Стечишин М.С., Олександренко В.П., Машовець Н.С., Білик Ю.М.

Зносостійкість композиційних електролітичних покриттів

У статті проведено аналіз впливу композиційних електролітичних покриттів (КЕП) на зносостійкість конструкційних сталей.Розглянуті питання вибору матриці і різноманітні поєднання у композиційних покриттях різних хімічних елементів та сполук. У промисловості широко використовують покриття, в яких металевою основою є хром, нікель, залізо, мідь, кобальт та інші, але найбільш широке застосування мають композиційні покриття на основі нікелю. Нікель широко використовується в якості матриці для КЕП, тому що він має спорідненість до більшості частинок, що застосовуються як друга фаза і легко утворює з ними покриття. Дані покриття використовують з метою корозійного захисту, підвищення фізико-механічних та хімічних показників, підвищення твердості та зносостійкості, відновлення розмірів, надання поверхні самозмащувальних властивостей.

На базі створеної установки для нанесення КЕП досліджувалися покриття на нікелевій основі з наповнювачем SiC різних фракцій від розміру 100/80 мкм до наночастинок розміром менше 50 нм. Таким чином, в роботах використано порошки SiCз розмірами: менше 50 нм- наночастинки; М5; 28/20; 50/40; 100/80 мкм.

В проведених дослідженнях в електроліт додатково вводили ПАР-лаурилсульфат натрію в кількості 0,01…0,02 г/л, який сприяє включенню частинок SiCв покриття та покращує умови нарощування нікелевої матриці.

До карбідів кремнію в якості наповнювача додавали також порошки аморфного бору розміром біля 1 мкм, що пояснюється можливістю взаємодії бору та нікелю при наступній термічній обробці покриття і отримання нових його структур (тверді розчини, евтектика, дисперсійно-тверді сплави).

Практичний інтерес становить вивчення можливості підвищення фізико-механічних властивостей КЕП на нікелевій основі введенням у їх склад металів, спроможних у процесі термічної обробки, взаємодіяти з металевою матрицею з утворенням твердих розчинів заміщення і хімічних сполук (твердих фаз впровадження) та визначення триботехнічних характеристик цих покриттів.

Ключові слова: композиційні електролітичні покриття (КЕП),зносостійкість

Creation of progressive hole processing processes based on the study of contact phenomena during deforming broaching and finishing antifriction non-abrasive treatment in various technological environments

Ya.B. Nemyrovskyi[1], I.V. Shepelenko[1], E.K. Posviatenko[2], M.I. Chernovol[1], F.Y. Zlatopolskiy[1]

[1]Central Ukrainian National Technical University, Kropyvnytsky, Ukraine
[2]National Transport University, Kyiv, Ukraine
E-mail: kntucpfzk@gmail.com

Abstract

This work is devoted to the creation of progressive technological processes for processing holes. The relevance of studying this issue is substantiated, technological environments (TE) used in these operations are listed. The purpose of the work performed is to study the influence of TE on contact phenomena and quality parameters of the treated surface during deformation broaching (DB) and finishing antifriction non-abrasive processing (FANT) and the creation on this basis of new technological processes to obtain parts with improved performance. New methods have been developed for studying contact interaction in the case of DB using solid lubricants, as well as for modeling the FANT process. The conditions for the use of liquid lubricants in the DB are described. It has been established that, when them applied, the altitudinal roughness parameters decrease and the surface layer hardens to a considerable depth. It is shown that the use of solid lubricants in DB is mandatory when processing products from hard-to-work materials and alloys. When them applied, significant plastic deformations of the hole can be made. In this case, the surface layer of the workpiece is little different from the original. The change in the altitude parameters of the rough layer, as well as contact pressures using solid lubricants, was studied. Peculiarities of contact phenomena in the case of DB using solid lubricants are revealed. For this case, a functional relationship has been established between the altitude parameters of roughness and the relative contact pressure. An analytical dependence is proposed for their calculation. The boundary conditions for its application are determined. Formation FANT also occurs when using the TE. It was established that solid lubricants during FANT perform a dual function, namely, technological, like solid lubricant during processing, and operational - improve the quality parameters of the processed parts. The combination of DB and FANT operations allows us to develop a new technological process for processing holes of parts such as bushings and sleeves. This process consists in the use of DB as a roughing and finishing operations, and FANT as a finishing operation, which allows to improve the quality indicators of the machined part.

Key words: deforming broaching, finishing antifriction non-abrasive treatment, technological environment, solid lubricants, liquid lubricants, contact phenomena, roughness, hardening, quality of the processed surface

Introduction

The deforming broaching (DB) of products from ductile metals and alloys is always carried out using technological lubricants, which eliminates the setting of the tool with the workpiece material, reduces the energy consumption for the process, and also improves the quality of the processed surface [1].

The technology of finishing anti-friction non-abrasive treatment (FANT), based on the use in the process of friction, setting and selective transfer, also requires the use of a special technological fluid - a technological environment (TE). It moistens the treated surface, loosens the oxide film, plasticizes the surface and creates the conditions for the setting of metals [2].

The most widely used in DB are liquid lubricants, which are used both in finishing and rough operations. When finishing processing, they allow you to get high performance properties of the processed surface of the workpiece. In this case, there is direct contact between the treated surface and the deforming element under liquid lubrication conditions. The treated surface receives hardening and a textured layer to a depth to 0.2 mm, compressing residual stresses that exceed the yield strength of the processed material, low roughness (Ra $\leq$ 0.1 μm), improved microrelief. All this helps to improve the operational characteristics of the finished part [3].

Literature review

According to work [1], the most common liquid lubricants are oil-based lubricants: sulfofresol, mineral oils of the MR class, as well as oils of plant origin. For the processing of non-ferrous materials, a 10% solution of soap in water is used.

The formation of the antifriction coating FANT on the surface of steel or cast iron is also carried out using a technological envirenment, which includes a number of chemical elements that ensure, under specific conditions, the interaction of materials and the presence of surface self-organization processes [4]. Since in this case the coatings are applied without significant changes in the composition and structure of the tool and the applied coating (the tool material is transferred to the steel (or cast-iron) surface of the part), the role of the TE is primarily to clean the surface of the part from oxides. In this case, the layer of applied anti-friction coating can also play the role of a solid lubricant.

The role of the lubricant during broaching by carbide deforming elements becomes especially significant when deforming parts from hard-to-work materials: chromium-nickel-molybdenum and stainless steels of austenitic class, titanium alloys. In these cases, significant deformation of the hole when broaching with liquid lubricants becomes impossible due to the adhesive setting of the tool with the part. Then use solid lubricants, which are characterized by high shielding properties [1].

This makes it possible to use deformation broaching for such materials as a rough shaping operation, the main purpose of which is to increase the utilization of the material in subsequent machining operations. In this case, the main characteristic of the lubricant used should be not anti-friction, but shielding properties, that is, the ability to exclude direct contact of the tool with the product. A number of solid lubricants meet this requirement, which also provide adhesive properties. They must be firmly fixed on the treated surface and localize large shear deformations in the lubricant layer itself.

A series of solid lubricants based on epoxy resins and solid fillers such as graphite, molybdenum disulfide, boron nitride, etc. have been developed at ISM NAS of Ukraine. They are sometimes modified with organosilicon compounds to improve the shielding properties. This allows you to process up to 10% of the holes in billets made of the following materials during deformation: stainless and heat-resistant alloys, hardened steels 30HGSA, EI643, 30HNMA, 38HMYuA, heat-treated aluminum alloys AK6, D16, tubes made of vanadium and niobium, as well as parts from VT1-0, VT6, VT22 titanium alloys.

Purpose

The study of the influence of solid lubricants on contact phenomena and the quality parameters of the treated surface during the DB and FANT and the creation on this basis of new technological processes for processing holes to obtain parts with improved performance.

This will reveal the features of the processes flow and establish their influence on the quality indicators of the treated surface. In turn, research will expand the scope of DB and FANT due to the creation of new technological processes for processing hard-to-work materials and the intensification of the FANT process.

Research methodology

The experiments were carried out on bushings made of 12H18N10T steel with dimensions: hole diameter d_0 = 35 mm, wall thickness t_0 = 35 mm, length l_0 = 250 mm. The initial surface roughness of the hole after boring is Ra = 3–4 μm. And also on bushings made of titanium alloy VT1-0 with dimensions: d_0 = 35 mm, t_0 = 4; 7; 9 mm, l_0 = 250 mm and d_0 = 19 mm, t_0 = 4; 7; 9 mm, l_0 = 150 mm.

The broaching was carried out on a horizontally broaching machine mod. 7B520 and at a special stand developed at the ISM NAS of Ukraine, which allows flashing a workpiece with a force of up to 100 kN. When broaching billets of steel 12H18N10T, solid lubricant ASM-6 was used, which included varnish F-9-K, molybdenum disulfide MoS_2 and toluene. It was previously established that this lubricant can withstand contact pressures of about 2.5 GPa and very significant hole deformations (up to 15%) without breaking. When broaching the VT1-0 titanium alloy preforms, a solid lubricant based on diane epoxy resin with anhydride hardener and filler – colloidal graphite, modified by introducing organosilicon compounds and a highly dispersed carbon filler [5] was used. The specified grease withstands without destruction contact pressure up to 3.2 GPa, which allows for very significant deformation during the expansion of the hole.

The roughness was measured by the parameter Ra along the generatrix of the hole after each deformation cycle, that is, after each missed deforming element, and surface profilograms were taken before and after processing. The measurement was carried out on a "Talysurf-5M-120" profilometer-profilograph and on a VEI-Caliber mod. 201. After each broaching cycle, a portion of the machined sleeve 10–15 mm long was cut off, with which the solid lubricant was removed with acetone, and roughness was measured. In some cases, the study of the roughness and conditions of contact interaction was carried out using transverse sections on the "Micron-gamma" devices, designed by the National Aviation University of Ukraine. Vickers hardness of the samples was measured on a HPO-250 hardness tester, and microhardness was measured on a PMT-3 instrument at loads of 50 and 200 grams. The FANT process was studied by modeling it by the interaction of the peaks of microprotrusions in the form of cutters from cast iron SCh20 and a sample from brass L63. In this case, a brass sample in the form of a plate was fixed on the working table of the milling machine, and a cast-iron micro-cutter was installed in a special device, the geometry of the cutting part of which simulated a separate microroughness of the surface. The front angle of the cutter γ varied from $+50 \div -150°$, and the cutting depth from 0.1 to 0.6 mm. The load on the sample was provided by the vertical feed mechanism of the machine and was controlled by an indicator head. In this case, the force P_e was measured with a special dynamometer. The thickness of the cut was insignificant and comparable with the radius of blunting of the cutting edge, that is, the contact interaction corresponded to the actual conditions of the interaction of the microprotrusion with a brass tool. Glycerin was used as TE. Measurement of the wear of the cutter, as well as the adhesion area of brass L63 on the rear surface of the cutter and its continuity, were performed on a ZEISS EVO 50XVP electron microscope.

Results

In fig. 1, the quality parameters of a surface treated by deforming broaching of steel sleeves 12H18N10T using solid lubricant based on molybdenum disulfide are given.
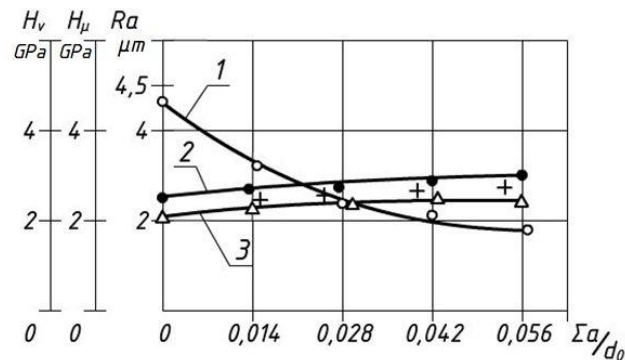
Fig. 1. The dependence of roughness (*Ra*), hardness *HV*, microhardness $H_{\mu50}$ on the total deformation when machining bushings made of steel 12H18N10T: when using solid lubricant ASM-6: 1 – *Ra*, 2 – $H_{\mu50}$ (● – on the surface, + – at a depth of 0.5 mm), 3 – *HV*

As can be seen, the altitude parameters of roughness decrease with an increase in the total expansion deformation, however, the decrease does not occur as intensively as with the use of liquid lubricants [6], which, apparently, indicates a decrease in shear deformations in the surface layer. The roughness profile of the machined surface of the sleeve made of 12H18N10T steel previously bored and stretched using solid lubricants (Fig. 2, a) also remains almost unchanged. The supporting surface also changes slightly at the midline level (Fig. 2, b).

a   b
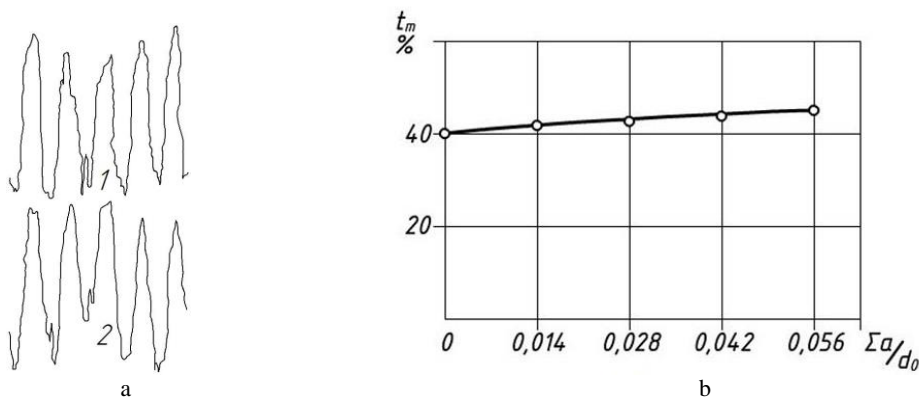
Fig. 2. The profile of the initial and processed surface (a) and the reference length of the profile at the midline level (b): 1 – the initial surface after boring, 2 – the surface after 4 cycles of deformation

After boring, the initial area of the supporting surface was 40%, and after 4 cycles of deformation, it increased by only 6–7%. This is also confirmed by the results of measuring the hardness of the treated surface (Fig. 1, curve 3), the microhardness of the surface and the microhardness of the material at a certain depth from the treated surface (Fig. 1, curve 2).

Similar results were obtained during the deformation of VT1-0 titanium alloy billets with applied hole deformations of up to 6% (Fig. 3). When processing these blanks, solid lubricant was also used, the composition of which is given in work [7].
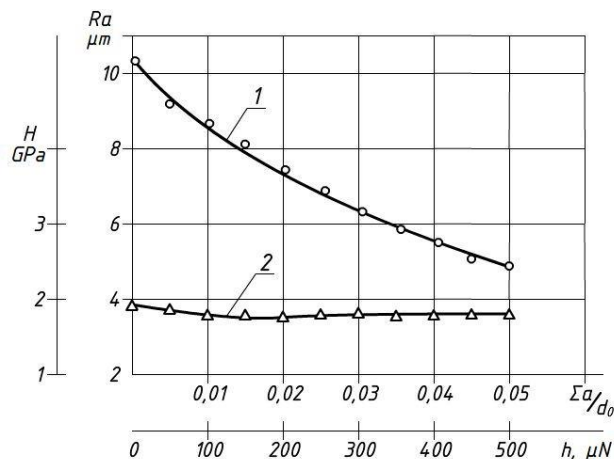
Fig. 3. The dependence of roughness (1) and microhardness (2) on the total deformation when processing bushings from titanium alloy VT1-0 with t_0/d_0=0,21 using solid lubricant based on diane epoxy resin ED-5 with colloidal graphite as a filler and modified organosilicon compounds

In this case, there are also no noticeable shear deformations in the surface layer, which is confirmed by the data shown in Fig. 3. It follows from them that the altitude parameter Ra decreases slightly after each cycle, which is due to the influence of mainly circumferential deformation of the hole. Therefore, the change in microhardness along the wall thickness is almost imperceptible. This is qualitatively different from the known nature of the change in this indicator when using liquid lubricants, which cause the formation of texture and the creation of a significant gradient of changes in hardening along the wall thickness [6].

The indicated features of the deformation of the surface layer when using solid lubricants are confirmed by photographs of the thin sections of the contact zone obtained on "Micron-gamma" device. It allows you to get not only a real picture of the interaction of the tool with the treated surface, but also to determine the height of microroughnesses using a scale ruler (1 division - 10 μm). As can be seen (Fig. 4), a layer of solid lubricant is present between the contacting surfaces, which, due to its screening properties, localizes shear deformations in itself. Microgeometry of the treated surface layer differs little from the original. That is, as indicated above, its change is caused mainly by the influence of the circumferential deformation of the hole – $\Sigma a/d_0$.
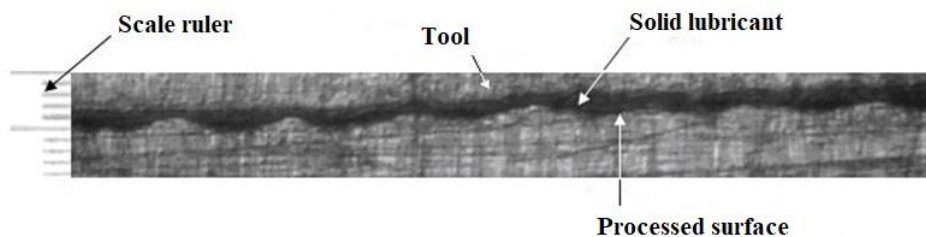
Fig. 4. Contact of the tool with the processed surface when using solid lubricant

Some differences in roughness values (Figs. 1 and 2) are due to its different initial values. For relative roughness $R_a/R_{a\ init}$, the experimental points for different materials lie practically on the same curve (Fig. 5), which apparently indicates close shielding properties of the applied solid lubricants.

When these bushings were deformed, normal contact pressures were determined. Their change depending on the deformation is shown in Fig. 6.

An analysis of the results showed that the existing models for determining the roughness of the treated surface after deforming broaching, given in [8], are not suitable for describing the process of changing the roughness during broaching using solid lubricants.

One of these models, used for low-cycle deformation, is built on the basis of a cone or prism precipitation scheme. In this case, the relationship between the altitude parameters of the rough layer and the total contact pressure Σq accumulated during each deformation cycle was analytically established [8].
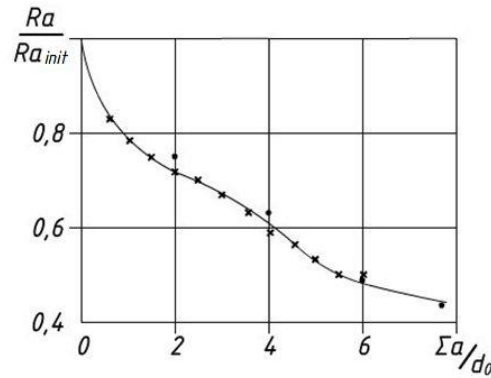
Fig. 5. The dependence of the parameter $R_a/R_{a\,init}$ when processing bushings: × – from titanium VT1-0: t_0/d_0=0,21, : a_0/d_0=0,005; ● – from stainless steel 12H18N10T: t_0/d_0=0,22, : a_0/d_0=0,014
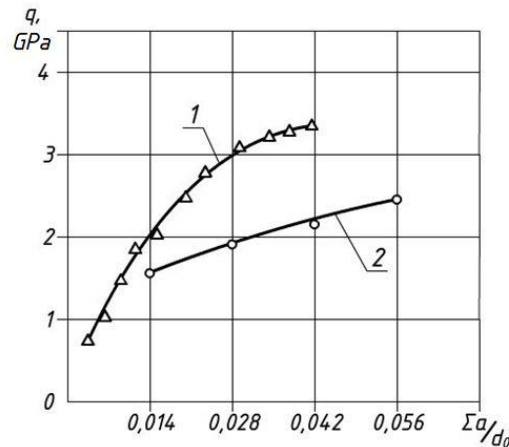
Fig. 6. The dependence of contact pressure on the total deformation during the processing of the bushings: 1 – from titanium VT1-0: t_0/d_0=0,21, a_0/d_0=0,028, l = 0.65 mm; 2 – from stainless steel 12H18N10T: t_0/d_0=0,22, : a_0/d_0=0,014, l = 1.5 mm

Another model of this work was obtained for calculating the change in the altitude parameters of roughness during multi-cycle deformation and takes into account the influence of not only normal loads, but also tangential ones due to friction between contacting surfaces. In this case, the process of reducing the altitude parameters of roughness occurs not only from compression under the action of a normal load, but also from mass transfer caused by the "roll-over" of microroughnesses under the action of the friction force that occurs when using liquid lubricants (Fig. 7). Moreover, with an increase in the number of deformation cycles, the influence of the friction force on the microrelief increases. Along with a decrease in the height of microroughnesses, cavities are filled due to the mass transfer of the material of the microprotrusions from the action of friction.
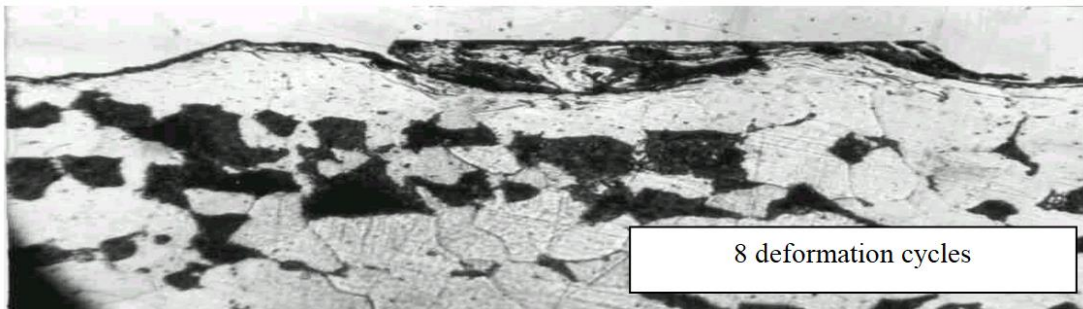
Fig. 7. The nature of the deformation of the microprotrusion of a workpiece made of steel 45 with the number of deformation cycles equal to 8; × 500

When broaching using solid lubricants, the following occurs. In this case, the expansion process occurs in the absence of friction forces on the surface of the workpiece, which are localized in the solid lubricant layer (Fig. 4). Therefore, when using large tension on the deforming element and small angles of the working cone of the tool, when the contact pressures are low and do not exceed the critical contact pressure for a given workpiece material [6], the expansion pattern will be close to the expansion of the pipe by internal pressure.

For technological calculations related to forecasting and ensuring the required roughness in case of DB, it is necessary to establish a relationship between the altitude parameters of roughness and contact pressure q.

As is known [6], value q is proportional to the hardness of the material being processed. Let us analyze the dependence of the relative roughness $R_a/R_{a\,init}$ on the dimensionless contact pressure q/HV (Fig. 8).
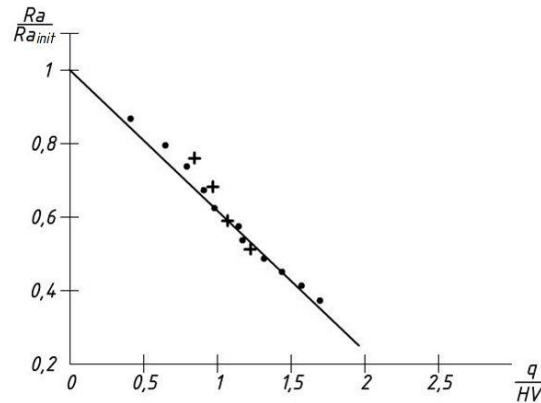
Fig. 8. The dependence of the relative altitude parameter of roughness on the relative contact pressure during the processing of titanium billets VT1-0 (●): t_0/d_0=0,21, a_0/d_0=0,028; from stainless steel 12H18N10T (×): t_0/d_0=0,22, a_0/d_0=0,014

It can be seen that this dependence is almost linear and does not depend on the material being processed and is approximated by the following expression:

$$\frac{Ra}{Ra_{init}} = 1 - 0,36\frac{q}{HV} .$$ (1)

In [1,6], based on the analysis of a significant amount of experimental data, empirical calculated dependences are proposed for determining q depending on technological factors and properties of the materials being processed.

For this, the axial force of broaching and the contact length l are experimentally determined. By the formula (2), the average value of the contact pressure is calculated:

$$q = \frac{Q\cos\eta}{\pi d_0 l \sin(\alpha + \eta)},$$ (2)

where η is the angle of friction, $\eta = arctgf$, f is the coefficient of friction, α is the angle of inclination of the generatrix of the working cone of the deforming element.

The friction coefficient for solid lubricants was determined experimentally and was approximated by the dependence:

$$f = C_{fm}q^{-xm} .$$ (3)

The values of the coefficients C_{fm} and xm for our processing conditions are shown in table 1.

Table 1

The value of the coefficients C_{fm} and xm for various processed materials

Lubricant for processed material	C_{fm}
stainless steel 12H18N10T	0,087
titanium alloy VT1-0	0,048

In [10], a calculation scheme was proposed for determining q during processing with small tension of substantially thick-walled workpieces with "infinite wall thickness" [6], when $t_0 \geq d_0$. However, it is correct for calculating the contact pressure when its value exceeds the critical pressure [6].

In our case, for technological calculations of the roughness parameters, we need to know the contact pressure, the hardness of the processed material and the initial roughness of the hole surface.

Based on the results obtained in this paper, we can propose a theoretical method for calculating contact pressures when expansion by DB with respect to thin-walled workpieces with large tension, small angles when contact pressure is below critical. Note the relevance of this issue. Large degrees of expansion are used for rough forming operations, and for this processing of workpieces from the above-described difficult-to-handle materials, it is used solid technological lubricants.

Since, as shown above, the roughness of the treated surface depends only on the total degree of deformation of the hole, it is natural to assume that in the case of using solid lubricants, the deformation process will be close to the internal pressure expansion pattern of the pipe. As shown in [8, 9], such a design scheme is acceptable for deformation broaching when determining the fracture deformation of workpieces and their geometric parameters after broaching.

Therefore, we use this model to determine contact pressures for our case. The design scheme is presented in Fig. 9.

Let the hardening of the workpiece material be approximated by the dependence:

$$\sigma_0 = \sigma_T + Ae_0^n, \tag{4}$$

where σ_0 and e_0 are the stress intensity and the intensity of plastic deformations; σ_T - yield strength; A and n are empirical coefficients.
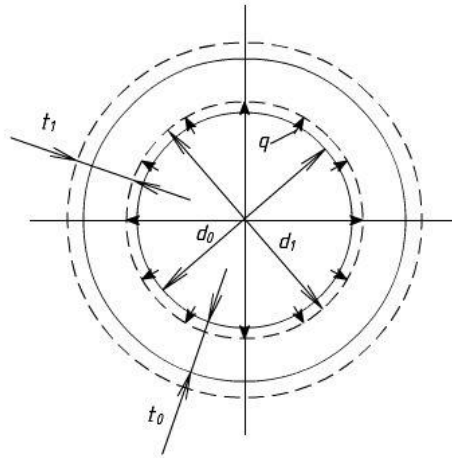
Fig. 9. The calculated expansion scheme

For relatively thin-walled workpieces, average circumferential deformation:

$$e_\varphi = \frac{\sum a}{d_0} = \sum \overline{a}. \tag{5}$$

In the absence of axial tightness

$$e_0 = e_\varphi = \sum \overline{a}. \tag{6}$$

Then

$$\sigma_0 = \sigma_T + A\left(\sum \overline{a}\right)^n. \tag{7}$$

Specific work of plastic deformations (per unit volume):

$$A^* = \sigma_0 e_0 = \sigma_T e_0 + Ae_0^{n+1}. \tag{8}$$

Full work of plastic deformations

$$A = A^* \cdot V_0, \tag{9}$$

where V_0 is the initial volume of the workpiece, which does not change during deformation:

$$V_0 = \pi d_0 t_0 L_0, \tag{10}$$

where L_0 is the length of the workpiece.
In view of (10)

$$A = \pi d_0 t_0 L_0 \left[\sigma_T \sum \overline{a} + A\left(\sum \overline{a}\right)^{n+1}\right]. \tag{11}$$

Elementary work on increment diameter $d\left(\sum \overline{a}\right)$

$$dA = \pi d_0 t_0 L_0 \left[\sigma_T d\sum \overline{a} + A(n+1)\left(\sum \overline{a}\right)^n d\left(\sum \overline{a}\right)\right]. \tag{12}$$

On the other hand, it is produced by the current contact pressure q at increment $d\left(\sum \bar{a}\right)$:

$$dA = q\pi d_0 t_0 L_0 d\left(\sum \bar{a}\right). \tag{13}$$

Equating expressions (12) and (13) we obtain

$$q = \frac{t_0}{d_0 + \sum \bar{a}}\left[\sigma_T + A(n+1)\left(\sum \bar{a}\right)^n\right]. \tag{14}$$

It has been taken into account that the current value of the hole diameter is $d_1 = d_0 + \sum \bar{a}$.

To calculate contact pressures according to dependence (14), it is necessary to know the dimensions of the workpiece and the hardening curve of its material. We define the area of use of formula (14) by comparing the calculated and experimental (according to [6]) q values (Fig. 10) for the case of processing workpieces made of steel 20 and steel 45.

For steel 20, the flow curve was approximated by the dependence $\sigma = 220 + 624e^{0,473}$ (MPa), and for steel 45 – $\sigma = 350 + 1180e^{0,5}$ (MPa). As can be seen, good coincidence between the calculated and experimental data (Fig. 10, a, curves 2 and 3 and 10, b, curve 2) is observed at contact pressures below critical values, which, according to the data of [6], lead to the appearance in the deformation zone local zone of plastic deformation in the form of an influx. It causes the appearance of the axial flow of the processed material and large shear deformations (textures). In the presence of critical contact pressures, the calculated contact pressures are much lower than the experimental ones (Fig. 10, a, curves 1 and 2 and Fig. 10, b, curves 1 and 2).
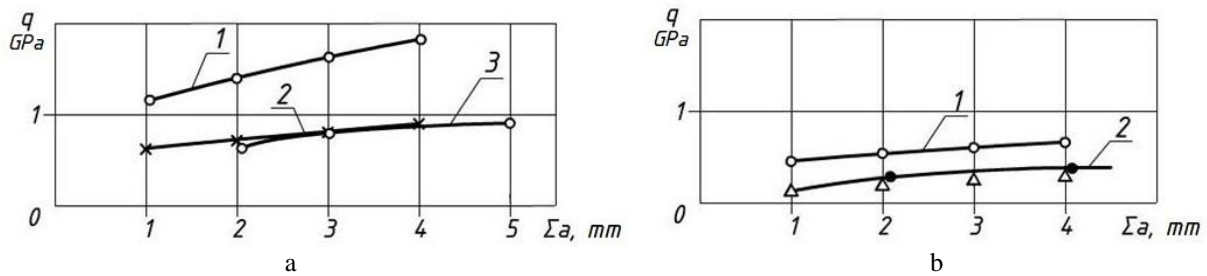
Fig. 10. The dependence of contact pressures on the total deformation during processing of billets: a) from steel 45: $t_0/d_0=0,136$, $a_0/d_0=0,015$: 1 – experiment, 2 – calculation according to (14), 3 – $a_0/d_0=0,03$ (experiment and calculation according to (14)); b) from steel 20: $t_0/d_0=0,65$, $a_0/d_0=0,015$: 1 – experiment, 2 – calculation according to (14) ($\triangle$); $a_0/d_0=0,03$ ($\bullet$) – calculation according to (14) and experiment

This is due to the mismatch of the conditions of deformation of the workpiece to the expansion pattern of the pipe with internal pressure. The following conclusion can be drawn from this: the theoretical calculation of contact pressure according to dependence (14) can be performed at contact pressures less than critical. The authors of [6] found that for steel 45 the critical contact pressures are 0.87 GPa, and for steel 20 – 0.78 GPa. At contact pressures equal to and above critical, their calculation must be carried out according to dependence (2) or according to the method described in [10]. The value of q depends on the modes of broaching and the size of the workpiece.

The wall thickness at which critical contact pressures appear depends on the tension on the element, the angle α, as well as the broaching pattern and is determined from the experimentally obtained relationships (15) and (16) for tensile and compression patterns, respectively [11]:

$$t_0/d_0 = 3,39\left(a/d_0\right)^{0,75} \cdot \alpha^{-\left(0,17+14,3\,a/d_0\right)}; \tag{15}$$

$$t_0/d_0 = \left(0,11+10,24\,a/d_0\right) \cdot \alpha^{-\left(0,17+11,6\,a/d_0\right)}. \tag{16}$$

They allow us to determine the conditions for using formula (14).

Consider the conditions of contact interaction with FANT. The process of contact interaction of the surface of the workpiece with rubbed material can be divided into two stages: 1) micro cutting of the starting material with the tips of microprotrusions; 2) adhesive adherence and seizure of particles formed as a result of

micro-cutting with the surface onto which transfer and subsequent micro-smoothing takes place. In [12], the FANT process was studied at the stage of micro cutting and the role of the latter in the formation of a high-quality antifriction coating. It was established that in order to intensify the FANT process due to micro-cutting, it is necessary to create a regular microrelief of a rough surface with a front cutting angle $\gamma \geq 0°$, and the angle $\gamma = 5°$ is the best option.

In the process, the cutting edge of the microroughness is intensely blunting, the rounding radius increases, which intensifies the next stage of the FANT process – the interaction of the back surface of the tool with the brass surface.

In the contact zone of the processed tool on the back surface there are high contact loads, approximately 3 times higher than the yield strength of brass and approximately equal to its HV hardness. Therefore, a layer of plastically hardened material is created on the back surface of the simulated micro-cutter (microroughness) and a skin of adhesively adhering brass appears (Fig. 11).

Fig. 11. The sticking of brass L63 on the rear surface of the cutter made of cast iron SCh20 when rubbing

This skin begins to play the role of a third body, that is, solid lubricant, preventing further blunting of the microroughness peaks, and a further increase in the radius of rounding of the cutting edge, which is confirmed by the experimental data shown in Fig. 12.
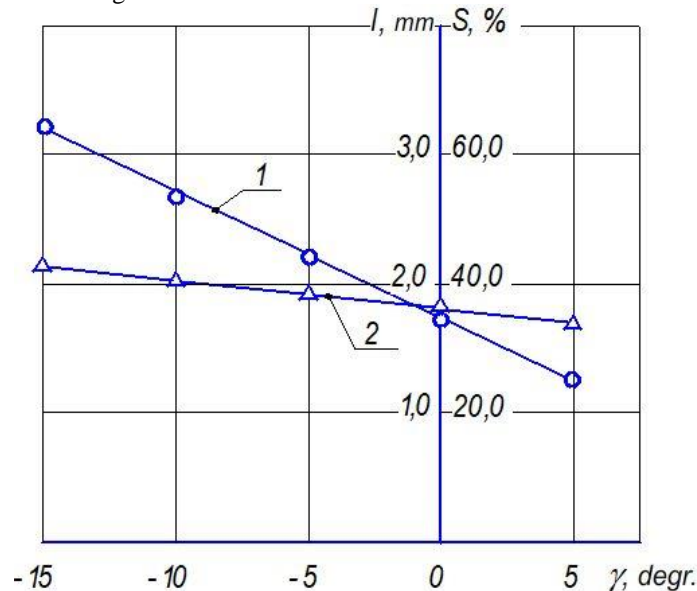
Fig. 12. Dependence of the brass coverage area of the contact surface *S* (curve 1) and the contact length *l* **(curve 2) on the angle *γ* when modeling micro-cutting with a SCh20 cast iron cutter with a brass surface L63**

So, the contact length along the rear face *l* depends on the angle *γ*, and with increasing *γ* the value of *l* increases (Fig. 12, curve 2), which is possibly due to the absence of micro-cutting at $\gamma < -5°$ and an increase tension on the radius section of the rear face. The adhesive interaction of the back surface of the cutter model with brass also increases with decreasing angle *γ* and reaches its maximum at $\gamma = -15°$. This is evidenced by curve 1 (Fig. 12), which shows the change in the percentage of the area covered with brass, referred to the total

contact area. With a further cycle of interaction, an adhesively fixed brass layer plays the role of a technological solid lubricant, and the process of applying an antifriction coating is significantly intensified. The coating layer becomes solid, which indicates an increase in its quality. Subsequently, the formed brass coating increases the quality parameters of the machined part, which improves its durability and is of practical importance.

Thus, a feature of the use of solid lubricants in FANT is that they perform a twofold function, namely, technological – as solid lubricant during processing and operational - increases the quality parameters of the processed part, and therefore its durability and wear resistance.

Our studies of the FANT process [13, 14] showed that the surface layer is significantly hardened. However, the depth of this hardening is negligible. This does not allow the use of the hardening effect when operating the part for a long time. Therefore, it is advisable to combine these two operations, which will allow you to get the processed surface with improved physical, mechanical and geometric characteristics. In this case, the DB will provide a substantial hardening of the surface layer by 30–40% and its bedding to a depth of 0.25 mm, and the FANT process will allow obtaining an equilibrium roughness that coincides with the operational roughness, regardless of the initial roughness.

Given the capabilities of the DB and FANT, the following conclusion can be drawn. To improve the operational properties of a part such as bushings and sleeves, it is necessary to build the technological process of processing according to the following scheme: the first operation is rough shaping using DB, which increases the utilization of metal, bringing the workpiece closer to the size of the part. When processing workpieces from hard-to-work materials, solid lubricant is used according to the recommendations received. In this operation, the bulk of the plastic deformation of the hole is carried out. The next operation is the final deforming broaching of the hole, during which the remainder of the plastic deformation is performed. The treated surface acquires the required macrorelief, roughness, the necessary hardening and the depth of its bedding. Then, given that the antifriction layer has an insignificant thickness $\delta < 5$ μm, we perform the FANT operation, which is the finish and can improve the performance of the treated surface. In this case, the necessary microrelief is provided, obtaining equilibrium roughness, as well as applying solid lubricant from antifriction material.

Conclusions

Analysis of the above material allows us to formulate the following conclusions:

- an analysis of the conditions for the effective use of solid lubricants was performed, and the features of contact phenomena during DB using solid lubricants were revealed.

- a functional relationship has been established between the altitude parameters of roughness and the relative contact pressure during processing using solid lubricants.

- a theoretical dependence has been obtained for calculating contact pressures and it has been established that the field of its effective application is limited by the condition whereby these pressures should not exceed their critical value.

- it was found that in the FANT process, solid lubricants can perform two functions: technological, like solid lubricant during surface treatment of a part, ensuring the quality of the coating, and operational. This improves the quality of machining parts, reduces the wear rate by 2–2.5 times, reduces the running-in time by 2 times and the friction coefficient by 20%.

- a new technological process has been proposed for processing holes of parts such as bushings and sleeves, which consists in combining DB as rough and finishing operations and the FANT finishing operation, which allows to improve the quality indicators of the machined part.

References

1. Rosenberg A.M., Rosenberg O.A., Posvyatenko E.K. et al. (1978). Calculation and design of carbide deforming broaches and broaching process. Academy of Sciences of the Ukrainian SSR, ISM, Kiev, Ukraine: Nauk. dumka, p. 256. [in Russian].

2. Shepelenko I. (2020). The study of surface roughness in the process of finishing anti-friction non-abrasive treatment. Problems of Tribology, V. 25, 1/95, pp. 34−40. [in English]. https://doi.org/10.31891/2079-1372-2020-95-1-34-40.

3. Rosenberg A.M., Rosenberg O.A., Gritsenko E.I. et al. (1977). The quality of the surface treated by deforming broaching. Kyiv, Ukraine: Nauk. dumka, p. 188. [in Russian].

4. Shepelenko I.V., Posviatenko E.K., Cherkun V.V. (2019). The mechanism of formation of anti-friction coatings by employing friction-mechanical method. Problems of Tribology, №1, pp. 35−39. [English]. https://doi.org/10.31891/2079-1372-2019-91-1-35-39.

5. Rosenberg O.A., Pashchenko E.A., Sheikin S.E. et al. (2007). On the selection of technological lubricants for deforming broaching of parts made of titanium alloys. Technological systems, vol. 2 (38), pp. 27–32. [in Russian].

6. Rosenberg A.M. and Rosenberg O.A. (1990). Mechanics of plastic deformation in cutting and deformation broaching processes, P.R. Rodin., Ed. Kiev, Ukraine: Nauk. dumka, p. 320. [in Russian].

7. Nemirovsky Ya.B., Posyavtenko E.K., Rostotsky I.Yu. et al. (2019). Features of contact phenomena during deformation broaching using solid lubricants. News of the National Technical University "KhPI". Ser.: Technologies in mechanical engineering: collection of scientific works. Kharkiv, Ukraine: NTU "KhPI", vol. 19 (1344), pp. 61–68. [in Russian]. DOI: 10.20998 / 2079-004x.2019.1.011.

8. Balaganskaya E.A., Golodenko B.A., Nemirovsky Ya.B. et al. (2001). Mathematical modeling of deforming broaching process. Ministry of Education of the Russian Federation, Voronezh state. technol. Acad, Voronezh, Russia: Voronezh state. technol. Acad., p. 194. [in Russian].

9. Tsekhanov Yu.A. and Sheikin S.E. (2001). The mechanics of forming blanks during deformation broaching. Ministry of Education of the Russian Federation, Voronezh state. technol. Acad, Voronezh, Russia: Voronezh state. technol. Acad., p. 200. [in Russian].

10. Tsekhanov Yu.A., Rosenberg O.A. and Del G.D. (1976). Stress state during deformation broaching of a thick-walled pipe. University proceedings: Mechanical engineering, no. 5, pp. 153–156. [in Russian].

11. Nemirovsky Ya.B., Tsekhanov Yu.A. and Balaganskaya E.A. (2005). Investigation of the change in the dimensions of hollow axisymmetric blanks when they are expanded by deforming broaching. Forging and stamping. Processing of materials by pressure, no. 2, pp. 12–15. [in Russian].

12. Shepelenko I., Tsekhanov Y., Nemyrovskyi Y., Posviatenko E. (2020). Power Parameters of Micro-cutting During Finishing Anti-friction Non-abrasive Treatment. In: Karabegović I. (eds) New Technologies, Development and Application III. NT 2020. Lecture Notes in Networks and Systems, vol 128. Springer, Cham, pp. 194−201. [in English]. https://doi.org/10.1007/978-3-030-46817-0_22.

13. Shepelenko I. (2021). Technological factors influence on the antifriction coatings quality. Problems of Tribology, 26(2/100), pp.50−57. https://doi.org/https://doi.org/10.31891/2079-1372-2021-100-2-50-57.

14. Shepelenko I., Tsekhanov Y., Nemyrovskyi Y., Posviatenko E. (2020). Improving the Efficiency of Antifriction Coatings by Means of Finishing the Antifriction Non-abrasive Treatment. In: Tonkonogyi V. et al. (eds) Advanced Manufacturing Processes. InterPartner 2019. Lecture Notes in Mechanical Engineering, Springer, Cham, pp. 289−298. [in English]. https://doi.org/10.1007/978-3-030-40724-7_30.

Немировський Я.Б., Шепеленко І.В., Посвятенко Е.К., Черновол М.І, Златопольський Ф.Й.

Створення прогресивних процесів обробки отворів на основі дослідження контактних явищ при деформуючому протягуванні та фінішній антифрикційній безабразивній обробці в умовах різних технологічних середовищ

Виконано дослідження впливу технологічного середовища (ТС) на контактні явища і параметри якості обробленої поверхні при використанні операцій деформуючого протягування (ДПР) і фінішної антифрикційної безабразивної обробки (ФАБО). Описано умови застосування рідинних мастил при ДПР. Розроблені нові методики вивчення контактної взаємодії при ДПР з використанням твердих мастил. Доведено необхідність застосування твердих мастил при обробці виробів з важкооброблюваних матеріалів і сплавів. Досліджено зміну висотних параметрів шорсткості поверхневого шару, а також контактних тисків при використанні твердих мастил. Розкрито особливості контактних явищ при ДПР з використанням твердих мастил. Встановлено функціональний зв'язок між висотними параметрами шорсткості і відносним контактним тиском при ДПР. Показано, що тверді мастила при ФАБО виконують двояку функцію, а саме – технологічну, як тверде мастило при обробці, і експлуатаційну – покращують параметри якості оброблених деталей. Поєднання операцій ДПР і ФАБО дозволило розробити новий технологічний процес обробки отворів деталей типу втулок з покращеними експлуатаційними властивостями.

Ключові слова: деформуюче протягування, фінішна антифрикційна безабразивна обробка, технологічне середовище, тверді мастила, рідкі мастила, контактні явища, шорсткість, зміцнення, якість обробленої поверхні

Structure research of nanoscaled silicon carbide detonation coatings of tribotechnical application

A.H. Dovhal*, L.B. Pryimak

National Aviation University, Ukraine
*E-mail: andrii.dovhal@npp.nau.edu.ua

Abstract

Presented studies are related to the spheres of wearproof coating development. World wear resistance improvement technology experience has accumulated a huge amount of statistical material on the failure due to increased level of parts wear. That is why the issue of research and improvement of anti-wear properties of machine elements is one the components when considering the priority directions of ensuring the reliability of operation motor vehicles and friction units. The SiC coating has been deposited on the medium carbon steel using detonation deposition. It has been established that it is very sensible for modes of coating deposition and different physical and chemical phenomenon have been detected. The structure of the obtained coating has been thoroughly researched on the electronic microscope. The obtained coating has been developed for testing on the friction bench modeling the friction process that is taking place in the couple of main and rod journals of internal combustion engines. The coating has also the corrosion protection. The new magnet modified method of detonation coating deposition has been tested for deposition of nanoscaled coating on mild carbon steel. The optimal modes of the magnet modified coating deposition for silicon carbide powders batch mixture from the viewpoint of structure formation have been detected.

Key words: wear, wear resistance, coating, adhesion, nanoscaled coating, detonation coating deposition.

Introduction

Means of powered equipment and automated equipment of airports are equipped with power plants as energy sources for technological operations on ground handling of aircraft.As such power plants on aircraft ground equipment electric motors, gas turbine engines, internal combustion engines can be used. Operating experience has shown that internal combustion engines have the highest energy efficiency and safety, because electric engines have low starting torques, and gas turbine engines are designed for operation at altitudes of the cruising flight of aircraft and at ground level have low fuel efficiency and stability. Thus, an internal combustion engine (ICE), which can be either fuel or diesel, is the main power unit of aviation ground equipment. The lifetime of the ICE can be improved by wearproof coatings

Review of the latest research

Silicon carbide materials has attracted scientific attention of researchers from many countries. So in the works [1,2] the features of structure formation of ceramic materials of the constituents SiC–C with oxides Al_2O_3 and Y_2O_3, as well as titanium hydride under free sintering and hot pressing are considered. Effect of ceramics dispersion strengthening by nanoscaled particles of silicon carbide and titanium carbide has been established. In the publication [3] micromechanical properties of composition materials made of SiC, acquired by activated sintering has been researhed.

Authors of the work [4] has researched high temperature, corrosion resistant, mechanical properties of nanoporous structures made of silicon carbide, which was intended for eletrical and technical application.

In the publication [5], researchers had been learning oxidation resistance of composites of the constituents $SiC–TiB_2–B_4C$, acquired by hot pressing at temperature $2150^{\circ}C$, which have improved physical and mechanical properties. The samples porosity made less than 8%.

The structure formation of ceramics made of constituents $SiC–TiB_2$, where the silicon carbide was the composite major, was researched in details in warks [6, 7]. In particular, optimal technological modes of ceramic materials acquisition concerning the bending strength, crack- and wear resistance had been determined.

Attempts of properties optimization of self-bonded silicon carbide are undergoing nowadays. So, in the works [8] different from conventiona technologies technique of high-dense ceramic products on the basis of self-bonded silicon carbide, which blankpieces are made by the method of slip casting of thermal plastics under the pressure had been developed. The content of multifractional batch mixture and amount of temporary bonds with rheological properties, that provide the high density of products, has been justified.

One of the prominent scientific direction of silicon carbide application is the nanostructured composites and coatings. So, the researchers of article [9] the microstructure and properties of alumina-silicon carbide nanocomposites fabricated by pressureless sintering and post hot-isostatic pressing have been investigated. There the grain growth of Al_2O_3 matrix had been eliminated due to the grain growth inhibition by nano-sized SiC particles (about 150-250 nm). It improved the fracture strength of acquired composite.

In the scientific paper [10] the synthesis of SiO_2 and SiC micro/nanostructures of nanowires (about 100 nm) and nanorod (about 50-200 nm) shapes had been held by thermal evaporation method (CVD).The scientific findings were intended for core-shell coaxial nanocables.

The researchers of work [11] have acquired nanocomposites of C-SiC content. The composite is the carbon fibers covered by SiC nanocoatings. The material was intended for radiation resistant fabric concerning the fabric strength. And the scientists of paper [12] had acquired the nanostructured coatings of silicon carbide by novel method. the thickness of the coating was about 2-9 nm and the coatings were suitable to application in metallurgy, nuclear power engineering, microelectronics and high-temperature stoves.

In order to create the metal ceramic materials, effect of iron millings on the technological modes of acquisition of ceramic materials of the system $SiC-Al_2O_3$, their structure and properties have been researched. Tribological performances of acquired materials have been tested. Wear rate of these materials together with the steel counterbody is 3,8 microns per kilometer, and together with ceramic counterbody it is 4,1 microns per kilometer. In both cases oxidative wear mechanism takes place [13].

As have already been mentioned the specific way acqured batch mixture of $SiC-Al_2O_3$ content was used for acquisition of wearproff composited [13] the same batch mixture was applied for coating deposition by detonation method modified by magnetic field [14]. So it had been established on direct poalrity of coil magnet the microparticles of silicon carbide and alumina had been deposited on the substrate. The coating had demonstrated not only high wear resistanse [14], but also high wear resistanse at elevated temperatures [15]. The last metioned composition had been widely used for coating deposition by different technique and several results had been acquired. And changing the polarity of coil magnet only the nanosized particles of silicon carbide had been deposited on the substrate to which investigation this scientific paper is devoted.

Research aim

Scientific development of nanoscaled composition coatings for crank shaft journal of internal combustion engines of aircraft ground support equipment.

Originating from the aim of article papper the following tasks of research were preset:

1. Outlook of the reference sources on the topic of the article paper and on its basis the topic urgency had been confirmed.

2. Algorythm development of the complex scientific research, selection of the necessary laboratory equipment for coating deposition and tribotechnical research.

3. Preparation of the coating batch mixture, manufacture of the specimens and deposition of the coating.

4. Research of the coating structure and its description.

Research methodology

For study of interactions between properties of coatings with their phase composition and structure, and also an external factors influence the choice of research methods has the great importance. The receiving of reliable results of research in this work is provided with the use of modern equipment and devices, approved methodologies, necessary productivity of experiments, by careful treatment of specimens before and after the experiment, strict adherence of order of experiment carrying out.

For receiving a charge of carbide silica ceramics with aluminum oxide admixtures, the starting powders were used: silicon carbide grade 64C (ГОСТ 26 327-84) with an average size of 45-55 µm, aluminum oxide (ТУ 6-09-03-350-73) with particles of average size 45 -50 microns.

The chemical composition of the starting powders is given in Table 1.

Table 1

Results of analysis of initial powders in masses. %

Powder name	Al	Si	Mg	Fe	Ni	Cr	Ti	Ca	Zr	Ag	Cu
SiC	10^{-3}	major.	10^{-4}	10^{-3}	-	-	-	10^{-4}	-	-	-
Al_2O_3	major.	-	10^{-3}	>0,1	>1	0,01	-	-	-	10^{-4}	10^{-3}

An integral operation for the formation of composite materials from the initial powders is their mutual mixing and grinding.

To obtain a SiC-based ceramic charge with Al_2O_3 admixture, the powder components in the appropriate proportions were mixed with simultaneous grinding for 5 hours in the laboratory planetary mill Sand-1 in an alcohol medium.

In this case, the rotational speed was 648 rpm, the drum rotation frequency was 1620 rpm. To prepare the charge, laminated aluminum oxide and steel drums of 340 cm^3 and steel grinding media from steel of ШХ15 with a diameter of 10-15 mm and SiC-Al_2O_3 ceramics grinding media were used.

The ratio of the mass of the charge to the mass of grinding media is 1: 3. After grinding, the charge was dried and sifted. The granulometric composition of the resulting mixtures after milling was determined in aqueous media on a laser microanalyzer "SK Lazer Micron Sizer PRO 7000"

Coatings in the work was applied by the detonation method on the installation described below. The "Dnepr-3M" (table. 2.) detonation-gas installation is intended for coating metal powders, hard alloys, ceramics and composite materials on the surfaces of machine parts, devices, apparatuses and tools during their manufacture, as well as reconditioning.

According to their purpose, coatings can be wear-resistant, frictional, antifriction, corrosion-resistant, heat-resistant, electrically conductive, electrical insulating, etc.

Table 2

Technical data and specifications

#	Specification	Value
1.	Working gases	oxygen, acetylene, nitrogen, compressed air.
2.	Pressure of working gases, MPa - oxygen - acetylene - nitrogen - air	 0,2 0,14 0,4 0,4
3.	The consumption of working gases per shot, m^3 - oxygen - acetylene - nitrogen - air	 $27*10^{-5}$ $23*10^{-5}$ $5*10^{-4}$ $5*10^{-4}$
4.	Powder consumption per shot, m^3	$1.5 * 10^{-8}$
5.	Water consumption, m^2/s	$3 *10^{-5}$
6.	Frequency of fire, Hz	1-10
7.	The diameter of the booster section of the barrel, m	0,022
8.	Coating thickness per shot, microns	5-20
9.	Productivity at a coating thickness of 10 microns, m^3/h	0.8-3.5
10.	Installation	remote control
11.	Overall dimensions, m - a gun - gas remote - control panel	 1,8*0,6*1,1 1.8*0.63*0.61 0.5*0.3*0.22
12.	Mains supply: - frequency, Hz - voltage, V - power consumption, VA	 50-60 220 200
13.	Sound pressure level, dB (A)	140
14.	Relative humidity of air,%	40-75

For getting such compositions the following conditions have been determined. Working gas is a mixture of C_2H_2-O_2. Consumption of C_2H_2 is 30 points, O_2 is 70 points. Powder supply is 30 points. Blowing the barrel at the end of the cycle is air. Scavange gas is air. Shots speed is 4 shots per second. The diameter of the spot is 22

mm. Spraying distance is170 mm. For research of the effect of a constant magnetic field a cylindrical solenoid at the output has been used, which provided the magnetic field strength H = 150 A/m. For deposition of nanoparticles of the coating the reverse magnetic field had been applied during the shots (fig. 1.).
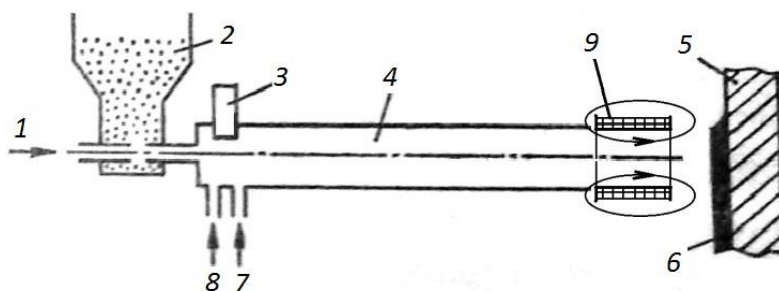
Fig. 1. Magnet modified detonation installation simplified diagram:
1 – carrying gas; 2 – charge bin; 3 – spark plug; 4 – gun tube of plant; 5 – substrate (specimen); 6 – coating; 7 – flushing gas between shots; 8 – combustible gas; 9 – solenoid coil (direct polarity when it is toward substrate, reverse polarity when it is backward from substrate.).

For research of structure and phase composition of the structure and phase storage of ceramic on the basis (SiC-Al$_2$O$_3$), and also their friction surfaces was conducted by metallography, X-ray-phase (RPA) and micro X-ray spectral (MRSA) analyses. The metallography analysis of the investigated materials was carried out on the optical microscopes МИМ-8 and «НЕОФОТ».

Radio-phase analysis of specimens was executed on the X-ray diffractometers ДРОН-2.0 (see fig. 2.5.1.) in Cu$_{k\alpha}$ -radiation. Micro X-ray spectral analysis and receving of electronic images of surfaces was conducted on electron microscope РЭМ-106И

Research results and discussion

Composite coatings SIAL-M32 (SiC-Al$_2$O$_3$ – 32 hours milling) has a high wear resistance in a compact form due to the formation of films of complex oxide systems SiO$_2$, Al$_2$O$_3$ on the surface of the friction, which, as a result of the dissolution of iron oxide, form secondary structures. In the process of grinding in the steel vessels, steel milling bodies in the batch mixture form pieces of iron, which have a size from 250-400 nm (fig. 2.). Large particles can be easily removed by magnetic clean. Nanoscale particles cannot be removed from the charge with magnetic clean. Particles of this size are evenly distributed in the batch mixture without bundle and segregation, and their size is not sufficient to absorb larger particles of silicon carbide during the formation of silicides. The presence in the batch mixture of particles of iron millings should intensify the process of coating deposition using the magnetic field flux (double sided).

a)   b)
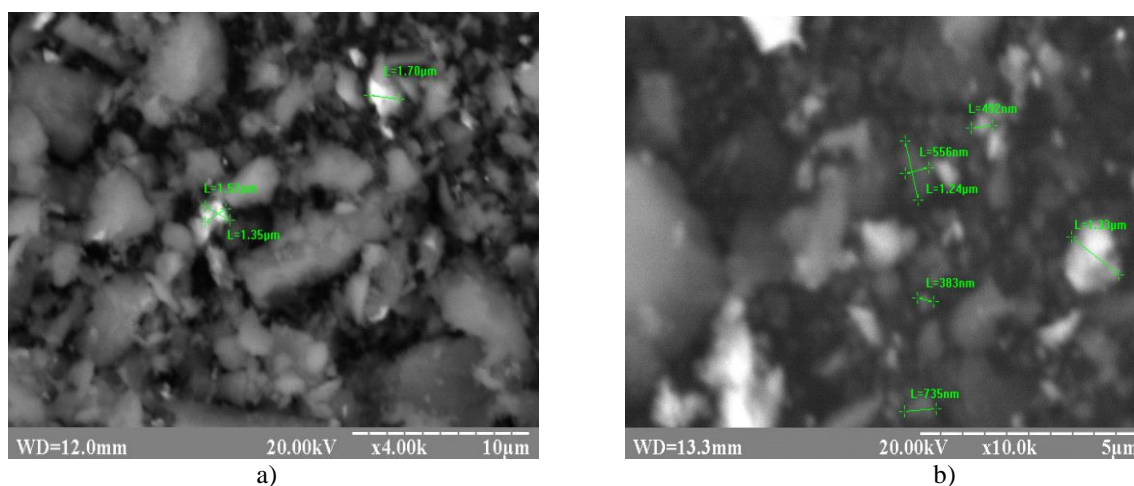
Fig. 2. SEM image of SiC-Al$_2$O$_3$ composite powders after mixing and grinding in steel vessels by steel milling bodies for 32 hours; a – 4000 zoom; b – 10,000 zoom. (250-400 nm particles are detected).

In order to investigate the formation of a grinding of iron in the process of grinding of the components of SiC-Al$_2$O$_3$ batch mixture, the kinetics of the change in the content of particles of iron millings was determined experimentally, depending on the duration of grinding. As a result of the grinding of SiC-Al$_2$O$_3$ batch mixture powders with varying the duration of process, the following regularities were established (table 3.).

Table 3

Powders content of SiC-50% Al₂O₃ composition depending on the time of grinding

Grinding time, h	1	2	4	8	16	32
Material designation *	SIAL M1	SIAL M2	SIAL M4	SIAL M8	SIAL M16	SIAL M32
Average size of charge particles, µm	28,7	14,9	6,8	4,8	2,2	2,1
The content of iron particles,% wt	1,5	3,4	6,8	10,9	16,3	19,3

The phase content of the milled batch mixture is shown on fig. 3.

Fig. 3. X-ray diagram of powder SIAL-M32 composition.

The comprehensive detonation coating research is on the fig. 4. There the zoom kinetics and general imagination of the coating surface roughness and pattern is shown.

a)

b)

c)

d)

e)
f)
Fig. 4. SEM image of nanoscaled coating of different zoom of the same area: a) 550; b) 1000; c) 2000; d) 4000; e) 8000; f) 20000

While milling the silicon carbide the nanosized particles can be obtained [4]. During the milling the metal particles are acquired in the batch mixture and they are affecing crucially on the coating formation in the magnetic fields. In particular, applying the magnetic field the microsized coatings are acquired and well invrstigated [9]. This coating is acquired by the technoque described in paper [9,10] on the direct flux (from S to N) of the magnetic field, merely, enspeeding the metal particles to the substrate. Changing the polarity of the magnetic flux (from N to S) permanent magnet coil the microscopic particles are retained in the detonation shots stream and only nanosized particles of the batch mixture are reaching to the surface and depositing there (fig. 4. and 5.).
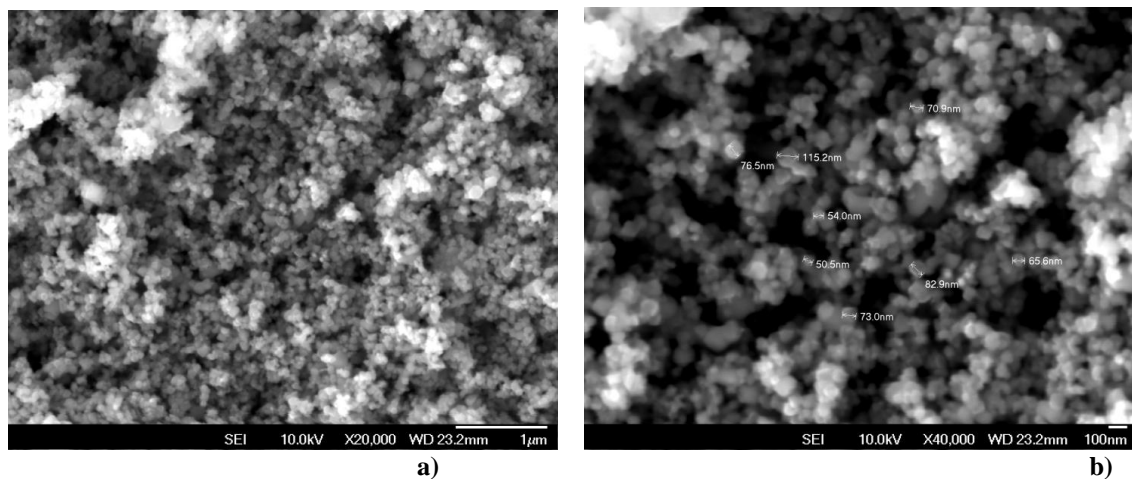
a)
b)
Fig. 5. SEM-images of the Top Raw View of the Nanoscaled Detonation Coatings of SiC on the Specimens of Steel 45 for Rolling-Sliding Friction: a) 20 000 zoom; b) 40 000 zoom

The scanning electronic image (SEM) is supplied on the fig 5. Within the 20 000 electronoc zoon (fig. 5. a) the sirface of the coating appeared to be very rough and containing the nanosized particles. Within the 40 000 electronoc zoon (fig. 5. b) the particles of 70,9, 115,2, 76,5, 54,0, 50,5, 65,6, 82,9 and 73,0 nanometers are acquired.

The content of the nanoparticles is about 85% of SiC, 10% of Al_2O_3 and 5% of Fe_2C. No metalic particles were detected in the coating content. Coating thickness was about 50-60 micrometers.

Conclusions

Using the gas detonation deposition from the batch mixture which contanis the the silicon carbide and aluminium oxide particles, which have a size from 250-400 with the steel millings, on the direct polarity the fine grained microstructure is acquired and on the reverse polarity the nanostructure the particles of 70,9, 115,2, 76,5, 54,0, 50,5, 65,6, 82,9 and 73,0 nanometers had been acquired.

References

1. Гадзыра Н. Ф., Давыдчук Н. К., Гнесин Г. Г. Структурообразование композиционной керамики на основе сверхстехиометрического карбида кремния при свободном спекании и горячем прессовании. Порошковая металлургия. 2009. № 5/6. С. 81–87.

2. Gadzira M., Gnesin G., Mykhaylyk O. et al. Synthesis and Structural peculiarities of Nonstoichiometric □-SiC. Diamonds and Related Materials. 1998. N 7. P. 1466–1470.

3. Орданьян С. С., Арцутанов Н. Ю., Чупов В. Д. Активированное спекание керамики на основе SiC и ее механические свойства. Огнеупоры и техническая керамика. 2000. № 11. С. 8-11.

4. Уваров В. И., Боровинская И. П., Закоржевский В. В., Малеванная И. Г. Градиентные нанопористые структуры на основе карбида кремния и нитрида бора в процессах самораспространяющегося высокотемпературного синтеза. Порошковая металлургия. 2010. № 7/8. С. 122–125.

5. Швец В. А., Лавренко В. А., Субботин В. И. и др. Особенности анодного окисления композитов системы SiC–TiB2–B4C в 3–%–ном растворе NaCl Порошковая металлургия. 2010. № 11/12. С. 107–113.

6. Grigoriev O. N., Subbotin V. I., Kovalchuk V. N. Structure and properties of SiC-TiB2 ceramics. Journal of Materials Processing and Manufacturing Science. 1998. Vol. 7, N 1. P. 99-110.

7. Grigoriev O. N., Subbotin V. I., Gogotsi Yu. G. et al. Development and properties of SiC-B4C-MeB2 ceramics. Journal of Materials Processing and Manufacturing Science. 2000. N 5/6. P. 29-42.

8. Майстренко А. Л., Кулич В. Г., Ткач В. Н. Формирование высокоплотной структуры самосвязанного карбида кремния. Сверхтвердые материалы. 2009. № 1. С. 18-35.

9. Young-Keun JEONG, Koichi NIIHARA Microstructure and properties of alumina-silicon carbide nanocomposites fabricated by pressureless sintering and post hot-isostatic pressing. Trans. Nonferrous Met. Soc. China 21(2011) s1−s6.

10. G. Zhu, X.P. Zou, J. Cheng, M. F. Wang, Y. Su Synthesis and Characterization of SiO$_2$ and SiC micro/nanostructures. Archives of metallurgy and materials. Volume 53. 2008 Issue 3. P 727-734.

11. П.А. Александров, Н.Е. Белова, К.Д. Демаков, Л.М. Иванова, Ю.Ю. Кузнецов, Н.В. Степанов, С.Г. Шемардов Получение и структурные исследования нанокомпозита на основе С—SiC. Вопросы атомной науки и техники. Сер. Термоядерный синтез, 2007, вып. 1, с. 68—75.

12. К. Н. Филонов, В. Н. Курлов, Н. В. Классен, Е. А. Кудренко, Э. А. Штейнман Особенности свойств наноструктурированных карбидокремниевых пленок и покрытий, полученных новым способом. Известия РАН. Серия физическая, 2009, том 73, № 10, с. 1457–1459.

13. A. P. Umanskii, A. G. Dovgal', V. I. Subbotin, I. I. Timofeeva, T. V. Mosina and E. N. Polyarys Effect of grinding time on the structure and wear resistance of SiC–Al$_2$O$_3$ceramics // Powder Metallurgy and Metal Ceramics, Vol. 52, Nos. 3-4, July, 2013- pp. 189-196.

14. A. Dovgal, L. Pryimak, I. Trofimov A Modified Method of Applying Detonation-Sprayed Composite Coatings by a Magnetic Field.// Eastern-European Journal of Enterprise Technologies.– Volume 6/5 (84). – 2016. – P. 33-38.

15. L. Pryimak, A. Dovgal, Ye. Puhachevska Analysis of Structure and Tribitechnical Properties of Plasma Carbide-Silicon Coatings Under Conditions of Elevated Temperatures // Eastern-European Journal of Enterprise Technologies. – Volume 1/5 (85). – 2017. – P. 46-53.

Довгаль А.Г., Приймак Л.Б. Дослідження структури нанорозмірних карбідокремнієвих покриттів триботехнічного призначення

Представлене дослідження пов'язане з розробкою зносостійких покриттів. Світовий досвід підвищення зносостійкості накопичив велику кількість статистичного матеріалу відмов деталей через зношування. Тому питання дослідження та покращення зносостійких властивостей деталей машин є одним із пріоритетних компонентів при розгляді напрямків забезпечення надійності експлуатації транспортних засобів та вузлів тертя. Покриття із SiC булинаннесені на середньовуглецеву сталь детонаційним напиленням. Бкло встановлено, що воно дуже чутливе до режимів нанесення покриттів та бкли виявлені різні фізичні та хімічні явища. Структура отриманих покриттів була вивчена методами електронної мікроскопії. Отримані покриття були розроблені для подальших триботехнічних випробувань на машинах тертя, що моделюють процеси тертя, що мають місце у у парах корінних та шатунних шийок двигунів внутрішнього згоряння. Покриття мають також і коррозійно захисні властивості. Було випробувано новий магнітно модифікований метод детонаційного напилення нанорозмірних покриттів на середньовуглецеву сталь. Було визначено оптимальні режими магнітномодифікованого нанесення покриттів для карбідокремнієвої шихти стосовно структури

Ключові слова: знос, зносостікість, покриття, адгезія, нанорозмірне покриття, детонаційне нанесення покриттів

Influence of heat treatment on tribocorrosion properties of Ni-B composite coatings

M. Khoma[1], R. Mardarevych[1], V. Vynar[1], Ch. Vasyliv[1], Yu. Kovalchyk[2]

[1]*Karpenko Physico-Mechanical Institute of NAS of Ukraine*
[2]*Lviv National Agrarian University*
E-mail:vynar.va@gmail.com

Abstract

Various surface protection technologies, in particular, electrochemical, are used to increase the wear and corrosion resistance of steels and alloys. Composite electrochemical coatings (CEC) technology is more promising than "pure" galvanic coatings. Application of CEC increases the wear, corrosion and fatigue failure resistance of metals. Nickel often is chosen as a CEC matrix because it easily forms uniformly filled defect-free composite structures with many particles of the dispersed phase (DP).

Physical and mechanical properties of metal coatings determine practical application of such composition. The characteristics of nickel-based CEC are: high hardness and strength, significant corrosion resistance in atmospheric environment, as well as in alkali and mild acidy environments. An effective composition coating with tribological designation can be CEC Ni-B, received in the process of electrolysis from suspension of amorphous boron in nickel electrolyte. A new composite structure of matrix filled type Ni-Ni$_3$B is formed after heat treatment. Composition and structure of coating is determined by regimes of diffusion annealing. Ni-B coatings increase wear resistance of steel in chlorine-based environments. The influence of low-temperature thermal treatment of Ni-B CEC on steel 09Mn2Si on their tribocorrosion behavior is investigated. It is shown that the structural factor has a decisive influence on the efficiency of such friction pairs. The CEC has the least wear and the most positive compromise electrode potential after vacuum annealing at 450°C, when the initial stage of solid-phase interaction of coating components with the formation of Ni-Ni$_3$B occurs.

Key words: composition electrochemical coating, low temperature thermal treatment, tribocorrosion, friction coefficient.

Introduction

Various surface protection technologies, in particular, electrochemical, are used to increase the wear and corrosion resistance of steels and alloys. Composite electrochemical coatings (CEC) technology is more promising than "pure" galvanic coatings. Application of CEC increases the wear, corrosion and fatigue failure resistance of metals. Nickel often is chosen as a CEC matrix because it easily forms uniformly filled defect-free composite structures with many particles of the dispersed phase (DP). Nickel-Boron CEC is an effective composite coating for tribotechnical application. It is obtained by electrolysis of a suspension "amorphous boron - the nickel electrolyte" [1]. A new composite structure Ni-Ni3B of matrix-filled type is formed in the process of subsequent thermal treatment (TT) [3,4]. The composition and structure of composite are determined by the diffusion annealing parameters. The wear resistance of steels with Ni-B CEC after TT at 900… 1000°C increases by 1.5… 3 times compared to solid galvanic chromium or diffusion boride coatings [4]. It is due to formation of Ni3B boride grains with high microhardness (9… 12.5 GPa). It is shown, that Ni-B CEC in the initial state also increase the wear resistance of steels under conditions of corrosion and mechanical wear in chloride-containing environments, but the effect is smaller due to increased electrochemical activity of solutions [5,6].

Ni-B coatings after low-temperature TT can also be promising for surface protection of alloys [7, 8]. Therefore, the aim of the work was to investigate the influence of low-temperature thermal treatment parameters on the structure, hardness and tribocorrosive behavior of Ni-B CEC on steel 09Mn2Si.

Materials and research methods

Preliminary preparation of steel 09Mn2Si samples was performed according to the requirements [9]. CEC Ni-B was precipitated from a suspension of amorphous boron in the sulfate chloride electrolyte of nickel plating at a cathode current density of 5 A/dm2, temperature 40...45°C and hydrodynamic electrolysis regimes, recommended in [10]. Sodium dodecyl sulfate was used as an anti-pitting agent and suspension stabilizer. The thickness of the coatings was 45...50 µm, and the boron content in them was 4.8 ... 5.2 wt.%. Samples with coatings were annealed in vacuum at temperatures of 200, 300 and 450°C for 2 h. X-ray diffraction analysis of the coatings was performed on a DRON-3M diffractometer in Cu-Kα radiation. The parameters of the fine structure (the size of the coherent scattering regions, the magnitude of the microdeformation and the dislocation density) were calculated by the method of approximation of the expansion of the diffraction line profile (111) and (222) [11]. Electron microscopic studies of the coatings were performed on a scanning electron microscope EVO-40XVP (Carl Zeiss) with an X-ray microanalysis system INCA Energy. The microhardness of the coatings was determined on a microhardness tester PMT-3M. Tribocorrosion studies of coated samples were performed according to the scheme rotating disk–counter-body in the form of a segment (block) on the SMC-2 test rig at a contact load P = 280 N. The sliding speed was 0.67 m/s, the test time was 1 h. Coatings were applied to the cylindrical surface of the "disk" specimens made of steel 09Mn2Si. Counter body - "pad" of steel ШХ 15 (100Cr6), HRC 60…63. Electro-insulating coating was applied to the non-working surfaces of the disks. Working environment - glycerin with the addition of 10% NaCl (pH = 5.9). The change in the electrode potential of the friction pairs was measured using a chlorine-silver reference electrode. Measurements of the friction moment were performed with a non-contact inductive sensor mounted on the shaft of the installation. Electrical signals (mV), from the measurement of these parameters, were transmitted to an analog-digital device and simultaneously recorded by a personal computer with a recording step of 0.2 s. The wear of the samples after the tests was determined gravimetrically with an precision $\pm$ 0.0001 g.

Results and discussion

Structure and microhardness of CEC after TT. Thermal treatment significantly changes the properties of CEC. TT is carried out to increase adhesion to the substrate material, to do partial dehydration and to reduce the level of residual stresses. TT is even more effective for CEC Ni-B, because annealing is accompanied by diffusion interaction of components with partial or complete dissolution of boron particles in the matrix and the formation of solid solution and nickel borides. In addition, the newly formed structural components occupy a larger volume in the matrix, than the dispersed particles in the initial state. Therefore, TT is an additional factor, that increases the content of the reinforcing phase in the coating. Electrochemical deposition without TT does not provide optimal volumetric filling of the matrix by the dispersed phase (30… 50%) to ensure high tribotechnical characteristics. CEC Ni-B, obtained by the above modes of electrolysis, have significant filling of the matrix with boron particles and their uniform distribution in the layer (Fig. 1a). Only diffraction lines of nickel are presented on the coating diffraction pattern. The absence of boron lines - indicates the amorphous state of its structure (Fig. 1 b).

The dislocation structure of the electrodeposited coating is formed in the presence of inclusions. Stress fields of inclusions are an effective barrier to dislocation displacement and cause higher (50… 60%) microhardness of CEC, compared to "pure" nickel coating (Fig. 2). The hardness is affected by effect of dispersed hardening of the matrix by boron particles. The hardness also depends on crystal structure, due to the new conditions of crystallization in the electrolyte suspension. The stress state of the CEC is evidenced by the results of diffractometric studies of fine crystal structure parameters. The magnitude of lattice microdeformation and dislocation density increase 1.6 and 4 times, respectively, compared to values for galvanic nickel, and substructure block sizes decrease from 54… 57 to 30 … 32 nm.

Low-temperature thermal treatment of nickel and composite coatings causes similar structural changes. Kinetics of these process is different, therefore development and the degree of conversion at certain temperatures occur differently. A polygonized structure with 50… 70% higher microhardness is formed after the heating of the nickel coating at 200… 230°C, due to the migration of point and linear defects to the grain and subgrain boundaries. The lattice microdeformation decreases after annealing at a temperature of 300°C, due to annihilation of dislocation, and the size of subgrain blocks increases to 94 nm, which affects the decrease in microhardness. When the heating temperature exceeds 360°C, recrystallization transformations start in nickel. Corresponding changes of fine structure cause a significant decrease in hardness [11,12].

The inclusion of boron particles in the CEC slows down the relaxation processes at the stage of pre-recrystallization annealing at 200… 300°C. Slight change in the parameters of the fine structure is observed. In

contrast to the nickel coating, the size of the substructure blocks increases to only 33… 34 nm, the microdeformation of the lattice decreases from $1.5 \cdot 10^{-3}$ to $1.2 \cdot 10^{-3}$, and the density of dislocations - from $0.29 \cdot 10^{12}$ to $0.24 \cdot 10^{12}$ sm^{-2} after annealing of the CEC at 300°C. Heating within 400… 450°C determines the initial stage of solid-phase interaction of components, which is confirmed by the results of differential-thermal [12] and X-ray diffraction methods of analysis (Fig. 1 d). The development of the interaction between boron particles and the nickel matrix, which is carried out by the type of reaction diffusion, leads to a marked change in the microstructure of the coating (Fig. 1 c).
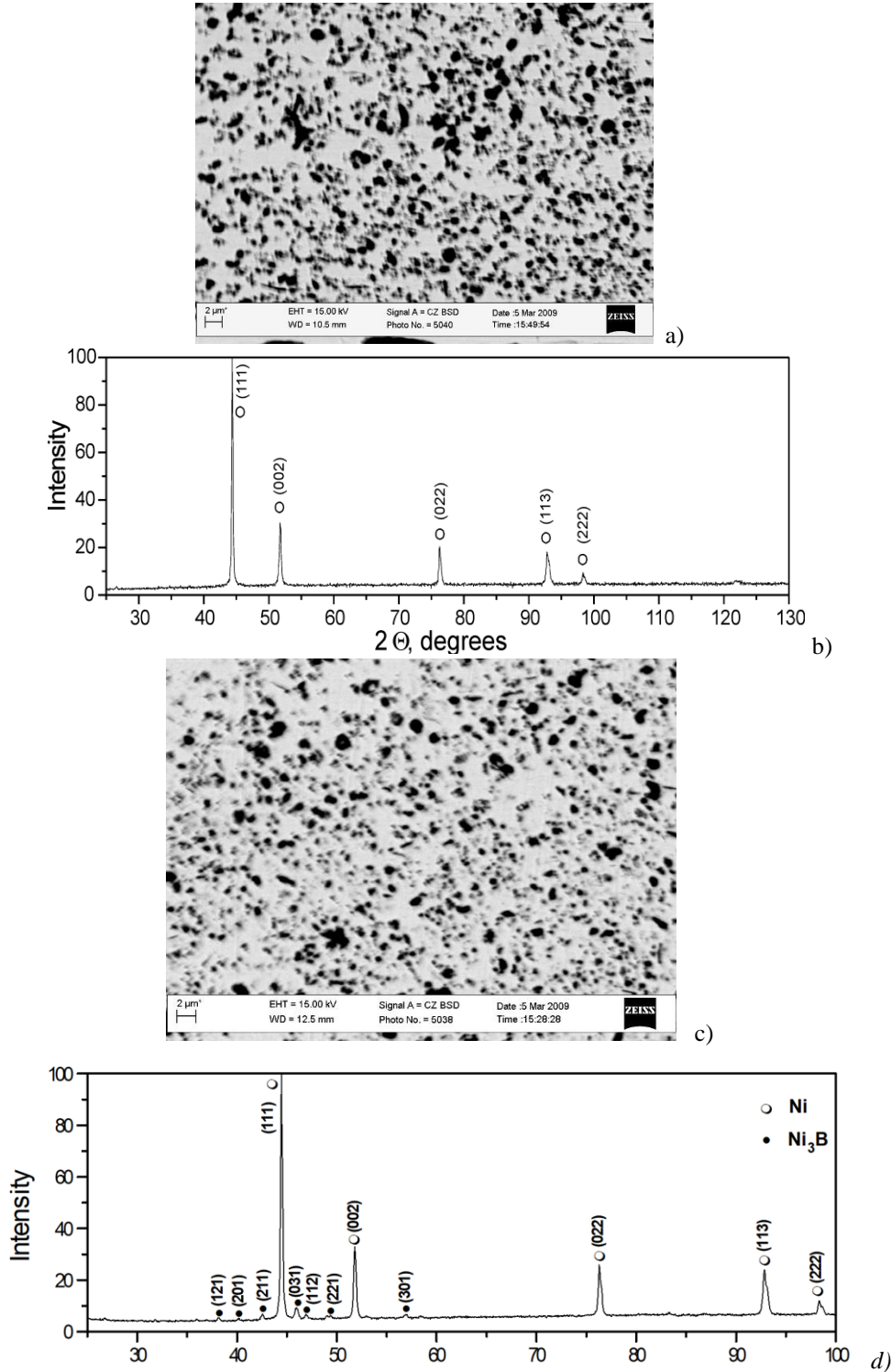
Fig.1. Microstucture (a, c) and X-ray diffraction patterns of CEC Ni-B in initial state (a, b) and after thermal treatment at 450°C (c, d)

The highly developed and branched surface of boron particles in the initial state gradually acquires more rounded shapes, framed by newly formed boride zones. It is due to the diffusion of boron atoms into the adjacent volumes of the Nickel matrix. Stresses are removed insufficiently, the high level of microdeformation remains, the sizes of blocks increase insignificantly. X-ray diffraction analysis showed a significant amount of Ni_3B phase. It is the main reason for the increase in the microhardness. The coating, obtained after this mode of TT is significantly different from pure nickel coating (Fig. 2).
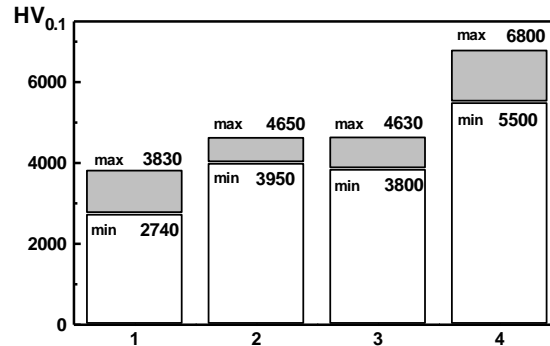
Fig.2. Microhardness of CEC Ni-B after the different thermal treatment parameters. (1) – without TT; after TT: (2) – 200°C; (3) – 300°C and (4) – 450°C. The minimum and maximum values of microhardness are given

Tribocorrosive behavior of CEC. Changes in the electrode potential and friction coefficient (Fig. 3 a, b) during frictional interactions in pairs "steel - Ni-B CEC after different TT" in glycerol + NaCl were studied. Test stages: I - 0… 600 s - contact of friction pairs occurred through a layer of work environment, without load, II - 600… 1200 s friction pairs in contact, III - 1200… 5000 s load is applied, IV - 5000… 6000 s friction pair is unloaded (Fig.3 a, b). The compromise electrode potential is the most positive in the friction pair "steel - CEC-Ni-B after TT at 450□C (E ≈ - 235 mV) (Fig. 3 a), and the most negative - without TT (E ≈ - 370 mV). The coefficient of friction is the lowest in the first case ≈ 0,005 (Fig.3 b), and the highest - in the last ≈ 0.018. The electrode potential in the friction pair "steel - CEC-Ni-B after TT at 300°C is E ≈ - 300 mV, and the coefficient of friction changes randomly from 0.005 to 0.008 during the tests.

a)

b)
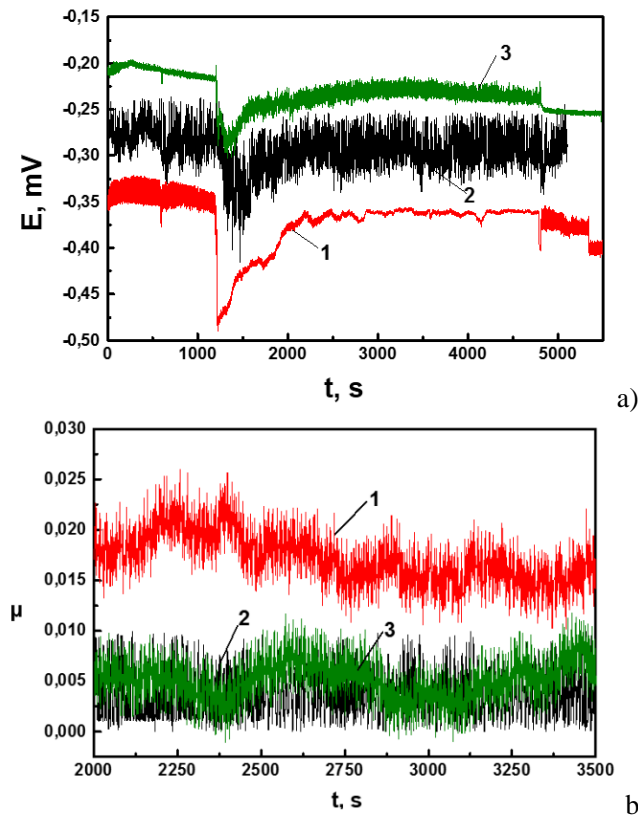
Fig.3. General changes of mixed electrode potential (*a*) and friction coefficient (*b*) of friction couples steel – CEC Ni-B in the environment of glycerin + 10% NaCl at the contact loading 280 N. Friction couples – CEC Ni-B without thermal treatment (*1*), after vacuum annealing at 300°C (*2*) and 450°C (*3*)

After unloading, the electrode potentials of the friction pairs "steel - CEC Ni-B after TT at 450°C" and "steel - CEC Ni-B without TT" became more negative. This indicates, that the friction surfaces are in the activated state for some time after the test. The values of the compromise electrode potential of the friction pair "steel - CEC Ni-B after TT at 300°C" do not change after unloading and are at the same level for some time.

Wear resistance of CEC without TT is the worst, after TT at 300°C is slightly better, and after TT at 450°C is the best (Fig. 4).
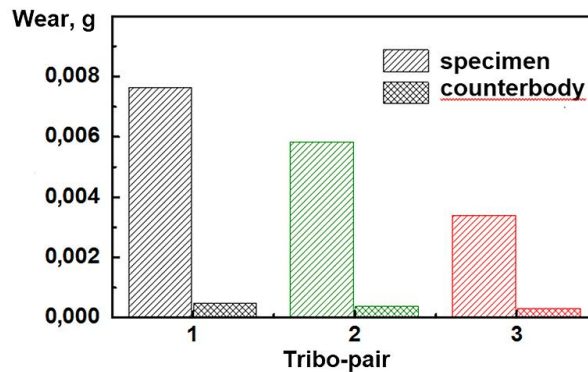
Fig.4. Wear of the friction pairs "steel - CEC Ni-B", load 280 N. CEC Ni-B: (*1*) – without thermal treatment, after vacuum annealing at 300°C (*2*), and 450°C (*3*)

Toporaphy of friction surfases CEC Ni-B after tribocorrosin investigations was analysed. Cracks were found on the surface of the CEC without TT. Working environment penetrates through cracks during friction (Fig. 5 a), and galvanic pairs are formed between CEC and base steel. Oxide films are absent and stresses increase at the places of friction contact. It is sufficient for the development of shift processes and accumulation of the defects with the subsequent formation of surface and near-surface cracks. The growth and propagation of cracks ends with the separation of individual fragments of the coating.

In addition, significant areas of plastic deformation were also found on the surface. Such morphological changes in the structure of CEC without TT are due to the frictional interaction of the contact surfaces in an aggressive environment and leads to a significant shift of the electrode potential towards the negative values.

a)

b)

c)
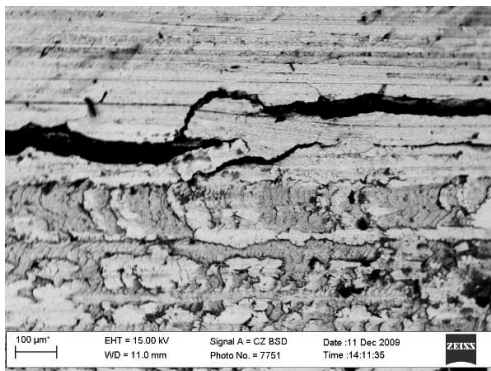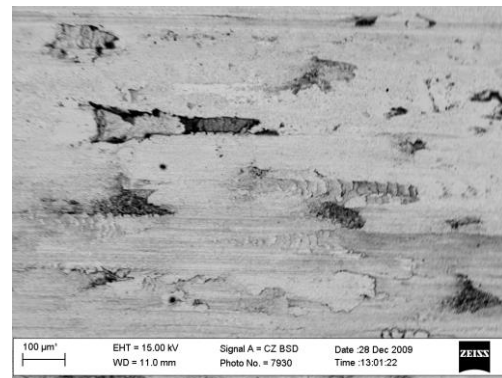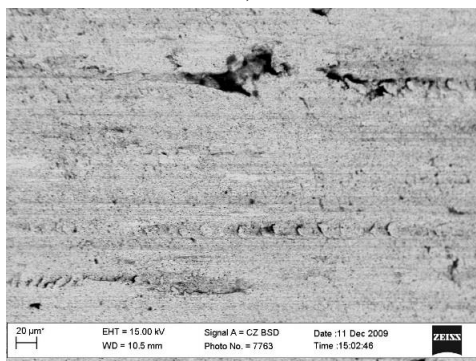
Fig.5. Toporaphy of friction surfases CEC Ni-B after tribocorrosion investigations in glycerin + 10% NaCl: (*a*) without thermal treatment, after vacuum annealing at 300°C (*b*) and 450°C (*c*)

There are no microcracks of friction surfaces of Ni-B CEC after TT at 300°C. Scores occurs mainly due to insufficient volume content of boride grains. The low hardness of the coating facilitates plastic deformation of the friction surface (Fig. 5 b). Defects in the structure are accompanied by a simultaneous shift of the compromise electrode potential toward negative values and an increase in the coefficient of friction at the local time intervals of the test.

Scores are practically not detected on the friction surfaces of Ni-B CEC after TT at 450°C, when the initial stage of solid-phase interaction of coating components with the formation of Ni-Ni$_3$B occurs (Fig.5 c). The friction process is stable, as it is evidenced by changes in the values of the compromise electrode potential and the coefficient of friction.

Conclusion

The influence of low-temperature thermal treatment of Ni-B CEC on steel 09Mn2Si on their tribocorrosion behavior is investigated. It is shown that the structural factor has a decisive influence on the efficiency of such friction pairs. The CEC has the least wear and the most positive compromise electrode potential after vacuum annealing at 450°C, when the initial stage of solid-phase interaction of coating components with the formation of Ni-Ni$_3$B occurs.

References

1. Fedorchenko I. M., Guslienko Yu. A., Luchka M. V. Chemical-thermal treatment of metals and alloys with electrochemical coatings // Protective coatings on metals. - 1981. - Issue. 15. - p. 24–27.

2. A. Mazurek, W. Bartoszek, G. Cieślak, A. Gajewska-Midziałek, D. Oleszak , M. Trzaska Influence of heat treatment on properties of Ni-B/B composite coatings .Arch. Metall. Mater.- 65.- 2020.- 2.-P. 839-844. DOI: 10.24425/amm.2020.132829

3. E. Ünal, A. Yaşar and İ. H. Karahan A review of electrodeposited composite coatings with Ni–B alloy matrix // Materials Research Express.- 2019.- Vol. 6, No 9.

4. Mardarevych R. S., Dalisov V. B., Guslienko Yu. A. Influence of the structure of composite electrochemical coatings on the strength of carbon steel / / Protective coatings on metals - 1986. - Issue 20.–p. 80-83.

5. R. Oriňáková, K. Rošáková, A. Orinak, M. Kupková Electrodeposition of composite Ni–B coatings in a stirred heterogeneous system//Journal of Solid State Electrochemistry.- 2011.-15(6).-P.1159-1168. DOI:10.1007/s10008-010-1177-7

6. Khaldeev GV, Koskov VD, Yagodkina LM Structure and corrosion-mechanical properties of nickel-boron composite coatings // Protection of metals. - 1982. - Issue. XVIII, No. 5. - P. 719-724.

7. Formation of composite boride coatings under conditions of low-temperature annealing of an electrolytic deposit / I. M. Fedorchenko, Yu. A. Guslienko, T. N. Tikhonovich, A. A. Agarkov // Powder metallurgy. - 1985. -№4. - P. 29–31.

8. Mardarevych R.S., Chervinska N.R., Vynar V. A. Influence of heat treatment regimes of composite coatings of Ni-B system on their electrochemical properties // Scientific Bulletin of the Chernivtsi University. Issue 401: Chemistry.– Chernivtsi, 2008. – p.102-104.

9. B 252-87 (1999) e1. Standart Guide for Preparation of Aluminium Alloys for Electroplating. Book of Standart Volume: 02.05.

10. Mardarevich R.S. Investigation of the process of electroplating of composite coatings in the nickel-boron system // Bulletin of the National Technical University "KhPI". -2005. -No.15. – P.107-110.

11. Smyslov E.F. Ratios for determining block sizes and microdistortion values in the X-ray approximation method // Apparatus and methods of X-ray analysis. – 1983.–Issue 29.–p.75-78.

12. Pokhmurskii V., Mardarevych R., Wielage B., Pokhmurska H., Wank A. Structure-phase transformation in electrochemical boron containing coatings by thermal treatment // Tagungsband zum 8. Werkstofftechnischen Kolloquium. Chemnitz. -2005. – Band 22. – P. 33-40

Хома М., Мардаревич Р., Винар В., Василів Х., Ковальчик Ю. Вплив термічної обробки на трибокорозійні властивості композитних покриттів Ni-B

Для підвищення зносостійкості та корозійної стійкості сталей і сплавів застосовуються різні технології захисту поверхонь, зокрема, електрохімічні. Технологія композитних електрохімічних покриттів (КЕП) є більш перспективною, ніж «чисті» гальванічні покриття. Застосування КЕП підвищує стійкість металів до зносу, корозії та втомного руйнування. Нікель часто вибирають в якості матриці КЕП, оскільки він легко утворює рівномірно заповнені бездефектні композитні структури з великою кількістю частинок дисперсної фази (ДФ).

Фізико-механічні властивості металевих покриттів визначають практичне застосування такого складу. Характеристиками КЕП на основі нікелю є: висока твердість і міцність, , а також корозійна стійкість в лужних та слабкокислих середовищах. Ефективним композиційним покриттям з високими трибологічними властивостями є композиційне електрохімічне покриття Ni-B, отримане в процесі електролізу із суспензії аморфного з сульфатхлоридного електроліту нікелювання за катодної густини струму 5 А/дм^2, температури 40...45°C. Встановлено, що після термічної обробки формується нова композитна структура з наповненою матрицею типу Ni-Ni$_3$B. Покриття Ni-B суттєво підвищують зносостійкість сталі в середовищах з хлоридами. Досліджено трибокорозійну поведінку КЕП Ni-B у вихідному стані та після низькотемпературної термічної обробки. Показано, що структурний фактор має вирішальний вплив на ефективність таких пар тертя. КЕП на основі нікелю має найменший знос і найбільший позитивний компромісний електродний потенціал після вакуумного відпалу при 450°C, за якого відбувається початкова стадія твердофазної взаємодії компонентів покриття з утворенням Ni-Ni$_3$B.

Ключові слова: композиційне електрохімічне покриття, нікель, бор, структура, твердість, низькотемпературна термообробка, трибокорозія, коефіцієнт тертя

Experimental verification between the functioning of tribosystems in the conditions of boundary lubrication

A.V. Voitov

State Biotechnological University, Kharkiv, Ukraine
E-mail: K1kavoitov@gmail.com

Abstract

The paper presents an experimental test of modeling the limits of stable operation of different structures of tribosystems (robustness criteria) in the conditions of extreme lubrication. The results of the experimental test confirmed the previously concluded conclusion that not all structures of tribosystems lose stability in terms of the coefficient of friction, i.e. the appearance of burrs on the surfaces of the friction. At low values of the coefficient of shape and low values of the quality factor of the tribosystem, the loss of stability occurs due to accelerated wear of materials.

Expressions for calculation of criteria of robustness of tribosystems taking into account speed of change of loading on tribosystem are received. The rate of change of load is taken into account by the coefficients of dynamism, which are obtained taking into account the right-hand side of the differential equation of the dynamics of the functioning of tribosystems. Analysis of the obtained theoretical results on the assessment of the robustness of tribosystems and their comparison with the results of the experiment, suggest that the obtained conditions for stable operation of tribosystems (criteria of robustness) allow theoretically, with error 10,3 - 13,3 %, determine the boundaries of sustainable work.

Criteria for the robustness of the tribosystem by wear rate and friction coefficient should be used in the design of tribosystems.

Key words: tribosystem; stability of tribosystems; burr of friction surfaces; accelerated wear; the stability limit of the tribosystem; robustness of the tribosystem; the robustness range of the tribosystem; criterion of robustness of the tribosystem.

Introduction

Stable operation of tribosystems in the entire load-speed range of operation is the most important characteristic on which the reliability of machines and mechanisms depends. The range of stable operation of tribosystems is predicted at the stage of design development of new machines and is mainly performed on experimental data of previous designs or experimental data of laboratory and bench tests. To implement this approach, it is necessary to ensure the identity of operating conditions and laboratory (bench) tests, which is associated with high material costs during the development of new machines.

The most promising area is the mathematical modeling of the limits of sustainable operation of tribosystems, which will significantly reduce material resources when designing new equipment. The development of such models is based on the theoretical foundations of the stability of technical systems, developed by O.M. Lyapunov, who created a modern theory of stability of motion of mechanical systems determined by a finite number of parameters.

This work is a continuation of the work [1], where the results of theoretical research to determine the limits of sustainable operation of tribosystems. The purpose of this study is to experimentally test the modeling of the limits of stable operation of different structures of tribosystems (robustness criteria) in the conditions of extreme lubrication with the calculation of modeling error.

Literature review

In work [1] the concept of stability of tribosystems is formulated. The stability of the tribosystem is understood as the ability to restore the original mode of operation after the removal of external influences. An important parameter is also the limit of loss of stable operation of the tribosystem, i.e. the magnitude of the load and the sliding speed when there is a burr or accelerated wear. According to the results of theoretical research, the definition of robustness of the tribosystem is formulated. Robust range is a dimensionless quantity that characterizes the range of loads and sliding speeds, taking into account design and technological features, where the mode of wear without damage to friction surfaces.

In work [1] developed criteria for robustness of tribosystems, which, unlike previously known, are not empirical and do not meet a certain type of design or transmission. The criteria are based on the theory of stability of technical systems and can be applied to a large class of structures. The limits of the values of the developed criteria when tribosystems lose stability are theoretically substantiated. Criteria allow to define loss of stability not only on a bully, but also on the beginning of the accelerated wear that will allow to increase forecasting of reliability of tribosystems during designing.

In work [2] Problems in estimating the stability of tribosystems based on the results of analysis of oscillations in the normal and tangential directions of frictional interaction are considered. The authors argue that one of the most effective ways to study nonlinear friction systems is the method of their physical and mathematical modeling. The quasilinear subsystem is described by a system of differentiated equations, according to which an equivalent model of a mechanical subsystem is built. Friction processes are described by criterion equations. According to the offered criterion equations conditions of physical experiment which provide reception of the correct results corresponding to natural conditions are formed. The authors conclude that the use of spectral characteristics can greatly simplify the apparatus of analysis and synthesis of oscillatory processes in a dynamic system on the actual contact spots.

To solve the problems of dynamic monitoring of friction systems and identification of the dynamic state (stability of tribosystems) in the works [3–6] it is proposed to use integrated estimates: dissipation and degree of dissipation in the tribosystem. The first assessment indirectly determines the friction losses, i.e. the dissipative properties of the friction system and the friction process as a dynamic system. The second estimate determines the amount of damping of the friction process as a dynamic connection.

According to the authors [3–6] integrated estimates allow to estimate the ratio of elastic-inertial and dissipative forces of friction interaction, identify mechanisms of loss of stability, conditions of irreversibility in the contact area and formulate a new direction in building systems for dynamic monitoring of friction systems during their operation.

The methodological approach used to analyze the stability of tribosystems and set out in the works [2–6], allows to analyze tribosystems only at the level of actual contact spots, i.e. at the micro level. Methodical approach presented in the work [1], allows you to perform stability analysis at the macro level, taking into account design, technological and operational factors. This approach takes into account the speed of dissipation on the actual contact spots, which is presented in the paper [7].

The analysis of the works devoted to definition of limits of steady functioning of various designs of tribosystems allows to draw a conclusion that at development and substantiation of such criteria it is necessary to consider constructive, technological and operational factors of tribosystems. The geometrical dimensions of tribocouples, physical and mechanical properties of connected materials of triboelements, tribological properties of lubricating medium, roughness of friction surfaces are insufficiently taken into account in the works listed above. The account of the listed factors will allow to extend the received criteria to a wide class of tribosystems and to make such analysis system.

Purpose

The purpose of this study is to experimentally test the modeling of the limits of stable operation of different structures of tribosystems (robustness criteria) in the conditions of maximum lubrication, which are given in [1].

Methods

To substantiate the methodological approach in research, we use the equation of the dynamics of the functioning of the tribosystem, which is given in [8]. The third-order differential equation is written in operator form:

$$(T_1 T_2 T_3) p^3 + (T_1 T_2 + T_1 T_3 + T_2 T_3) p^2 + (T_1 + T_2 + T_3 + K_2 K_3 T_1) p + K_2 K_3 + 1 =$$
$$= (K_1 K_2 T_3) p + K_1 K_2$$

(1)

p - a differentiation operator that is equivalent to a record d/dt;

T_1, T_2, T_3 – time constants, dimension s;

K_1, K_2, K_3 – gain factors, dimensionless quantities.

Expressions to calculate time constants T_i and gain factors K_i, given in the work [9].

Analysis of the right-hand side of the differential equation shows that the processes of friction and wear in the tribosystem, especially the running-in processes, depend on the first load derivative, i.e. from the load speed. The load speed of the tribosystem can be taken into account by the coefficient of load dynamics, which is proportional to the right part of the differential equation (1):

$$k_d \approx (K_1 K_2 T_3) \frac{dW_i}{dt_l} + K_1 K_2 , \tag{2}$$

where the magnitude of the load (external influence during experimental studies) on the tribosystem is determined by expression:

$$W_i = N \cdot v_{sl} , J/s, \tag{3}$$

where N – load on the tribosystem, H;

v_{sl} – sliding speed, m/s.

t_l – load change time, s.

With the help of laboratory experimental studies on different structures of tribosystems at different values of the load on the tribosystem and different rates of change of load, an expression was obtained to calculate the coefficient of load dynamics.

When determining the robustness of the tribosystem by the parameter of the coefficient of friction:

$$k_{d(f)} = 0{,}62 \ln \left(\frac{K_1 \cdot K_2 \cdot T_{3(f)}}{t_l} \right) , \tag{4}$$

When determining the robustness of the tribosystem by the parameter of wear rate:

$$k_{d(I)} = 0{,}95 \ln \left(\frac{K_1 \cdot K_2 \cdot T_{3(I)}}{t_l} \right) , \tag{5}$$

Taking into account the expressions of the coefficients of load dynamics (4) and (5), which were obtained by the results of experimental studies, the formulas for determining the robustness of tribosystems, which are given in [1], we present in the following form.

To determine the robustness of the tribosystem by the coefficient of friction:

$$RR_f = \frac{\left((T_1 T_2 + T_1 T_{3,f} + T_2 T_{3,f}) \times (T_1 + T_2 + T_{3,f} + K_2 K_3 T_1) \right)}{\left(T_1 T_2 T_{3,f} K_2 K_3 + T_1 T_2 T_{3,f} \right) \cdot k_{d(f)}} \rangle 1. \tag{6}$$

To determine the robustness of the tribosystem by the wear rate:

$$RR_I = \frac{\left((T_1 T_2 + T_1 T_{3,I} + T_2 T_{3,I}) \times (T_1 + T_2 + T_{3,I} + K_2 K_3 T_1) \right)}{\left(T_1 T_2 T_{3,I} K_2 K_3 + T_1 T_2 T_{3,I} \right) \cdot k_{d(I)}} \rangle 1. \tag{7}$$

Criteria for robustness of the tribosystem RR_f and RR_I it is necessary to calculate for each load mode of the operational series of tribosystems, taking into account the rate of change of load. If the value of the criterion is more than one, then the tribosystem operates in a stable range. The greater the value of the criterion of robustness, the greater the margin of steady work.

If the value of the criterion is equal to one - the tribosystem operates on the verge of losing stability. If the value of the criterion is less than one - the tribosystem has lost stability, there is a burr or accelerated wear.

To answer the question of which parameter there was a loss of stability, it is necessary to calculate two criteria: the coefficient of friction, formula (6) and the rate of wear, formula (7). The value of the criterion, which first becomes less than one, answers the question of which parameter there was a loss of stability.

The standard deviation of the values of external influences during experimental research is represented by the formula:

$$S_{W_b} = \sqrt{\frac{1}{n}\sum_{i=1}^{n}\left(W_{b(i)} - W_{b(av)}\right)^2} \; , \tag{8}$$

where $W_{b(i)}$, $W_{b(av)}$, – the value of the magnitude of the external impact on the tribosystem at which there is a loss of stability (burr or accelerated wear), measured during the experiment and the average value for the number of repetitions n. Defined as the product of the load on the tribosystem and the sliding speed according to the formula (3).

The coefficient of variation of measurements of external influence, at which the event of loss of stability of the tribosystem occurs, was determined by the expression:

$$v_{W_b} = \left(\frac{S_{W_b}}{W_{b(av)}}\right) \cdot 100\% \; . \tag{9}$$

The relative error of modeling the limits of functioning of tribosystems in the conditions of marginal lubrication was determined by expressions:

$$e_{W_b} = \left|\frac{W_{b(ex)} - W_{b(m)}}{W_{b(ex)}}\right| \cdot 100\% \; , \tag{10}$$

where $W_{b(ex)}$, $W_{b(m)}$, – the value of the value of the external influence on the tribosystem at which there is a loss of stability (burr or accelerated wear), measured during the experiment and the results of modeling.

Experimental studies were performed on a universal friction machine, based on the friction machine 2070 SMT-1, according to the kinematic scheme "ring-ring". The design of the friction machine is presented in the work [10]. The test complex based on friction machines 2070 SMT-1 is presented in fig. 1.

Fig. 1. Experimental equipment based on the friction machine SMT-1

During the tests, the load on the tribosystem was increased at different load speeds: 1 s.; 10 s.; 20 s.

The loss of stability of tribosystems by the coefficient of friction was determined using the value of the moment of friction, which was registered by the friction recorder of the machine 2070 SMT-1. The loss of stability according to the parameter of the beginning of accelerated wear, was determined using the method of acoustic emission. The measuring complex and the method of registration of AE signals are given in the work [11]. To register acoustic radiation from the friction zone, the acoustic emission sensor was installed on a fixed triboelement. During the tests, the event that occurred first was recorded: either an increase in the coefficient of friction and the occurrence of burr; or the beginning of accelerated wear of triboelement materials. According to the results of three repetitions, the mean value of the burr load or the beginning of accelerated wear, the standard deviation of the values of the recorded values during experimental studies, the formula (8), coefficient of variation of measurements of external influence, at which the event of loss of stability of the tribosystem occurs, as a product of load and sliding speed (9), modeling error by the formula (10).

Results

The results of modeling the limits of stable operation of tribosystems and the results of experimental verification are presented in the table 1. The nature of the change in the value of the external influence on the tribosystem at which there is a loss of stability $W_{b(ex)}$ for different designs of tribosystems, which are estimated by the coefficient of form K_f, m^{-1} [12], presented in the first block of the table 1. Experimental studies of the

limits of sustainable operation of tribosystems were performed for tribosystem steel 40H + Br.AZh.9-4, lubricating medium E_u= 3,6·10^{14} J/m^3, (motor oil M-10G$_{2к}$, SAE 40, API CC), roughness of friction surfaces: Ra = 0,2 micron; Sm=0,4 mm. The sliding speed did not change and was equal to $υ_{sl}$ = 0,5 m/s. During the experiment, the values of the form factor of the tribosystem varied K_f = 6,25 - 22,6, m^{-1}. Such values were obtained by changing the values of the friction areas of the fixed triboelement. The following conclusions can be drawn from the presented results. Increasing the values of the shape factor of the tribosystem expands the range of robustness. In this case, the loss of stability of the tribosystem at low values K_f = 6,25 according to the parameter of wear rate, occurs when $W_{b(ex)}$ = 1200 N·m/s, and the parameter of the coefficient of friction $W_{b(ex)}$ = 1750 N·m/s. For the tribosystem with K_f = 12,5 loss of stability occurs at the same values $W_{b(ex)}$ = 1700 N·m/s. For the tribosystem with K_f = 22,6 loss of stability occurs when $W_{b(ex)}$ = 2000 N·m/s by the coefficient of friction. Tribosystems lose stability due to the burr of friction surfaces. The results of experimental studies of changes in the value of the external influence on the tribosystem in which there is a loss of stability when changing the tribological properties of the lubricating medium E_u, are presented in the second block of the table 1. The results are presented for the tribosystem: steel 40H + Br.AZh.9-4; coefficient of forms K_f = 12,5 m^{-1}; roughness of friction surfaces Ra = 0,2 micron; Sm=0,4 mm. Hydraulic oil was chosen as the changing factor MG - 15V, (E_u= 2,43·10^{14} J/m^3); motor oil M - 10G$_{2к}$, (E_u=3,6·10^{14} J/m^3); transmission oil TSp - 15K, API GL-4, (E_u= 4,18·10^{14} J/m^3). The sliding speed did not change and was equal to $υ_{sl}$= 0,5 m/s. Increasing the tribological properties of the lubricating medium from E_u = 2,43·10^{14} J/m^3 to E_u = 4,18·10^{14} J/m^3 contributes to the expansion of the range of robustness of tribosystems, both in terms of wear rate and friction coefficient.

Table 1

The results of checking the error of modeling the range of robustness of different designs of tribosystems

Tribosystem design	$W_{b(m)}$, N·m/s	$W_{b(ex)}$, N·m/s	S_{Wb}, N·m/s	v_{Wb}, %	e_{Wb}, %
40H + Br.AZh.9-4, motor oil M-10G$_{2к}$, E_u= 3,6·10^{14} J/m^3, K_f = 6,25 m^{-1}	1300 *(I)*	1200 *(I)*	200	16,6	8,3
40H + Br.AZh.9-4, motor oil M-10G$_{2к}$, E_u= 3,6·10^{14} J/m^3, K_f = 12,5 m^{-1}	1900	1700 *(I, f)*	300	17,6	11,7
40H + Br.AZh.9-4, motor oil M-10G$_{2к}$, E_u= 3,6·10^{14} J/m^3, K_f = 22,6 m^{-1}	2300	2000 *(f)*	400	20,0	15,0
40H + Br.AZh.9-4, K_f = 12,5 m^{-1}, hydraulic oil MG-15V, (E_u= 2,43·10^{14} J/m^3)	850	1000 *(f)*	200	20,0	15,0
40H + Br.AZh.9-4, K_f = 12,5 м$^{-1}$, motor oil M-10G$_{2к}$, (E_u=3,6·10^{14} J/m^3)	1900	1700 *(I, f)*	300	17,6	11,7
40H + Br.AZh.9-4, K_f = 12,5 m^{-1}, transmission oil TSp-15K, (E_u= 4,18·10^{14} J/m^3).	2600	2350 *(I)*	350	14,8	10,6
steel 40H+ steel 40H, ($RS_{TS(max)}$ = 326,7; m^{-1}); K_f = 12,5 m^{-1}, motor oil M-10G$_{2к}$, E_u= 3,6·10^{14} J/m^3	1300	1150 *(f)*	250	21,7	13,0
steel 40H+ Br.AZh.9-4, ($RS_{TS(max)}$ = 436,0; 1/m); K_f = 12,5 m^{-1}, motor oil M-10G$_{2к}$, E_u=3,6·10^{14} J/m^3	1900	1700 *(I, f)*	300	17,6	11,7
steel 40H+ LMcSKA 58-2-2-1-1, ($RS_{TS(max)}$ = 460,9; 1/m), K_f = 12,5 m^{-1}, motor oil M-10G$_{2к}$, E_u=3,6·10^{14} J/m^3	1950	1800 *(I, f)*	300	16,6	8,3
Tribosystem №1: steel 40H+ steel 40H, ($RS_{TS(max)}$ = 326,7; m^{-1}), K_f = 6,25 m^{-1}, hydraulic oil MG – 15V, (E_u= 2,43·10^{14} J/m^3), Q_0 = 1,12·10^{10} J/m^3.	650	750 *(f)*	150	20,0	13,3
Tribosystem №2: steel 40H+ Br.AZh.9-4, ($RS_{TS(max)}$ = 436,0; 1/m); K_f = 12,5 m^{-1}, motor oil M-10G$_{2к}$, E_u=3,6·10^{14} J/m^3, Q_0 = 5,5·10^{10} J/m^3.	1900	1700 *(I, f)*	300	17,6	11,7
Tribosystem №3: steel 40X+ LMcSKA 58-2-2-1-1, ($RS_{TS(max)}$ = 460,9; m^{-1}), K_f =14,5, m^{-1}; transmission oil TSp-15K, E_u=4,18·10^{14} J/m^3, Q_0 = 7,69·10^{10} J/m^3.	3100	2900 *(I)*	350	12,0	10,3

Loss of stability of the tribosystem when using hydraulic oil MG - 15V occurs when loading $W_{b(ex)}$ = 1000 N·m/s, by the coefficient of friction. With increasing tribological properties of the lubricating medium to E_u = 4,18·10^{14} J/m^3 (transmission oil TSp - 15K), the stability limit of the tribosystem increases to values $W_{b(ex)}$ = 2350 N·m/s. Loss of stability occurs according to the parameter of wear rate.

The results of experimental studies of changes in the value of the external influence on the tribosystem in which there is a loss of stability when changing the rheological properties of the structure of bound materials in the tribosystem $RS_{TS(max)}$, [13], presented in the third block of the table 1.

The results are presented for the tribosystem: coefficient form K_f = 12,5 m^{-1}; roughness of friction surfaces Ra = 0,2 micron; Sm=0,4 mm. Lubricating medium - motor oil M – 10G$_{2к}$, (E_u= 3,6·10^{14} J/m^3). The following was chosen as the changing factor: "steel 40H + steel 40H", ($RS_{TS(max)}$ = 326,7; 1/m); "steel 40H + Br.AZh.9-4", ($RS_{TS(max)}$ = 436,0; 1/m); "steel 40H + LMcSKA 58-2-2-1-1", ($RS_{TS(max)}$ = 460,9; 1/m).

Increasing the rheological properties of bound materials in the tribosystem from $RS_{TS(max)}$ = 326,7 m^{-1} to $RS_{TS(max)}$ = 460,9 m^{-1} contributes to the expansion of the range of robustness of tribosystems, both in terms of wear rate and friction coefficient. The following values were obtained for these parameters. When using the tribosystem "steel 40H + steel 40H", burr occurs at $W_{b(ex)}$ = 1150 N·m/s by the coefficient of friction. When using tribosystems with connected materials "steel 40H + Br.AZh.9-4" and "steel 40H + LMcSKA 58-2-2-1-1", loss of stability on the parameter of the coefficient of friction and wear rate does not differ and increases to the value $W_{b(ex)}$ = 1700 - 1800 N·m/s.

The results of experimental studies of changes in the value of the external influence on the tribosystem in which there is a loss of stability when changing all the above factors, which can be taken into account by the value of the quality factor of the tribosystem Q_0, presented in the fourth block of table 1. Determination of the quality factor of the tribosystem is given in the paper [14].

The results are presented for three tribosystems.

1.Tribosystem №1: "steel 40H + steel 40H", ($RS_{TS(max)}$ = 326,7; m^{-1}); K_f =6,25, m^{-1}; lubricating medium E_u= 2,43·10^{14} J/m^3, (MG-15V). Roughness of friction surfaces Ra = 0,2 micron; Sm=0,4 mm. The magnitude of the quality factor of the tribosystem Q_0 = 1,12·10^{10} J/m^3.

2.Tribosystem №2: "steel 40H + Br.AZh.9-4", ($RS_{TS(max)}$ = 436,0; m^{-1}); K_f =12,5, m^{-1}; lubricating medium E_u= 3,6·10^{14} J/m^3, (M-10G$_{2к}$). Roughness of friction surfaces Ra = 0,2 micron; Sm=0,4 mm. The magnitude of the quality factor of the tribosystem Q_0 = 5,5·10^{10} J/m^3.

3.Tribosystem №3: "steel 40H + LMcSKA 58-2-2-1-1", ($RS_{TS(max)}$ = 460,9; m^{-1}); K_f =14,5, m^{-1}; lubricating medium E_u= 4,18·10^{14} J/m^3, (TSp-15K). Roughness of friction surfaces Ra = 0,2 micron; Sm=0,4 mm. The magnitude of the quality factor of the tribosystem Q_0 = 7,69·10^{10} J/m^3.

Increasing the value of the quality factor of the tribosystem, which also takes into account the coefficient of form, tribological properties of lubricating medium, rheological properties of connected materials in the tribosystem, thermal conductivity of materials of movable and fixed triboelements, loading and speed of sliding, from values Q_0 = 1,12·10^{10} J/m^3, (tribosystem №1), to Q_0 = 7,69·10^{10} J/m^3, (tribosystem №3), contributes to the expansion of the range of robustness, both in terms of wear rate and the parameter of the coefficient of friction.

Loss of stability when using the design of the tribosystem №1 occurs at the value of external influences $W_{b(ex)}$ = 750 N·m/s by the coefficient of friction. As the quality factor increases (tribosystem №3), the stability limit of the tribosystem increases to values $W_{b(ex)}$ = 2900 N·m/s by the wear rate parameter.

The results of experimental studies suggest that not all designs of tribosystems lose stability in terms of the coefficient of friction, i.e. after the appearance of burr friction surfaces. There are options when the loss of stability occurs due to accelerated wear of materials.

The experimental data shown in table 1, obtained at the time of loading of the tribosystem equal to 20 s. With this value of the load time, the dynamics coefficients correspond to the minimum values: $k_{d(f)}$=3,42; $k_{d(I)}$=4,37, formulas (4) and (5). When the load time decreases, up to 1 s., the coefficients increase significantly, for example: $k_{d(f)}$=6,4; $k_{d(I)}$=7,38. Figure 1 presents the theoretical dependences of changes in the coefficients of dynamism of different structures of tribosystems on the parameters of the coefficient of friction and wear rate on the value of the load time.

Experimental dependences of the influence of dynamism coefficients on the value of the limit of loss of stability (burr or accelerated wear) are presented in fig..2.

The results of checking the modeling error and the coefficient of variation of the obtained experimental values when changing the magnitude of the external influence on the tribosystem, in which there is a loss of stability of different structures of tribosystems, allow us to draw the following conclusions.

Calculation of the error in determining the limit of stable operation of tribosystems according to the formula (10) when changing the shape factor of tribosystems allows us to say that the error value is equal to e_W= 8,3 - 15,0%, at the coefficient of variation v_W= 16,6 - 20,0%. As follows from the obtained results, increasing the coefficient of shape leads to an increase in modeling error.
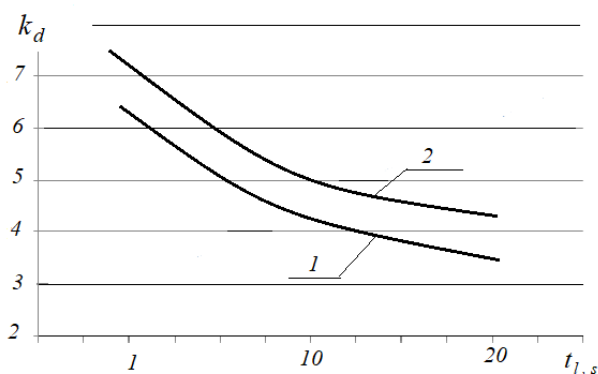
Fig. 2. Dependences of change of coefficients of dynamics of loading k_d different designs of tribosystems from the value of the load time t_l: 1 – by the coefficient of friction; 2 – by the wear rate parameter
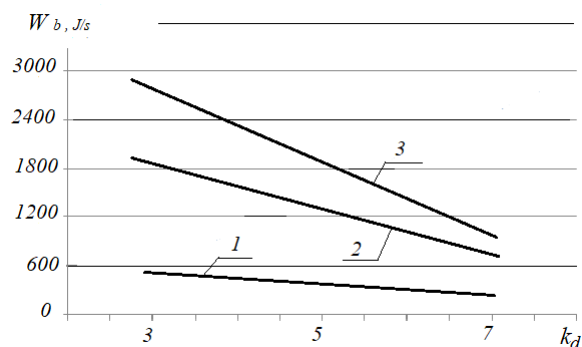
Fig. 3. Dependences of change of size of limit of loss of stability of various designs of tribosystems W_b from the value of the load factors k_d: 1 – tribosystem №1; 2 – tribosystem №2; 3 – tribosystem №3

The calculation of the error in determining the limit of stable operation of tribosystems when changing the tribological properties of the lubricating medium allows us to say, that the value of the simulation error is within e_W= 10,6 - 15,0%, at the coefficient of variation v_W= 14,8 - 20,0%. Greater error is inherent in the use of lubricating media with low values of tribological properties.

Comparison of experimental results with modeling results at change of rheological properties of the connected materials in a tribosystem allows to assert, that the error value is within e_W= 8,3 - 13,0%, at the coefficient of variation v_W= 16, - 21,7%. Greater error is inherent in the use of bonded materials with low values of rheological properties.

Comparison of experimental results with simulation results when changing all the above factors, which can be taken into account by the quality factor of the tribosystem Q_0, allow to state that the value of modeling error is within e_W= 10,3 - 13,3%, at the coefficient of variation v_W= 12, - 20,0%. Greater error is inherent in the use of tribosystems with low quality values.

The introduction of coefficients of dynamism (4) and (5) in the calculated expressions for determining the robustness of tribosystems (6) and (7) reduces the modeling error.

Conclusions

An experimental test of modeling the limits of stable operation of various structures of tribosystems (robustness criteria) in the conditions of maximum lubrication, which were developed in [1]. The results of the experimental test confirmed the previously concluded conclusion that not all structures of tribosystems lose stability in terms of the coefficient of friction, i.e. the appearance of burrs on the surfaces of the friction. At low values of the coefficient of shape and low values of the quality factor of the tribosystem, the loss of stability occurs due to accelerated wear of materials.

Expressions for calculation of criteria of robustness of tribosystems taking into account speed of change of loading on tribosystem are received. The rate of change of load is taken into account by the coefficients of dynamism, which are obtained taking into account the right-hand side of the differential equation of the dynamics of the tribosystems. Analysis of the obtained theoretical results on the assessment of the robustness of tribosystems and their comparison with the results of the experiment, allow us to state that the obtained conditions of stable operation of tribosystems (robustness criteria) in the form of expressions (6) and (7), allow theoretically, with error 10,3 - 13, 3%, define the limits of sustainable work.

Criteria for robustness of the tribosystem by wear rate and friction coefficient should be used in the design of tribosystems. By changing the design and technological parameters of the structure, it is possible to ensure the operation of the tribosystem, which is designed in a given load-speed range without damage and with a margin of safety.

References

1. Vojtov V., Voitov A. Simulation of boundaries of tribosystems functioning in the conditions of border oiling // Problems of Friction and Wear, 2021, №. 4 (93). – pp. 58-69. https://doi.org/10.18372/0370-2197.4(93).16262 [Ukraine]

2. Shapovalov V.V., Sladkovski A., Erkenov A.CH. Aktual'nyye zadachi sovremennoy tribotekhniki i puti ikh resheniya / Izvestiya vysshikh uchebnykh zavedeniy. Mashinostroyeniye, 2015, №1(658), s. 64-75. [Russian]

3. Ozyabkin A.L. Dinamicheskiy monitoring tribosistemy «Podvizhnoy Costav–put'» / Vestnik RGUPS, 2011, № 2, s. 35–47. [Russian]

4. Ozyabkin A.L., Kolesnikov I.V. Metody povysheniya nadezhnosti rez'bovykh soyedineniy tormoz-nykh sistem vagonov / Vestnik RGUPS, 2011, № 4, s. 66–75. [Russian]

5. Ozyabkin A.L., Kolesnikov I.V., Kharlamov P.V. Monitoring tribotermodinamiki friktsionno-go kontakta mobil'noy tribosistemy / Treniye i smazka v mashinakh i mekhanizmakh, 2012, № 3, s. 25–36. [Russian]

6. Ozyabkin A.L. Teoreticheskiye osnovy dinamicheskogo monitoringa friktsionnykh mobil'nykh si-stem / Treniye i smazka v mashinakh i mekhanizmakh, 2011, № 10, s. 17–28. [Russian]

7. Vojtov V.A., Zakharchenko M.B. Modelirovaniye protsessov treniya i iznashivaniya v tribosiste-makh v usloviyakh granichnoy smazki. Chast' 1. Raschet skorosti raboty dissipatsii v tribosisteme. // Problemi tribologii. – 2015. - № 1. – S. 49-57. [Russian]

8. Voitov A. Structural identification of the mathematical model of the functioning of tribosystems under conditions of boundary lubrication / Problems of Tribology, 2021, V. 26(2/100), p. 26-33. https://doi.org/10.31891/2079-1372-2021-100-2-26-33 [English]

9. Voitov A. Parametric identification of the mathematical model of the functioning of tribosystems in the conditions of boundary lubrication / Problems of Tribology, 2021, V. 27(3/101), p. 6-14. https://doi.org/10.31891/2079-1372-2021-101-3-6-14 [English]

10. Vojtov V.A., Bazderkin V.A. Universal'naya mashina treniya / Treniye i znos, 1992, T.13, №3, s.501-506. [Russian]

11. Vojtov V.A., Fenenko K.A., Voitov A.V. Metodyka diahnostuvannya riznykh konstruktsiy trybosy-stem metodom akustychnoyi emisiyi // Problemy tertya ta znoshuvannya. 2021. – №. 2 (91). – S.18-26. DOI: 10.18372/0370-2197.2(91).15525 [Ukraine]

12. Vojtov V.A. Printsipy konstruktivnoy iznosostoykosti uzlov treniya gidromashin / V.A. Voy-tov, O.M. Yakhno, F.KH. Abi Saab – K.: Nats. tekhn. un-t «Kiyev. politekhn. in-t», 1999. – 190 s. [Russian]

13. Voitov A. V. Zalezhnosti zminy reolohichnykh vlastyvostey struktury spoluchenykh materialiv u trybosystemi pid chas prypratsyuvannya // Problemy tertya ta znoshuvannya. 2020. – №. 3 (88). – S. 71-78. http://dx.doi.org/10.18372/0370-2197.3(88).14921 [Ukraine]

14. Vojtov V.A., Voitov A.V. Assessment of the quality factor of tribosystems and it's relationship with tribological characteristics // Problems of Tribology, V. 25, No 4/98 – 2020, 20-26. https://doi.org/10.31891/2079-1372-2020-98-4-20-26 [English]

Войтов А.В. Параметрична ідентифікація математичної моделі функціонування трибосистем в умовах граничного мащення

У роботі представлена експериментальна перевірка моделювання меж стійкого функціонування різних конструкцій трибосистем (критеріїв робастності) в умовах граничного мащення. Результати експериментальної перевірки підтвердили зроблений раніше висновок, що не всі конструкції трибосистем втрачають стійкість за параметром коефіцієнта тертя, тобто по появі задиру поверхонь тертя. При низьких значеннях коефіцієнта форми та низьких значеннях добротності трибосистеми, втрата стійкості настає за прискореним зношуванням матеріалів.

Отримано вирази для розрахунку критеріїв робастності трибосистем з урахуванням швидкості зміни навантаження на трибосистему. Швидкість зміни навантаження враховується коефіцієнтами динамічності, які отримано з урахуванням правої частини диференціального рівняння динаміки функціонування трибосистем. Аналіз отриманих теоретичних результатів з оцінки робастності трибосистем та їх зіставлення з результатами експерименту, дозволяють стверджувати, що отримані умови сталої роботи трибосистем (критерії робастності) дозволяють теоретичним шляхом, з похибкою 10,3 - 13, 3 %, визначити межі стійкої роботи.

Критерії робастності трибосистеми за швидкістю зношування і за коефіцієнтом тертя необхідно застосовувати при проектуванні трибосистем.

Ключові слова: трибосистема; математична модель; диференційне рівняння; параметрична ідентифікація; коефіцієнт посилення; постійна часу; граничне мастило; добротність трибосистеми; швидкість роботи дисипації

The influence of the alloying of the auger by the chromium on its wear during dehydration process of municipal solid waste in the garbage truck

O.V. Bereziuk[1], V.I. Savulyak[1], V.O. Kharzhevskyi[2]

[1]*Vinnitsa National Technical University, Ukraine*
[2]*Khmelnytskyi National University, Ukraine*
E-mail: berezyukoleg@i.ua

Abstract

The article is dedicated to the study of the influence of the alloying of the auger by the chromium on its wear during dehydration of solid waste in the garbage truck. Using the method of regression analysis, the hyperbolical dependencies of auger wear depending on the chromium content in its hardened steel for different values of the friction path are determined. Graphical dependences of augur wear depending on the chromium content in its hardened material as a function of the friction path are made up, and it confirms sufficient convergence of the obtained dependencies. Carried out additional regression analysis allowed to determine that that during two weeks of operation of the auger during dehydration of solid waste in the garbage truck increasing of the chromium content in its hardened material from 0.25% to 12% reducing the speed of the wearing and energy consumption of solid waste dehydration from 12.2% to 3.1%, and, consequently, to reduce the cost of the process of their dehydration in the garbage truck. It is shown the graphical dependence of the reduction of energy consumption of dehydration of solid household waste by the hardened auger due to its alloying by the chromium. It was established the expediency of further research to determine the rational content and structural state of the material of the auger and the ways to increase its wear resistance.

Key words: wear, chromium content, auger press, garbage truck, dehydration, solid waste, regression analysis

Introduction

The increasing of the wear resistance and reliability of machine parts is the important task of the municipal machine building [1, 2]. A promising technology for primary processing of municipal solid waste (MSW), aimed at reducing both the cost of transportation of solid waste and the negative impact on the environment is their dehydration, accompanied by pre-compaction and partial grinding. Dehydration of solid waste in the garbage truck is performed using a conical screw, the surface of which due to the existing friction wears out intensively. This is due to the fact that solid waste contains small metal parts, glass, ceramics, stones, bones, polymeric materials, which have abrasive properties. Besides, the presence of moisture 39-92% by weight in MSW creates an aggressive corrosive environment. For the manufacturing of the augers, the alloyed steels are widely used. The usage of steels and cast irons which are alloyed by chromium is well-grounded. Such alloys harden well and have high resistance to corrosion and abrasive wear. Therefore, the study of the influence of the chromium content in the hardened steel of the auger on its wear during dehydration of solid household waste in the garbage truck is a topical task.

Literature review

The results of experimental studies of wear resistance of different auger materials with different thermal and chemical-thermal treatment in a corrosive-abrasive environment on special friction machines that simulated the operating conditions of extruders in the processing of feed grain with saponite mineral impurities are published in the paper [3]. The authors found that the wear resistance of materials in a corrosive-abrasive
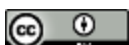
environment at elevated temperatures depends not only on the hardness of the friction surface, but also on its structure and phase composition and changes in the hardness gradient along the depth of the hardened layer. To ensure high wear resistance of extruders in the manufacture of animal compound feed with impurities of the mineral saponite, it is recommended to use for the manufacture of parts of the extrusion unit steel X12, hardened by nitro-hardening technology.

The paper [1] is dedicated to the research of the tribotechnical characteristics of cast high-chromium alloys followed by heat treatment.

The author of the article [4] investigated the influence of chromium alloying of structural steel on its abrasive wear resistance after high-temperature thermomechanical treatment. It is noted that the combined treatment, which consists of a combination of chromium alloying in the amount of 1 ... 5% and high-temperature thermomechanical treatment can be recommended for practical use as an effective means of increasing the strength of steels. The hardening of steel in this structural state reaches its maximum value after alloying by 1 ... 2% of chromium.

In the article [5], a mathematical model for calculating the wear rate of triboelements in a tribosystem operating in conditions of corrosion and abrasive wear was developed. The input factors were: active acidity, abrasiveness, roughness, load and sliding speed. Theoretically, the degree of influence of the above factors on the wear rate is established. It was found that abrasiveness is the most important factor, followed by the degree of decline – the level of active acidity and load.

Authors of the article [6] presented a new design of the auger with a sectional elastic surface, which is designed to reduce the degree of damage to the grain material during its transportation. The theoretical calculation of the interaction of the grain with the elastic section of the auger is carried out. A dynamic model has been developed to determine the influence of structural, kinematic and technological parameters of the elastic auger on the time and path of free movement of bulk material particles during their movement between sections, as well as to exclude the possibility of grain material interaction with the non-working surface of the auger working body to reduce the possibility of its damage.

In the paper [7] it was determined that restoration of the auger requires surfacing or spraying a layer of a certain thickness on the end part of the coil of the auger, while the width of the restored layer is usually a few millimeters. An algorithm for selecting the optimal composite powder material for plasma spraying in order to increase the wear resistance of the working surfaces of machine parts, in particular the auger, is described. Plasma spraying of composite powder materials, according to the authors, will increase the durability of the auger by 2-3 times, which will reduce repair costs by tens of times.

The influence of geometrical parameters on productivity and design of the briquetting machine using the model of pressure based on the theory of piston flow is investigated in the article [8]. An analytical model that uses a pressure model was also developed based on Archard wear law to study the wear of augers of biomass briquetting machines. The developed model satisfactorily predicted the wear of the auger and showed that the greatest influence on it have the speed of rotation and the choice of material. The amount of wear increases exponentially to the end of the auger, where the pressure is the highest. Changing the design of the auger to select the optimal geometry and speed with the appropriate choice of material can increase the life of the auger and the productivity of the machine for briquetting biomass.

The analysis of the process of screw briquetting of plant materials into fuel and feed is investigated in the work [9]. Regularities of this process are the basis for determining the rational parameters of the working bodies. When designing briquette presses it is necessary to consider deformation of biomass taking into account change of physical and rheological properties at the moment of interaction with the working surfaces of the auger.

In the article [10] the wear of a twin-auger extruder of rigid PVC resins is investigated. The pressures around the cylinder when extruding two rigid PVC resins in a laboratory extruder with a diameter of 55 mm were measured and the forces acting on the auger core were determined. Numerical simulation of the flow was performed using the power parameters of the viscosity of the resins.

The process of pressing wood chips in auger machines was investigated in the work [11]. The processes occurring in different parts of the auger are established, formulas are defined that allow to calculate the loads acting on the auger coils, as well as to determine the power required for pressing. The specific energy consumption and the degree of heating of raw materials during pressing are determined.

The results of experimental studies of the process of solid dehydration based on the planning of the experiment by the Box-Wilson method are shown in the article [12]. Quadratic regression equations with the 1st order interaction effects were obtained using rotatable central composite planning for such objective functions as humidity and density of pre-compacted and dehydrated MSW, maximum drive motor power, energy consumption of solid waste dehydration. This allowed to determine the optimal parameters of equipment for dehydration by the criterion of minimizing the energy consumption of the process (auger speed, the ratio of the radial gap between the auger and the body, and the ratio of the auger core diameter to the outer diameter of the auger on the last coil) for both mixed and "wet".

In the article [13] the improved mathematical model of work of the dehydration drive of MSW in the garbage truck is suggested that takes into account wear of the auger, which allowed to research numerically the dynamics of this drive during the start-up, and to define that with the increase of wear of the auger pressure of

working liquid on the speed of the auger it is significantly reduced. The power regularities of change of the nominal values of pressures at the inlet of the hydraulic motor, angular speed and frequency of rotation of the auger from values of its wear are defined, the last of which describes detuning from optimum frequency of rotation of the auger in the course of its wear. It is established that the wear of the auger by 1000 μm leads to an increase in the energy consumption of solid dehydration by 11.6%, and, consequently, to an increase in the cost of the process of their dehydration in the garbage truck and accelerate the wear process.

In the paper [14], the influence of carbon content in the auger material on its wear during dehydration of solid waste in the garbage truck was investigated by means of the regression analysis method. It was also found that during operation and the wearing process of the auger on the path s = 56850 m during dehydration of solid waste in the garbage truck, the increase of the carbon content in the auger material from 0.2% to 2.1% leads to a decrease in the growth rate of energy consumption of solid waste dehydration from 19.6% to 4.4%, and, consequently, to reduce the cost of dehydration in the garbage truck.

Purpose

Researching the influence of the chromium content in the hardened steel of auger on its wear during dehydration of solid waste in a garbage truck.

Methods

Determination of paired dependencies of auger wear from the chromium content in the hardened steel was performed by regression analysis [15]. Regressions were determined on the basis of literalizing transformations, which allow to reduce the nonlinear dependence to the linear one. The coefficients of regression equations were determined by the method of least squares using the developed computer program "RegAnaliz", which is protected by a copyright registration certificate, and is described in the article.

The following dependencies were used to determine the energy consumption of solid dehydration taking into account the auger wear [13]:

$$
\begin{aligned}
E = {} & 1504 - 15.92w_0 + 0.3214\rho_0 - 1.069n(u) - 2061(\Delta_{aug} + u)/(D_{min} - 2u) - 1947(d_{min} - \\
& - 2u)/(D_{min} - 2u) + 9.118 \cdot 10^{-4} w_0\rho_0 + 0.002142w_0 n(u) + 18.12w_0(\Delta_{aug} + u)/(D_{min} - 2u) - \\
& - 2.115w_0(d_{min} - 2u)/(D_{min} - 2u) + 4.392 \cdot 10^{-4}\rho_0 n(u) - 2.005\rho_0(\Delta_{aug} + u)/(D_{min} - 2u) + \quad (1) \\
& + 0.3361\rho_0(d_{min} - 2u)/(D_{min} - 2u) + 0.09031w_0^2 - 7.923 \cdot 10^{-4}\rho_0^2 + 0.008241n(u)^2 + \\
& + 104172[(\Delta_{aug} + u)/(D_{min} - 2u)]^2 + 1318[(d_{min} - 2u)/(D_{min} - 2u)]^2 \ [\text{kWh/tons}];
\end{aligned}
$$

$$ n = 52.43 - 1.276 \cdot 10^{-3} u^{1,5} \ [\text{rpm}], \qquad (2) $$

where E – is the energy consumption of solid waste dehydration, kW·h/tons; ρ_0 – initial density of solid waste, kg/m^3; w_0 – initial relative humidity of solid waste, %; n – the nominal speed of the auger, rpm; u - auger wear, m; Δ_{aug} - radial clearance between auger and housing, m; d_{min} – outer diameter of the auger on the last coil, m; D_{min} is the diameter of the auger core on the last coil, m.

Results

The values of auger wear for different values of chromium content in the hardened steel of auger and friction path are given in Table 1 [3]. As a result of regression analysis of the data in Table 1, it was determined the hyperbolical dependencies of wear of the auger depending on the hardness of its surface for different values of the friction path:

$$ u_{s=3000} = \frac{C_{Cr}}{0.02586C_{Cr} - 0.002768} ; \qquad (3) $$

$$ u_{s=6000} = \frac{C_{Cr}}{0.01402C_{Cr} - 0.001645} ; \qquad (4) $$

$$ u_{s=9000} = \frac{C_{Cr}}{0.009613C_{Cr} - 0.001109} ; \qquad (5) $$

$$ u_{s=12000} = \frac{C_{Cr}}{0.007314C_{Cr} - 0.0008353} , \qquad (6) $$

where u – wear, μm; C_{Cr} – chromium content in the hardened steel of auger, %; s – friction path, m.

Table 1

The results of regression analysis of the dependence of the wear of the auger depending on the chromium content in the hardened steel and the friction path [3]

№	Material of the auger	Chromium content in the auger material, %	Wear, μm, for the friction path, m			
			3000	6000	9000	12000
1	Steel 45	0.25	53	103	153	203
2	Steel ШХ15	1.5	43	80	116	152
3	Steel Х12	12	39	72	105	138

Fig. 1 shows graphical dependences of auger wear depending on the chromium content in the hardened steel for different values of the friction path, made up using the dependences (3 - 6), which confirmed the sufficient convergence of the obtained dependencies compared with the data in the Table 1.
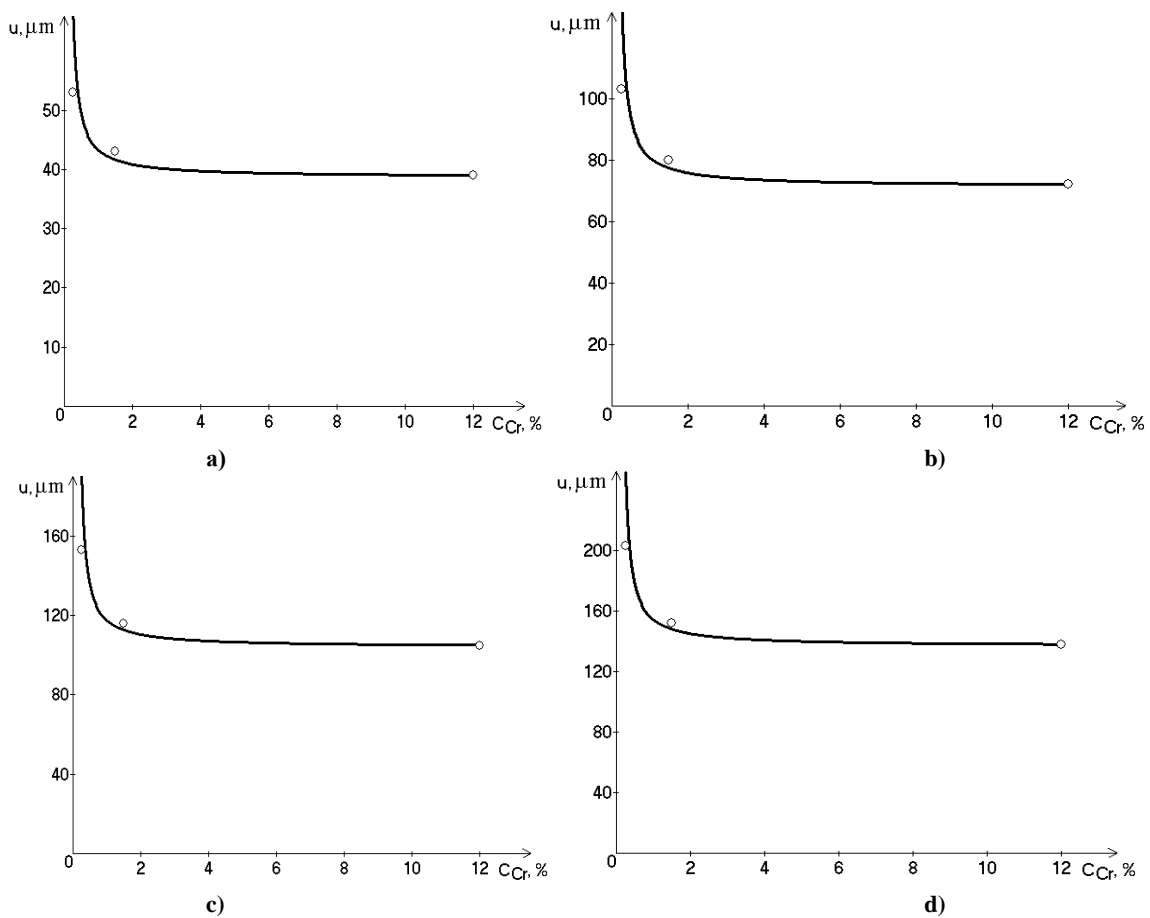
Fig.1 The wear of the auger depending on the chromium content in the hardened steel for different values of the friction path (a) – s = 3000 m, (b) – s = 6000 m, (c) – s = 9000 m, (d) – s = 12000 m: actual ○, theoretical —

Dependences (3 - 6) for different values of the friction path can be written in general as follows

$$u = \frac{C_{Cr}}{B(s)C_{Cr} - A(s)},$$ (7)

where $A(s)$, $B(s)$ – regression coefficients that depend on the path of friction.

After the additional regression analysis, the regression coefficients which depend on the friction path can be described by power laws:

$$A(s) = \frac{1}{66.64 + 0.09338s};$$ (8)

$$B(s) = \frac{1}{5.971 + 0.0109s} .$$ (9)

The results of the regression analysis are shown in Table 2, where the cells with the maximum values of the correlation coefficient R for each of the paired regressions are marked in gray. Figure 2 shows the graphical dependences of the regression coefficients on the path of friction, constructed using the dependences (8,9), which confirm the sufficient convergence of the obtained dependencies.

Table 2

The results of regression analysis of the dependence of the wear of the auger depending on the chromium content in the hardened steel for different values of the friction path

№	Type of regression	Correlation coefficient R for paired regressions					
		$u_{s=3000}{=}f(C_{Cr})$	$u_{s=6000}{=}f(C_{Cr})$	$u_{s=9000}{=}f(C_{Cr})$	$u_{s=12000}{=}f(C_{Cr})$	$A{=}f(s)$	$B{=}f(s)$
1	$y = a + bx$	0.78434	0.76548	0.74538	0.73568	0.95672	0.93902
2	$y = 1 / (a + bx)$	0.82777	0.81508	0.79543	0.78565	0.99911	1.00000
3	$y = a + b / x$	0.98985	0.99365	0.99664	0.99772	0.99597	0.99957
4	$y = x / (a + bx)$	0.99998	0.99998	0.99998	0.99999	0.98313	0.98541
5	$y = ab^x$	0.80603	0.79008	0.77000	0.76015	0.99128	0.98339
6	$y = ae^{bx}$	0.80603	0.79008	0.77000	0.76015	0.99128	0.98339
7	$y = a \cdot 10^{bx}$	0.80603	0.79008	0.77000	0.76015	0.99128	0.98339
8	$y = 1 / (a + be^{-x})$	0.99736	0.99873	0.99985	0.99998	0.98832	0.98832
9	$y = ax^b$	0.96900	0.96212	0.95287	0.94812	0.99742	0.99985
10	$y = a + b{\cdot}\lg x$	0.95954	0.95070	0.94075	0.93575	0.99540	0.98841
11	$y = a + b{\cdot}\ln x$	0.95954	0.95070	0.94075	0.93575	0.99540	0.98841
12	$y = a / (b + x)$	0.82777	0.81508	0.79543	0.78565	0.99910	0.99999
13	$y = ax / (b + x)$	0.97675	0.98128	0.98712	0.98955	0.91241	0.92863
14	$y = ae^{b/x}$	0.98414	0.98849	0.99284	0.99455	0.96816	0.98033
15	$y = a \cdot 10^{b/x}$	0.98414	0.98849	0.99284	0.99455	0.96816	0.98033
16	$y = a + bx^n$	0.72971	0.70897	0.68701	0.67645	0.89126	0.86559
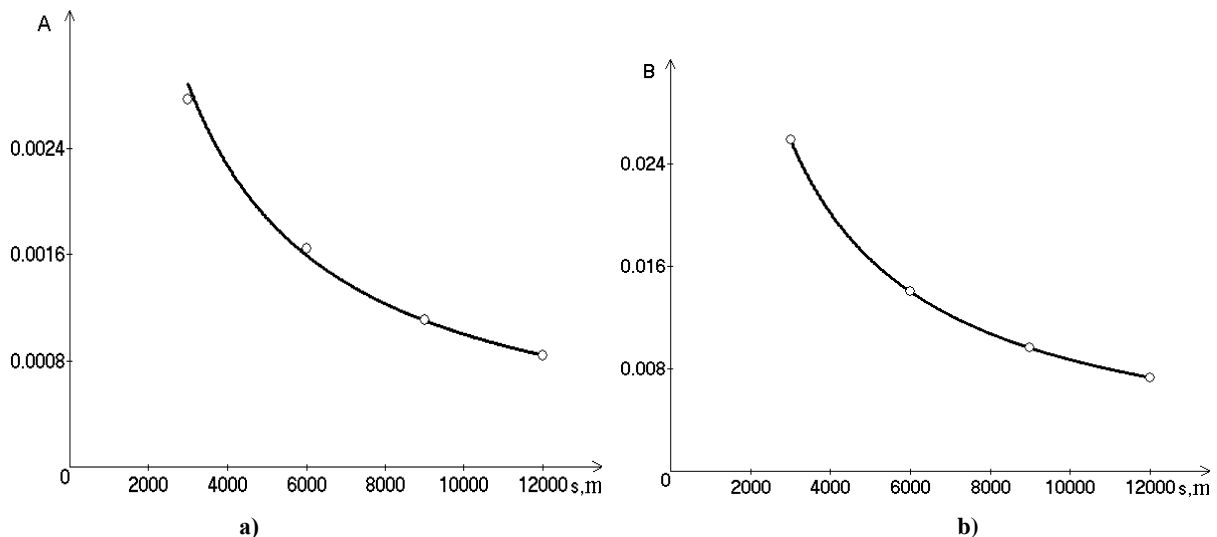
a)   b)
Fig. 2. Dependences of regression coefficients on the friction path (a) − $A = f(s)$, (b) − $B = f(s)$: actual○, theoretical —

After substituting the laws (8, 9) into the dependence (7), we obtain the law of wear of the auger depending on the chromium content in the hardened steel and the friction path

$$u = \frac{C_{Cr}}{C_{Cr}/(5.971 + 0.0109s) - 1/(66.64 + 0.09338s)} .$$ (10)

Fig. 3 shows a graphical dependence of the wear of the auger in the plane of the parameters of influence: the chromium content in the hardened steel and the friction path.
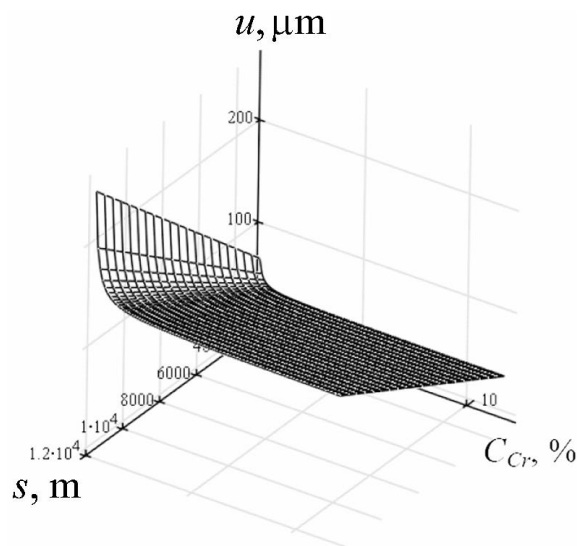
**Fig. 3. The dependence of the wear of the auger *u* in the plane of the parameters
of influence: the content of the chromium C_{Cr} in the hardened steel and the friction path *s***

Figure 4 shows the graphical dependence of the influence of the chromium content in the hardened steel of the auger of the device for dehydration of solid waste on the energy consumption of the process (*s* = 56850 m [14]), made up using dependencies (1, 2, 10).
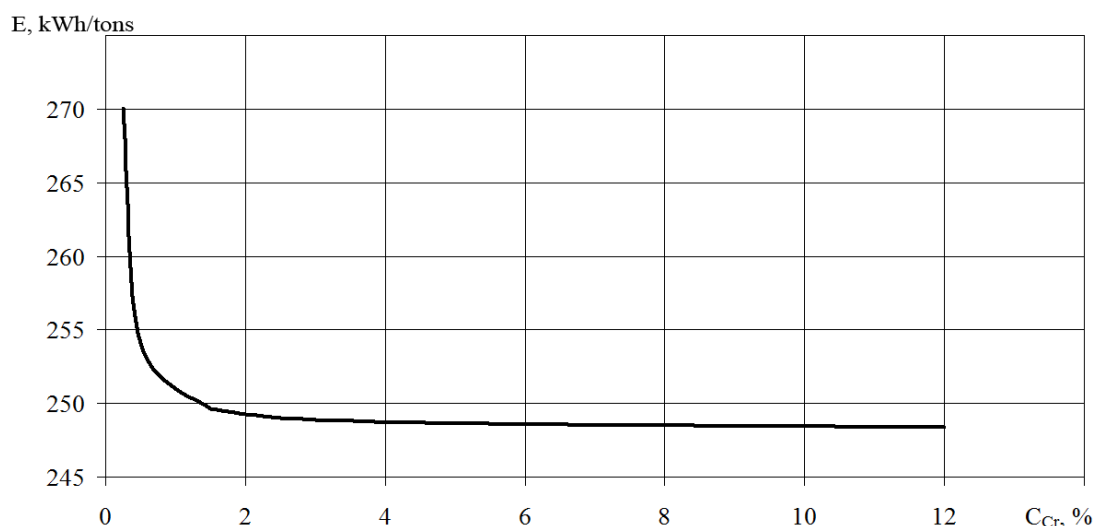
Fig. 4. The influence of increasing of the chromium content in the hardened steel of the auger on energy consumption of the MSW dehydration process after its operation and wear on the path s = 56850 m

As shown on the Fig. 4, after operation and wear on the path s = 56850 m during dehydration of MSW in the garbage truck, the increase in chromium content in the hardened steel of the auger from 0.25% to 12% leads to reduced energy consumption and to cheap the process of dehydration of solid waste in the garbage truck, which indicates the importance of determining the rational composition and structural state of the material of the friction surfaces of the auger and the ways to increase its wear resistance.

Conclusions

The hyperbolic dependencies of the auger wear depending on the chromium content in its hardened steel for different values of the friction path are determined. Carrying out additional regression analysis allowed to obtain the dependence of wear of the auger depending on the chromium content in its hardened steel and the friction path. It is established that on the way of auger wear s = 56850 m during dehydration of solid household waste in garbage truck, the increase of chromium content in auger steel from 0.25% to 12% allows to reduce energy consumption of solid waste dehydration from 12.2% to 3.1%, and, consequently, to reduce the cost of the process of dehydration in the garbage truck. Therefore, determining the rational composition and the structural state of the material of the friction surfaces of the auger and the ways to increase its wear resistance require further research.

Refrences

1. Kindrachuk M.V., Kutsova V.Z., Kovzel M.A., Hrebeneva A.V., Danylov A.P., Khlevna Yu.L. (2014) Tribotechnical properties of high chromium alloys are in the cast stay and after heat treatment. Problems of Tribology, 64(2), 58-63.

2. Dykha O.V. (2018) Rozrakhunkovo-eksperymentalni metody keruvannya protsesamy hranychnoho zmashchuvannya tekhnichnykh trybosystem: monohrafiya. [Computational and experimental methods for controlling the processes of maximum lubrication oftechnical tribosystems: a monograph.] Khmelnyts′kyi: KHNU.

3. Kaplun V.H., Honchar V.A, Matviishin P.V (2013) Pidvyshchennya znosostiykosti shneka ta ekstrudera pry vyhotovlenni kormiv dlya tvaryn iz domishkamy mineralnoho saponitu. [Improving the wear resistance of the auger and extruder cylinder in the manufacture of animal feed with impurities of the mineral saponite]. Visnyk of Khmelnytsky National University, 5, 7-11.

4. Dvoruk V.I. Vplyv lehuvannia khromom konstruktsiinoi stali na yii abrazyvnu znosostiikist pislia vysokotemperaturnoi termomekhanichnoi obrobky (VTMO) (2014). Problems of Tribology. 73. №. 3. S. 59- 65

5. Cymbal B.M. (2017) Pidvyshchennya znosostiykosti shnekovykh ekstruderiv dlya vyrobnytstva palyvnykh bryketiv u kyslotnykh ta luzhnykh seredovyshchakh [Increasing the wear resistance of auger extruders for the production of fuel briquettes in acidic and alkaline environments]: abstract dis. … cand. tech. sciences: 05.02.04 – Friction and wear in machines, Kharkiv, 20.

6. Hevko R.B., Zalutskyi S.Z., Hladyo Y.B., Tkachenko I.G., Lyashuk O.L., Pavlova O.M., ... & Dobizha N.V. (2019). Determination of interaction parameters and grain material flow motion on screw conveyor elastic section surface. INMATEH-Agricultural Engineering, 57(1).

7. Zhachkin S.Y., Trifonov G.I. (2017) Vplyv plazmovoho napylennya kompozytsiynykh poroshkovykh materialiv na znosostiykist′ detaley mashyn [Influence of plasma spraying of composite powder materials on the wear resistance of machine parts]. Master's Journal, № 1, 30-36.

8. Orisaleye J.I., Ojolo S.J., Ajiboye J. S. (2019) Pressure build-up and wear analysis of tapered screw extruder biomass briquetting machines. Agricultural Engineering International: CIGR Journal, 21(1), 122-133.

9. Eremenko O.I., Vasilenkov V.E., Rudenko D.T. (2020) Doslidzhennya protsesu bryketuvannya biomasy shnekovym mekhanizmom [Investigation of the process of biomass briquetting by auger mechanism]. Inzheneriya pryrodokorystuvannya, 3 (17), 15-22.

10. Demirci A., Teke I., Polychronopoulos N. D., Vlachopoulos J. (2021) The Role of Calender Gap in Barrel and Screw Wear in Counterrotating Twin Screw Extruders. Polymers, 13(7), 990.

11. Tataryants M.C., Zavynskyy C.S., Troshyn A.D. (2015). Rozrobka metodyky rozrakhunku navantazhen′ na shnek i enerhovytrat shnekovykh presiv [Development of a method for calculating auger loads and energy consumption of auger presses]. ScienceRise, 6 (2), 80-84.

12. Berezyuk O.V. (2018) Eksperymental′ne doslidzhennya protsesiv znevodnennya tverdykh pobutovykh vidkhodiv shnekovym presom [Experimental study of solid waste dehydration processes by auger press]. Visnyk Vinnyts′koho politekhnichnoho instytutu, № 5, 18-2413.

13. Bereziuk O.V., Savulyak V.I., Kharzhevskyi V.O. (2021) The influence of auger wear on the parameters of the dehydration process of solid waste in the garbage truck. Problems of Tribology, No 26(2/100), 79-86.

14. Bereziuk O.V., Savulyak V.I., Kharzhevskyi V.O., Osadchuk A.A. (2021) Research of the impact of carbon content in the auger material on its wear during dehydration in the solid waste garbage truck through regression analysis. –. – No 26(4/102). – P. 12-19.

15. Chatterjee S., Hadi A.S. (2015) Regression analysis by example. John Wiley & Sons.

Березюк О.В., Савуляк В.І., Харжевський В.О. Вплив легування хромом шнека на його знос під час зневоднення у сміттєвозі твердих побутових відходів

Стаття присвячена дослідженню впливу легування хромом шнека на його знос під час зневоднення твердих побутових відходів у сміттєвозі. За допомогою використання методу регресійного аналізу визначено гіперболічні закономірності зносу шнека залежно від вмісту хрому в його гартованій сталі для різних значень шляху тертя. Побудовано графічні залежності зносу шнека залежно від вмісту хрому в його гартованому матеріалі як функції шляху тертя, підтверджено достатню збіжність отриманих закономірностей. Додатковий регресійний аналіз дозволив встановити, що при двотижневій експлуатації шнека для зневоднення твердих побутових відходів у сміттєвозі збільшення вмісту хрому в гартованому матеріалі шнека з 0,25% до 12% дозволяє знизити швидкість зношування та енергоємність зневоднення твердих побутових відходів з 12,2% до 3,1%, а, отже, і до здешевлення процесу їхнього зневоднення у сміттєвозі. Показана графічна залежність зниження енергоємності зневоднення гартованим шнеком твердих побутових відходів внаслідок його легування хромом. Виявлено доцільність проведення подальших досліджень з визначення раціонального складу і структурного стану матеріалу шнека та шляхів підвищення його зносостійкості.

Ключові слова: знос, вміст хрому, гартування, шнековий прес, сміттєвоз, зневоднення, тверді побутові відходи, регресійний аналіз

Structure formation of abrasive-resistant coatings

V.I. Savulyak, V.Y. Shenfeld[*], O.P. Shylina, A.A. Osadchuk

Vinnytsia National Technical University, Vinnytsia, Ukraine
[*]E-mail: leravntu@gmail.com

Abstract

The paper presents the results of the study of abrasion-resistant coatings obtained by surfacing on alloying compositions Fe-Cr-Mo-V-C and Fe-Cr-B4C-Mo-C.It is established that with the increase of chromium in alloying compositions from 2% to 10%, the hardness and wear resistance of coatings increases due to the formation of a significant amount of complex alloyed carbides.The microhardness of the structural components of the deposited coatings correlates with the percentage of carbido-forming elements. Chromium-based coatings with the addition of vanadium, molybdenum and boron have shown high wear resistance under abrasive wear.

Key words: electric arc surfacing, alloying compositions, carbide inclusions, alloyed structures, microhardness.

Introduction

With the use of surfacing, parts are made that have special service characteristics of working surfaces, as well as their initial dimensions and operational properties of worn surfaces are repeatedly restored.Arc surfacing methods have become the dominant use in production practice. One of the most common methods is surfacing in shielding gases. And the development of surfacing technology using alloying elements is very important.

The main contribution to the wear resistance of the material is made by harder components, which are often carbides. Hence the desire to increase the amount of carbides in the structure of wear-resistant alloys. Sometimes their number is increased to 90% [1,2]. It is established that wear resistance is affected not only by size but also by the shape of carbides [3].

Grinding of carbide inclusions (for example, as a result of accelerating the crystallization of cast iron) increases wear resistance. Moreover, carbides in the form of isolated inclusions most intensively increase wear resistance. Less wear-resistant alloys have the structure of which contains ordinary cementite - an unstable phase. Under conditions of friction during operation, according to the modern theory of friction and wear, in the microzones of molecular adhesion there are so-called "high-temperature" points at which the substance can even pass into a plasma state. Under the influence of temperature, the wear-resistant components of the surface layer, in particular cementite, disintegrate, which leads to accelerated wear of working surfaces [5,6]. To stabilize cementite, it is necessary to introduce alloying elements that prevent the decomposition of cementite, namely: Cr, V, B, Mo and others.

One of the cheapest and most affordable elements is chrome, so it is most widely used in surface alloying of products [10]. The expediency of alloying the welded surfaces with chrome is due to the following circumstances:

- chromium cementite $(Fe, Cr)_3C$ has a higher hardness and therefore wear resistance than unalloyed Fe_3C cementite [1];

- doping with chromium increases the melting temperature of ledeburite, and hence the phenomenon of local melting at the points of high-temperature "flashes" in the "molecular" setting in the zone of friction and wear occurs much less frequently in alloyed cast iron;

- chromium increases chemical resistance and reduces oxidative wear at "setting points".

Studies of the processes of abrasive-corrosion wear of chromium steels [4,7,8,9] have shown that at low and moderate intensity of abrasive particles have sufficient resistance to steels with chromium content up to 14%. Instead of chromium often use V, B, Mo, forming carbides and carborides .

The introduction of boron into the deposited metal helps to change the critical ratios of carbide-forming elements to carbon, intensifies the release of special carbides [11] and carboborides $(Cr, Fe)_7(C, B)_3$ and $(Cr, Fe)_{23}(C, B)_6$), and also contributes to the grinding of the carbide phase, which significantly increases both the hardness and wear resistance of the weld metal [12]. Introduction to the alloy of 0.4 ... 0.6 wt. % boron shifts the eutectic point of alloys to the left, thereby promoting the loss of excess carbides and at the same time to increase the wear resistance of the weld metal, which works well even in conditions of intense abrasive wear without shock loads [2]. Other alloying systems use active carbides: tungsten, molybdenum, vanadium, titanium, niobium, tantalum, zirconium, which form monocarbides in the weld metal, increase its wear resistance, both at normal and at elevated temperatures. Excess alloying elements that are not involved in the formation of carbides, such as vanadium, molybdenum are soluble in solid solution, increase its strength at high temperatures. During heat treatment of welded products, or as a result of the thermal cycle of surfacing, as well as during their operation, supersaturated solid solutions can emit intermetallic compounds, which further increase the hardness of the metal [11]. Chromium-based coatings with the addition of vanadium, molybdenum and boron have shown high wear resistance under abrasive wear. The aim of the work is to create alloying compositions to counteract abrasive wear without shock loads.

Methods of experiments

On the original samples measuring 60x20x8 mm from steel sheet (steel 45) according to GOST 19903-2015 was applied prepared alloying composition (pre-mixed) in the form of a suspension in which the role of liquid dispersion medium was silicate glue (liquid glass according to GOST 13078-81), and the role of the solid dispersed phase is the powder charge (alloying complexes Fe-Cr-Mo-VC and Fe-Cr-B_4C-Mo-C).

In all cases, carbon was added to the composition in the form of graphite powder; alloying elements (chromium, molybdenum, vanadium) - respectively in the form of ferrochrome powders according to GOST 4757-91, ferromolybdenum according to GOST 4759-91, ferrovanadium according to GOST 27130-94; boron carbide. The applied suspension is quite viscous, after some time the samples were dried in an oven for 1 h at a temperature of 300oC. Surfacing of the prepared samples was performed on a surfacing unit UD-209M in carbon dioxide medium with copper-plated wire Sv-08G2S, 1.2 mm in diameter. Surfacing mode: current - 100 A, voltage - 25 V, surfacing speed - 5 m / h. Microstructural studies of the surface layers of the obtained samples were performed using MBS-6 and MIM-8 optical microscopes. Capturing images and converting them into digital form was carried out using a special eyepiece camera and computer. To perform microstructural studies, sections were made according to standard methods. Chemical etching of the sample surface was performed with a 4% solution of HNO3 in alcohol. Microhardness was measured with a microhardness tester PMT-3M.

Characteristics of prototypes

Used alloying compositions of the following composition:
1 - Cr-B4C-Mo-C - 2% chromium, 1% boron carbide, 0.5% molybdenum and 0.4% carbon;
2 - Cr-Mo-V-C - 5% chromium, 1% molybdenum, 1% vanadium, 0.8% carbon;
3 - Cr-Mo-V-C - 10% chromium, 1% molybdenum, 1% vanadium, 0.8% carbon.
Visible defects, micro- and macrocracks are absent for the deposited layers.

From the above data on the chemical composition of the components it is clear that the main alloying elements are chromium with the addition of vanadium, molybdenum or boron carbide in the presence of carbon.

Results of research and discussion

Figure 1 shows the structure of the base metal of steel 45, which is ferritic-pearlitic.
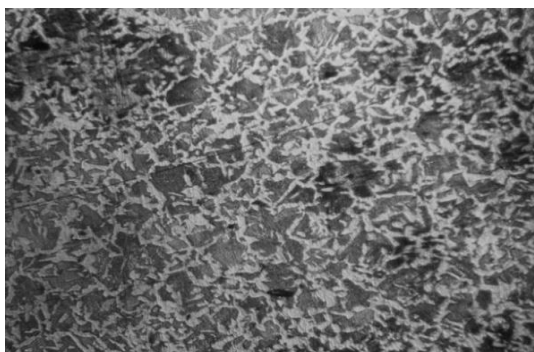
Fig.1. The structure of the base metal of steel 45 (x150)

The results of studies of the microstructures of the deposited coating system Fe-Cr-B4C-Mo-C are shown in Fig.2. In the transition zone (Fig. 2.a) a carbide grid was detected, which stood out along the grain boundaries. In the deposited layer (Fig. 2.b) this composition was ground grain due to the presence of carboborides with a limited amount of carbon.
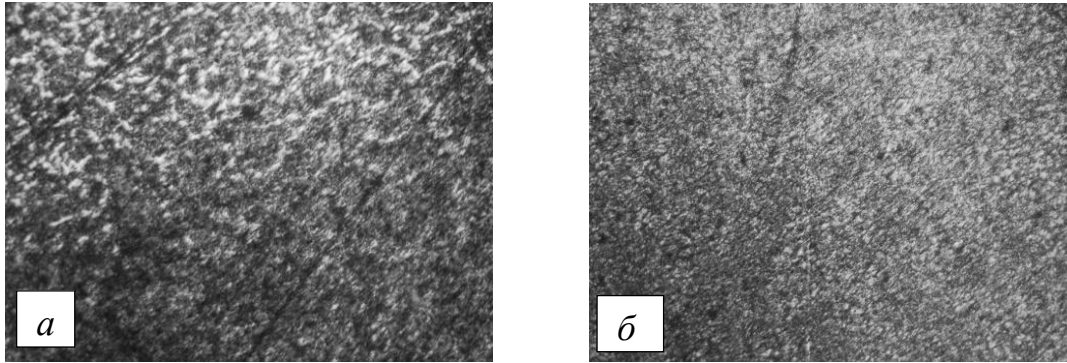
Fig.2. Microstructures of the deposited coating system Fe-Cr-B4C-Mo-C - 2% chromium, 1% boron carbide, 0.5% molybdenum and 0.4% carbon, thickness up to 0.5 mm (x150)

In fig. 3 shows the results of studies of the microhardness of the sample coated with the composition Fe-Cr-B4C-Mo-C, which is made on a microhardness tester PMT-3 with a step of 0.125 mm, starting from the coating surface to the base. The highest hardness is found on the surface of the coating and reaches ≈ 9500 MPa. Measurement of microhardness with a constant step leads to the fact that the indenter falls on different structural components. Carbides and carboborides show high hardness, and the matrix shows the hardness of hardened steel.
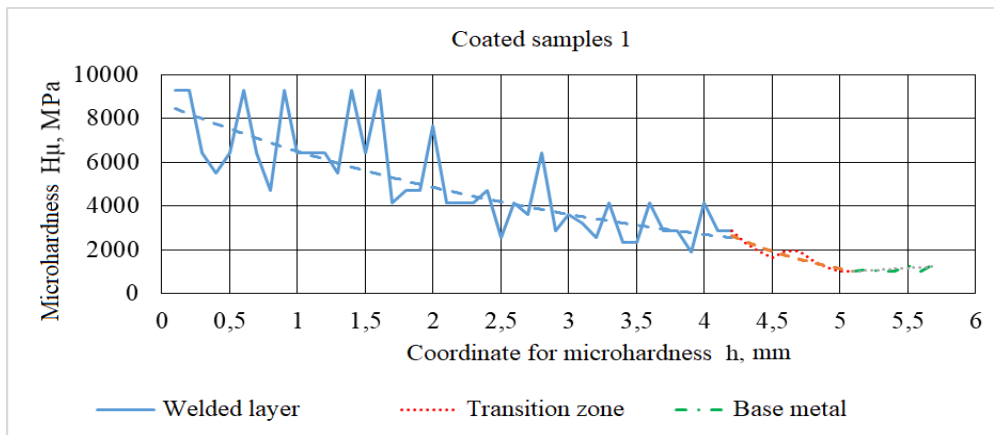
Fig. 3. Microhardness of the sample coated with the composition Fe-Cr-B4C-Mo-C - 2% chromium, 1% boron carbide, 0.5% molybdenum and 0.4% carbon

Figure 4 shows the microstructures of the transition zone (Figure 4, a) and the deposited coating of the Fe-Cr-Mo-V-C system (Figure 4, b). In the transition zone there are small inclusions and signs of stratification of structural components.
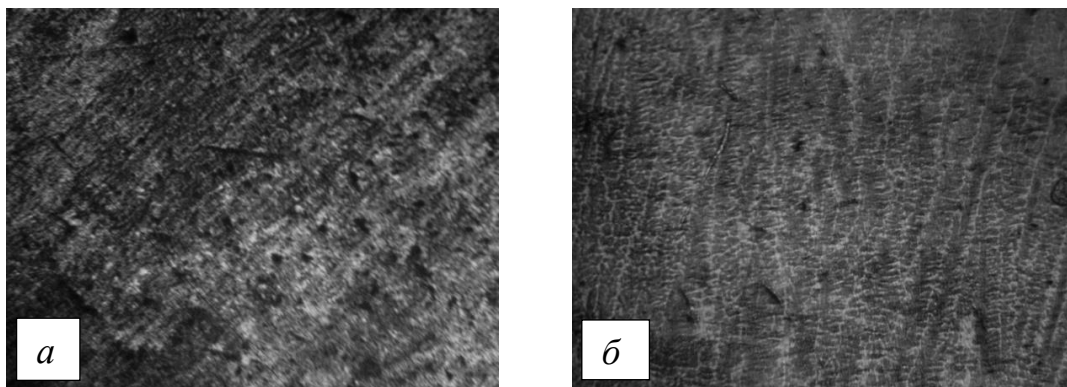
Fig.4. Microstructures of the deposited coating system Fe-Cr-Mo-V-C - 5% chromium, 1% molybdenum, 1% vanadium, 0.8% carbon, thickness up to 0.5 mm (x150)

In the deposited layer, a similar pain is also observed. The hardness of the surface layer (Fig. 5) was also measured with a hardness tester PMT-3 with a step of 0.125 mm from the surface to the depth of the coating. The maximum microhardness reaches ≈ 14000 MPa, and the microhardness of the matrix, as in the previous case for the Fe-Cr-B4C-Mo-C system, is ≈ 4500 MPa.
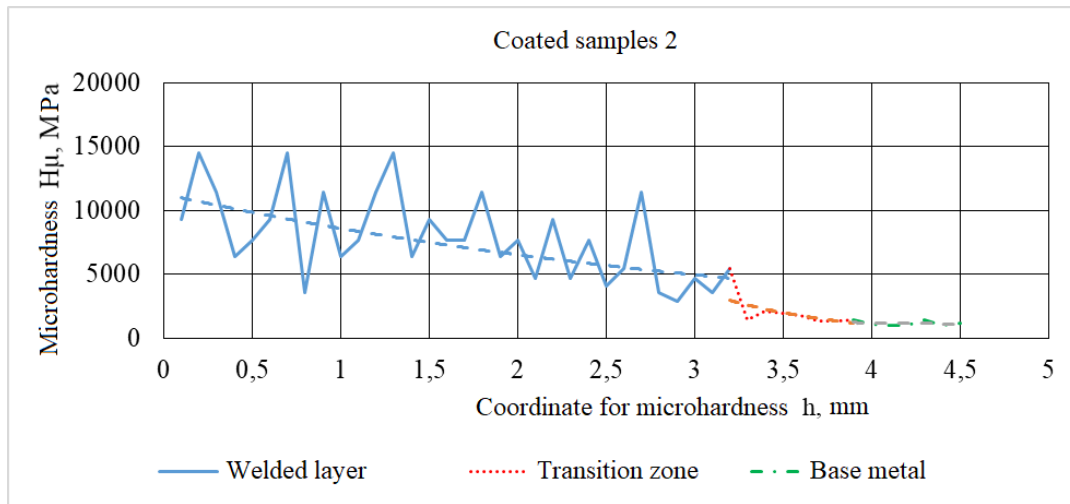
Fig. 5. Microhardness of the sample coated with the composition Fe-Cr-Mo-V-C - 5% chromium, 1% molybdenum, 1% vanadium, 0.8% carbon

Figure 6 shows the transition zone (Figure 6, a) and the deposited layer (Figure 6.b) of the Fe-Cr-Mo-V-C composition with high chromium content. In the transition zone, the inclusion of chromium defunted by various mechanisms is observed. Carbide mesh of the cementite type was formed in the deposited coating along the boundaries of small grains.
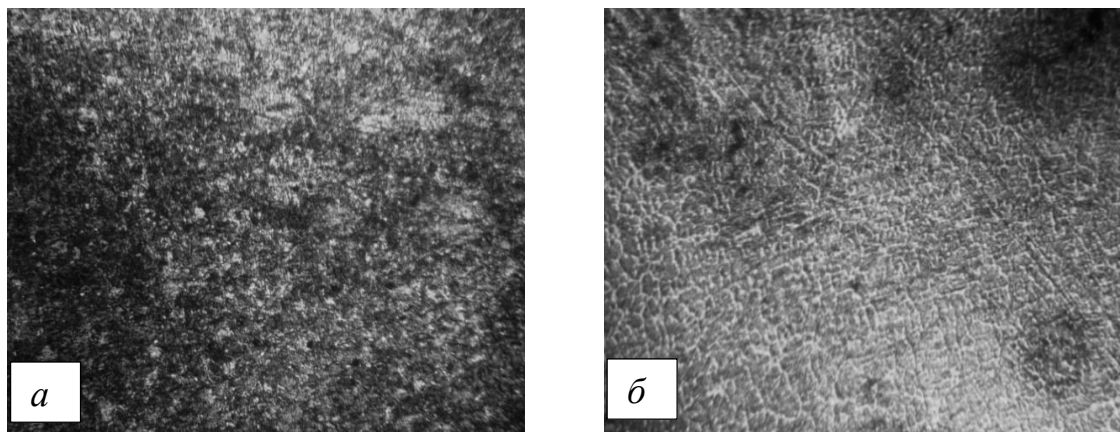
Fig.6. Microstructures of the deposited coating system Fe-Cr-Mo-V-C - 10% chromium, 1% molybdenum, 1% vanadium, 0.8% carbon, thickness up to 0.5 mm (x150)

The microhardness of the surface layer (Fig. 7) was measured by a similar method. The maximum microhardness reaches ≈ 15000 MPa, and the microhardness of the matrix, as in the previous case for the Fe-Cr-B4C-Mo-C system, is ≈ 8000 MPa due to doping.
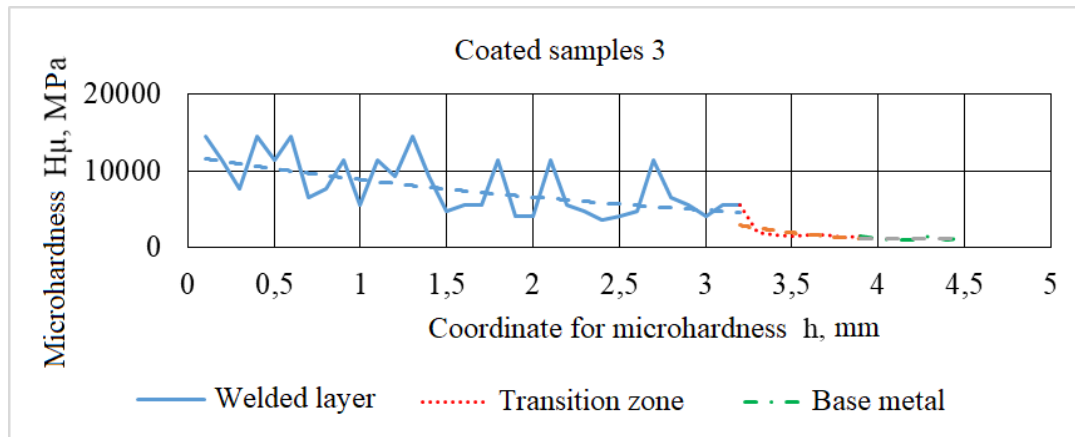
Fig. 7. Microhardness of the sample coated with the composition Fe-Cr-Mo-V-C - 10% chromium, 1% molybdenum, 1% vanadium, 0.8% carbon

The integrated hardness of the deposited layers is shown in Figure 8.
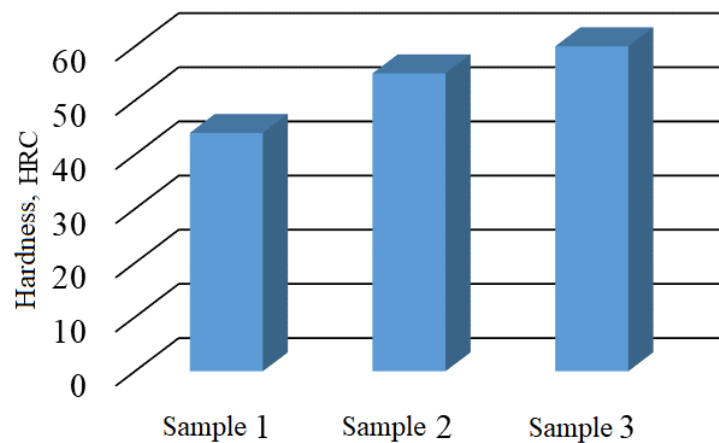
Fig.8 . Chart of hardness of prototypes

Coatings with hardness were obtained by the number of alloying elements: for the first sample (Cr-B$_4$C-Mo-C - 2% chromium, 1% boron carbide, 0.5% molybdenum and 0.4% carbon) - the hardness of the deposited surface was 44 HRC; for the second sample (Cr-Mo-V-C - 5% chromium, 1% molybdenum, 1% vanadium, 0.8% carbon) - 55 HRC; for the third sample (Cr-Mo-VC - 10% chromium, 1% molybdenum, 1% vanadium, 0.8% carbon) the surface hardness of the scale is 60 HRC, which is 5 units of HRC higher than the second sample due to different contents chromium (with the same content of other elements). Visible defects, micro- and macrocracks are absent for the deposited layers.

Conclusions

1. High wear resistance in abrasive wear showed chromium-based coatings with the addition of vanadium, molybdenum and boron.

2. With an increase in the amount of chromium in alloying compositions from 2% to 10%, the hardness and wear resistance of coatings increases due to the formation of a significant amount of complex alloyed carbides. The microhardness of the structural components of the deposited coatings correlates with the percentage of carbide-forming elements.

3. The introduction of boron carbides in the alloying composition promotes the grinding of grains.

References

1. Savulyak, V. I., Osadchuk, A.Yu. Savuliak, V. V. (2008) Contact melting of unalloed steel with graphite in diffusive unstazinary mode. / Bulletin of the polytechnic institute of Jasi, Rumuniia. – №LIV (LVIII). 85-90.

2. Popov, S. N. (2001) Optymyzatsyia khymycheskoho sostava naplavlennoho metalla detalei dlia raboty v uslovyiakh abrazyvnoho yznashyvanyia. Avtomatycheskaia svarka, № 4, 33 – 35.

3. Wieczerzak, K. [and etc.] (2016). Formation of eutectic carbides in Fe–Cr–Mo–C alloy during nonequilibrium crystallization. Materials & Design, № 94, 61-68.

4. Lin, C. [and etc.] Hardness, toughness and cracking systems of primary $(Cr,Fe)_{23}C_6$ and $(Cr,Fe)_7C_3$ carbides in high-carbon Cr-based alloys by indentation. Materials Science and Engineering, № 527, 5038-8.

5. Shakh, K. B., Kumar, S., Duvvedy D. K. (2006) Yznosostoikost naplavlennoho metalla systemy Fe-Cr-C. Avtomatycheskaia svarka, № 11, 27-31.

6. Osypov, M. Yu. (2014). Poysk y yssledovanye yznosostoikykh naplavochnыkh splavov dlia raboty v uslovyiakh abrazyvnoho yznashyvanyia pry povышennыkh temperaturakh. Novi materialy i tekhnolohii v metalurhii ta mashynobuduvanni, № 1, 52-57.

7.Kindrachuk M.V., Kutsova V.Z., Kovzel M.A., Hrebeneva A.V., Danylov A.P., Khlevna Yu.L. (2014) Tribotechnical properties of high chromium alloys are in the cast stay and after heat treatment. Problems of Tribology, 64(2), 58-638.8.Barker, K. S., Ball, A. (1989) Synergistic abrasive – corrosive wear of chromium containing stell. Brit. Cor, 24. № 3, 222-228.

9. Sokolov Kh. H. (2000) Vlyianye sootnoshenyia khroma, molybdena y uhleroda na strukturu y svoistva naplavlennoho metalla systemы Fe-Cr-Mo-C. Svarochnoe proyzvodstvo, № 11, 3-5.

10. Vosstanovlenye y povышenye yznososostoikosty y sroka sluzhbы detalei mashyn. Pod red. V. S. Popova. (2000). Zaporozhe, OAO «Motor Sych», 394.

11. Gang-chang Ji, Chang- Jiu Li, Yu-Yue Wang, Wen-Ya Li (2006) Microstrctural characterization and abrasive wear performance of HVOF sprayed Cr3C2- NiCr coating. Surface Coating & Technology (200) 6749-6757.

12. Messaadi, M., Kapsa, F. Wear behavior of high chromium sintered steel under dynamic impact-sliding: Effect of temperature. Tribology International, № 100, 380-387.

Савуляк В.І., Шенфельд В.Й., Шиліна О.П., Осадчук А.А. Структуроутворення нанесених абразивностійких покриттів.

В роботі показані результати дослідження абразивностійких покриттів, отриманих шляхом наплавлення на легувальні композиції Fe-Cr-Mo-V-C та Fe-Cr-B4C-Mo-C. Встановлено, що зі збільшенням кількості хрому в легувальних композиціях від 2% до 10%, підвищується твердість та зносостійкість покриттів за рахунок утворення значної кількості складнолегованих карбідів. Мікротвердість структурних складових наплавлених покриттів корелює з відсотком карбідотворних елементів. Високу зносостійкість в умовах абразивного зношування показали покриття на основі хрому з додаванням ванадію, молібдену та бору.

Ключові слова: електродугове наплавлення, легувальні композиції, карбідні включення, леговані структури, мікротвердість.

Determination of the dynamic hardness of greases as a characteristic of deformation properties in a tribocontact

O. Dykha*, A. Staryi, V. Dytyniuk, M. Dykha

Khmelnitskyi National University, Ukraine
*E-mail: tribosenator@gmail.com

Abstract

The efficiency of plastic oil is determined by the duration of its retention on the surface. Evaluation of the effectiveness of plastic lubricants depends on their mechanical properties. It is proposed to use the dependence of hardness on time when pressing a spherical indenter as one of the basic characteristics of the mechanical properties of plastic oils. The method of determining the function of oil hardness is based on the mechanics of contact interaction of a solid ball and a plane presented in this work, which has the property of creep according to the flow theory. One of the main methods of testing the deformation properties of plastic lubricants is to determine the number of penetrations. The number of oil penetrations is determined by the depth of indentation of the indenter; more informative for such a process is the ultimate pressure (hardness), which actually reflects the phenomenon of resistance to indenter indentation in the material. For uniform distribution of pressure under a spherical indenter the technique of construction of function of dynamic hardness of plastic materials is defined and on the basis of tests results of construction of dynamic hardness are received. Tests on contact creep of plastic lubricants are carried out, functions of dynamic hardness are received and the analysis of influence of character of change of dynamic hardness on wear processes in the presence of lubricants is carried out. To analyze the influence of deformation properties on the tribological properties of lubricants, comparative tests of the two above-mentioned types of lubricants on a four-ball friction device were performed. It was found that Litol-24 oil has the best wear resistance. The nonlinear period of running-in for this oil is practically absent that, obviously, under the given conditions of tests is connected with more stable in time deformation properties.

Keywords: grease, creep, penetration rate, dynamic hardness, test, wear.

Introduction

Plastic lubricants in the range of lubricants are the most common. Greases are thick oily products, which include: oil, thickener, solid carbon and various additives. A distinctive feature of plastic lubricants is that they are able, depending on working conditions, to have the properties of both solid and liquid substances. Under the action of small loads, lubricants behave like a solid body, can be held on vertical and inclined surfaces. The efficiency of plastic oil is determined by the duration of its retention on the surface. Evaluation of the effectiveness of plastic lubricants depends on their mechanical properties. Among the characteristics of mechanical properties, one of the most important is the shear strength of the oil. After the destruction of the frame, the oil begins to deform and flow like a liquid. Resistance to the flow of grease is characterized by viscosity. Typically, viscosity is determined at a single fixed strain rate. In the materials science of solids, the value of hardness is accepted as one of the mechanical characteristics. Hardness is the value of the average pressure under the indenter, which stabilizes the plastic deformation. In the mechanics of lubricants, the number of penetrations is analogous to the hardness of the lubricant. The number of penetrations is determined by pressing the cone into the flat surface of the grease and is measured in tenths of a millimeter for 5 seconds. With the help of the penetration number it is possible to estimate the effect of oil deformation at different temperatures. The disadvantage is that the number of penetrations is determined at one time point in the process that develops over time. At other time points of the penetration process, data on the hardness of lubricants can be obtained as opposed to those obtained at a holding time of 5 s. Also, the number of penetration of oil is

determined by the depth of indentation of the cone. For metals, hardness is defined as the ultimate pressure, which actually reflects the phenomenon of resistance to indenter indentation in the material.

Therefore, it is proposed to use the dependence of hardness on time when pressing the spherical indenter as one of the basic characteristics of the mechanical properties of plastic lubricants.

The method of determining the function of oil hardness is based on the mechanics of contact interaction of a solid ball and a plane presented in this work, which has the property of creep according to the flow theory.

Literatuter review

The study of the tribological properties of greases in world science is given quite a lot of attention. Based on modern methods of experimental and theoretical research, new highly effective lubricants are synthesized. The behavior and properties of lubricants are modeled under various operating conditions, under heavy loads, high heat, extreme speeds.

In paper [1] three kinds of new conductive lubricating greases were prepared using lithium ionic liquids as the base oil and the polytetrafluoroethylene as the thickener. The conductivities and contact resistances of the prepared lubricating greases were investigated using the conductivity meter and the reciprocating ball-on-disk sliding tester. The results suggest that the prepared lubricating greases have high conductivities and excellent tribological properties. The high conductivities are attributed to ion diffusion or migration of the lithium ionic liquids with an external electric field, and the excellent tribological properties depend on the formation of boundary protective films.

The study [2] investigates grease film evolution with glass disc revolutions in rolling elastohydrodynamic lubrication (EHL) contacts. The evolution patterns of the grease films were highly related to the speed ranges and grease structures. The transference of thickener lumps, film thickness decay induced by starvation, and residual layer were recognized. The formation of an equilibrium film determined by the balance of lubricant loss and replenishment was analyzed. The primary mechanisms that dominate grease film formation in different lubricated contacts were clarified.

In [3] the grease film distribution under a pure rolling reciprocating motion is observed on a ball-disk test rig. It is found that the reciprocating motion reduces the accumulation of the thickener fiber gradually with time. The maximum film thickness forms around the stroke ends. The life of grease lubrication under a transient condition is far below that under steady-state conditions. When increasing the maximum entraining speed of the reciprocating motion to a certain value, during which the thickener fiber is not expected to accumulate under a steady-state condition.

In paper [4] the technique of relative optical interference intensity and simple numerical calculations were used to investigate the lubricating behavior of grease lubricant films. Experimental results indicate that at a same entrainment velocity of the inlet, the central film thickness under deceleration is larger than that under acceleration. The numerical method can also be used to explain the behavior of the grease lubricating film under non-steady state conditions.

Thermal-induced changes in the viscous and viscoelastic responses of lubricating greases have been investigated sn [5]. Small-amplitude oscillatory shear and viscous flow measurements were carried out on a model conventional lithium lubricating grease. Two different regions, below and above this critical temperature, in the plateau modulus versus temperature plot have been detected. From this thermal dependence, a much larger thermal susceptibility of the lubricating grease is apparent. The thermo-mechanical reversibility of this material has been studied by applying different combined stress–temperature protocols. The experimental results obtained have been explained on the basis of the thermo-mechanical degradation of the lubricating grease microstructure.

In [6] a methodology for continuous monitoring of grease degradation subjected to mechanical shearing is proposed. It is hypothesized that the mechanical degradation of grease is akin to the running-in process in a tribo-pair with both transient and steady-state regimes. From the results, a more effective method using the entropy generation rate is proposed for continuous monitoring of grease degradation. The proposed method is extended to estimate the time for a grease subjected to mechanical shearing to degrade to a lower grade. The efficacy of this method is demonstrated via long duration testing in a custom-built ball-bearing test apparatus.

The tribological properties of a lithium calcium complex grease based on calcium sulfonate complex and lithium complex greases are investigated in [7]. The tribological properties of the latter greases are compared using an Optimol SRV reciprocating friction and wear tester. The morphologies of the worn surfaces are traced by a scanning electron microscope (SEM) and the chemical states of several typical elements on the worn surfaces are examined by x-ray photoelectron spectroscopy (XPS). The results indicate that the new grease has a low friction coefficient and good wear-resisting ability.

The dependence of the colloidal stability, effective viscosity, penetration, and yield stress of low-temperature polymeric greases on the composition and characteristics of the dispersion medium was investigated in paper [8]. Various types of low-viscosity oil with known fractional and group composition were used as base oils. The effect of the concentration of the two-component thickener of high- or low-molecular polypropylene and the proportions of its components on the main physicochemical characteristics of the polymer greases was determined. The dependence of the structure and properties of the polymer greases on the concentration of lithium stearate was established.

Also, the scientific works of the authors [9-12] are devoted to various aspects of the use of greases in technical applications. At the same time, the analysis of studies has shown that little attention has been paid to the study of the deformation properties of greases under various conditions of tribological contact.

Contact mechanics of the process of interaction between the sphere and the viscoplastic lubricant

The direct formulation of the problem of the interaction of a solid ball of radius with a plane in a state of creep includes three relations (Fig. 1):
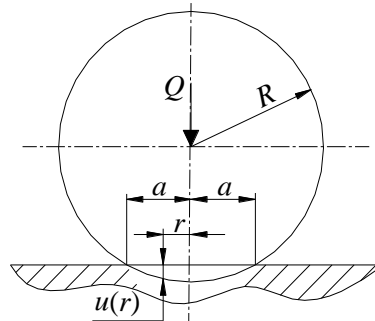
Fig.1. The scheme of contact of a ball and a viscoplastic plane

1) the model of constant creep of the lubricant material has the form:

$$\frac{du_c}{dt} = k_c \sigma^{m_c} ; \tag{1}$$

2) the condition of continuity in contact can be represented as:

$$u_c(t) = \frac{a^2(t) - r^2}{2R} ; \tag{2}$$

3) equilibrium condition in contact:

$$Q = 2\pi \int_0^a \sigma(t, r) r \, dr , \tag{3}$$

where $\sigma(t, r)$ is the time-dependent contact pressure distribution t ;

$a(t)$ is the radius of the circular area of contact;

r is the radial coordinate.

Differentiating condition (2) and equating (1) we have:

$$\sigma(t) = \left(\frac{1}{k_c} \frac{a}{R} \frac{da}{dt} \right)^{\frac{1}{m_c}} , \tag{4}$$

it is obvious that the pressure is evenly distributed over the contact area.
Substituting this expression in condition (3), we obtain:

$$Q = 2\pi \int_0^a \left(\frac{1}{k_c} \frac{a}{R} \frac{da}{dt} \right)^{\frac{1}{m_c}} r \, dr . \tag{5}$$

After integration we obtain a differential equation with respect to the function $a(t)$:

$$\left(\frac{Q}{\pi} \right)^{m_c} = a^{2m_c} \frac{a}{k_c R} \frac{da}{dt} . \tag{6}$$

Solving this equation, we have:

1) at $a(t = 0) = 0$:

$$a(t) = \left[(2m_c + 2) k_c R \left(\frac{Q}{\pi} \right)^{m_c} t \right]^{\frac{1}{2m_c + 2}} ; \tag{7}$$

2) at $a(t = 0) = a_0$:

$$a(t) = \left[(2m_c + 2) \left(k_c R \left(\frac{Q}{\pi} \right)^{m_c} t + a_0^{2m_c + 2} \right) \right]^{\frac{1}{2m_c + 2}} . \tag{8}$$

With a uniform distribution of contact pressures we have:

$$\sigma(t) = \sigma_0(t) = \frac{Q}{\pi a^2(t)} . \tag{9}$$

The maximum displacement from creep is obtained at $r = 0$:

$$u_{c0}(t) = \frac{a^2(t)}{2R} . \tag{10}$$

Example of calculating the size of the contact area when pressing the spherical indenter depending on (7).

Initial data:
1. Parameters of contact creep: $m_c = 1,82$; $k_c = 0,302$ МПа$^{-mc}$.
2. Spherical indenter radius $R = 6,35$ mm.
3. Indenter weight $Q = 1,9$ N.
Below are the results of the calculation obtained using the program MathCad.

t, min	2	3	7	17	37	67
$a(t)$, mm	1,47	1,58	1,83	2,14	2,46	2,73

Now suppose that the dependence of the radius of the contact $a(t)$ site on time is known from the experiment. It is necessary, using the solution of the direct problem, to determine the parameters k_c, m_c of the model of constant creep.

Consider the case of the initial zero contact site and present the experimental data in the form of a power approximation function:

$$a(t) = c_c t^{\beta_c} . \tag{11}$$

Substituting (11) into (7), we obtain:

$$c_c^{2m_c + 2} t^{\beta_c (2m_c + 2)} = (2m_c + 2) k_c R \left(\frac{Q}{\pi} \right)^{m_c} t . \tag{12}$$

From the condition that this equation is executable for any values of the argument t follows:

$$m_c = \frac{1 - 2\beta_c}{2\beta_c}.$$
(13)

For the second parameter from (12):

$$k_c = \frac{c_c^{\frac{1}{\beta_c}} \beta_c}{R\left(\dfrac{Q}{\pi}\right)^{m_c}}.$$
(14)

The obtained results can be used to describe the contact creep of solid balls covered with thin deformed layers of lubricant, which is promising in creating tribomechanics of thin lubricating layers.

У випадку ненульової початкової площадки контакту () необхідно визначати параметри моделі повзучості при заданій експериментальній функції:

In the case of a nonzero initial contact site ($a_0 \neq 0$), it is necessary to determine the parameters of the creep model k_c, m_c given a experimental function:

$$a(t) = a_0 + a(t).$$
(15)

The solution of the problem is performed provided that the values of the two experimental points are known:

$$(a_1, \ t_1); \ (a_2, \ t_2)$$
(16)

at $a_0 < a_1 < a_2$; $0 < t_1 < t_2$.

The solution of the direct problem (7) for two points is presented in the form:

$$\left. \begin{aligned} a_1^{2m_c+2} - a_0^{2m_c+2} &= (2m_c + 2)k_c R\left(\frac{Q}{\pi}\right)^{m_c} t_1, \\ a_2^{2m_c+2} - a_0^{2m_c+2} &= (2m_c + 2)k_c R\left(\frac{Q}{\pi}\right)^{m_c} t_2. \end{aligned} \right\}$$
(17)

Taking the ratio of equations, we obtain:

$$\frac{\alpha_1^{2m_c+2} - 1}{\alpha_2^{2m_c+2} - 1} = \frac{t_1}{t_2},$$
(18)

where $\alpha_1 = \dfrac{a_1}{a_0}$; $\alpha_2 = \dfrac{a_2}{a_0}$. This nonlinear equation can be solved numerically.

Це нелінійне рівняння можна розв`язати чисельним методом

Method for determination and research of dynamic hardness of plastic materials

The procedure for determining the parameters of the creep function of the oil at zero contact area is as follows.

The initial parameters of the process of pressing the ball into the surface of the grease are selected:

R is the ball radius; Q is the load to ball.

The ball is pressed into the surface of the oil with the measurement of the maximum depth of pressing u_{c_0}.

Using formula (10), determine the radius of the area of contact of the ball with the surface of the oil:

$$a(t) = \left[2Ru_{c_0}(t) \right]^{\frac{1}{2}}.$$

(19)

The experimental dependence of the radius of the contact site on time is represented as a power function:

$$a(t) = c_c t^{\beta_c}.$$

(20)

Approximation parameters c_c, β_c are determined by the method of least squares.

Parameters m_c, k_c models (1) of oil creep are determined by formulas (13) and (14).

The procedure for determining the parameters of the dynamic hardness of the oil is as follows.

The hardness of the oil H_L or the average pressure on the ball on the oil side is determined by the relationship of type (9):

$$H_L(t) = \frac{Q}{\pi a^2(t)}.$$

(21)

If the value of the radius of the contact site is known from the experiment, the hardness is determined immediately by formula (21).

If parameters are known for oil m_c, k_c model of contact creep, the function of dynamic hardness is determined by substitution (7) in (21) at the initial zero contact area:

$$H_L(t) = \frac{Q}{\pi \left[(2m_c + 2) k_c R \left(\frac{Q}{\pi} \right)^{m_c} t \right]^{\frac{1}{m_c+1}}}.$$

(22)

If it is necessary to compare the hardness of lubricants, functions are built $H_L(t)$.

When the non-zero contact area is set by the initial data R, Q and a_0. Conduct tests and obtain data for the function:

$$a(t) = a_0 + a(t).$$

Two points are chosen for the function:

$$(a_1, \ t_1); (a_2, \ t_2)$$

and write for them equation (18) in the form:

$$\frac{\alpha_1^x - 1}{\alpha_2^x - 1} = \bar{t}_{12},$$

(23)

де $x = 2m_c + 2$;

$\bar{t}_{12} = t_1/t_2$.

Numerically solve equations (23). The dynamic hardness of the oil is determined from the expression (22).

Investigation of dynamic hardness of plastic materials and its connection with wear

To implement the method of determining the parameters of contact creep of plastic materials, studies of bitumen and plasticine were performed by pressing a spherical steel indenter with a diameter of 12.7 mm and a

weight of 190 g. The results of research and calculations of the parameters of the contact creep model are given in table. 4.1 with graphical interpretation in Fig. 2.

Table 1

Test results for contact creep and determination of dynamic hardness of plastic materials

Material	Time t, min	Depth indentation, u_c, mm	The size of the contact area a_c, mm	Parameters approximations		Parameters models contact creep		Hrdness function, MPa
				c_c,	β_c	m_c	k_c	
plasticine	1	0,11	1,18	1,297	0,177	1,82	0,302	$H_L = 0,361t^{-0,35}$
	2	0,18	1,5					
	3	0,23	1,7					
	7	0,29	1,9					
	17	0,36	2,14					
	37	0,47	2,44					
	67	0,55	2,64					
bitumen	1	0,4	2,22	2,403	1,803	1,77	8,943	$H_L = 0,106t^{-0,36}$
	2	0,7	2,89					
	7	1,15	3,64					
	27	1,7	4,32					
	47	2,02	4,64					
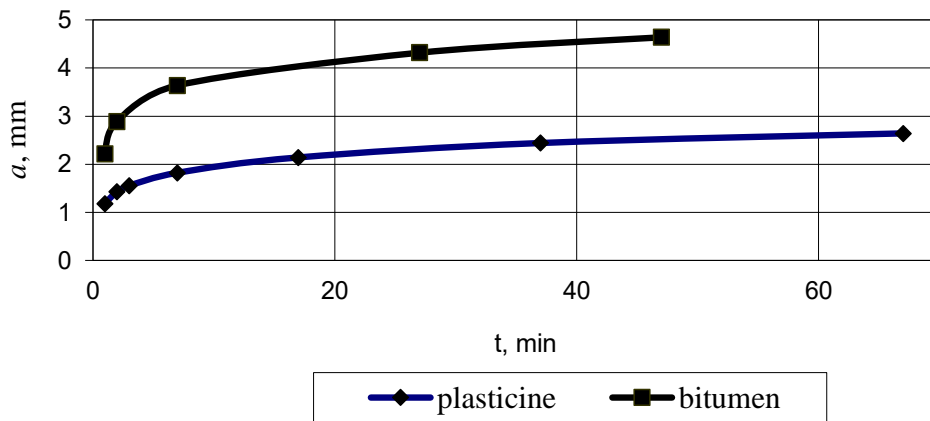
Fig. 2. The results of studies on contact creep

Results of tests of deformation properties of plastic oils by means of a ball with radius R= 15 mm are given in tab. 4 with graphical interpretation in Fig. 3.

Table 2

Test results of deformation properties of plastic lubricants

t, min	Ball, $d = 30$ mm, $m = 150$ g			
	Litol-24		Solidol C	
	a, mm	Δa, mm	a, mm	Δa, mm
0,08	12,75	0	9,86	0
0,6	12,99	0,24	10,09	0,23
2,6	13,15	0,4	10,30	0,44
7,6	13,36	0,61	10,51	0,65
17,6	13,64	0,89	10,71	0,85
47,6	13,89	1,14	10,9	1,04
107,6	14,07	1,32	10,99	1,13
227,6	14,2	1,45	11,09	1,23
407,6	14,44	1,69	11,18	1,32
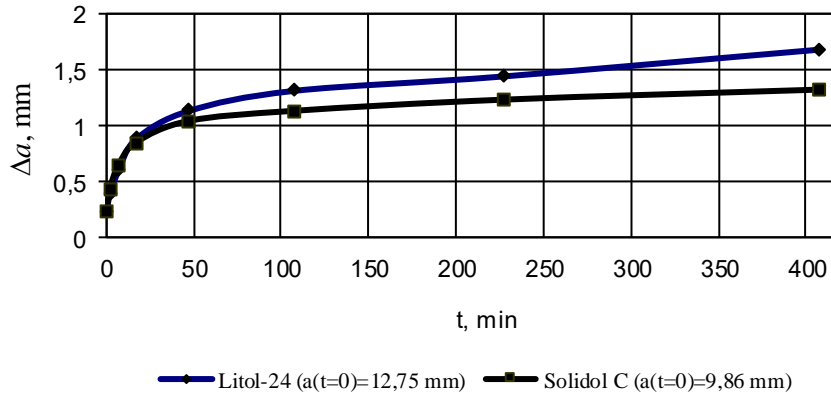
Fig. 3. The results of pressing the ball into the oil

The dependence (15) can be used to describe the process of pressing a cone and a ball with a non-zero initial contact pad.

As a result of processing the experimental data, the dependences for the contact site and the dynamic hardness when pressing the ball indenter into the surface of the plastic oil were obtained (Table 3).

Table 3

The results of determining the dynamic hardness for lubricants

Type of indentor	Solidol C	Litol –24
Steel ball, $R = 15$ mm	$a(t) = 9,86 + 0,334t^{0,258}$	$a(t) = 12,75 + 0,315t^{0,299}$
Dynamic hardness, MPA	$H_L(t) = Q / \pi a^2(t) = 0,48 / a^2(t)$	

According to the obtained results, graphical dependences of hardness for two types of investigated plastic lubricants are constructed, shown in fig. 4.
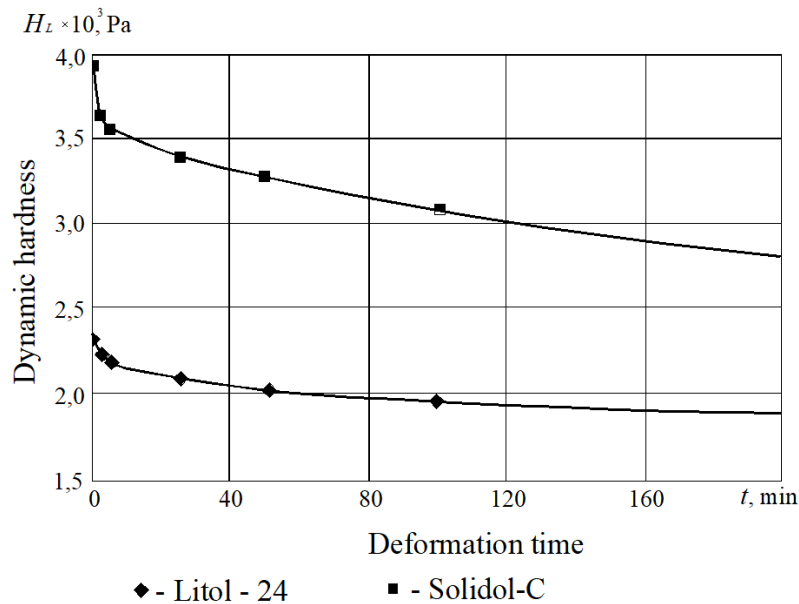
Fig. 4. Dynamic hardness of lubricants during deformation

Analysis of the obtained graphs shows that Litol - 24 oil has a lower dynamic hardness, but is characterized by more stable indicators over time. With a durability of almost 3 hours, the hardness of Solidol - 24 decreased by 40%, while Litol-24 decreased by only 20%, which indicates better stability of the load-bearing capacity of Litol -24 over time. The obtained dependences for the characteristic of dynamic hardness allow to

analyze the processes of deformation of lubricating layers of different lubricants under the action of applied loads.

To analyze the influence of deformation properties on the tribological properties of lubricants, comparative tests of the two above-mentioned types of lubricants on a four-ball friction device were performed. (V = 0.45 m/s; N = 350 N). As a result, the dependences of wear on the test time are obtained (Fig. 5).
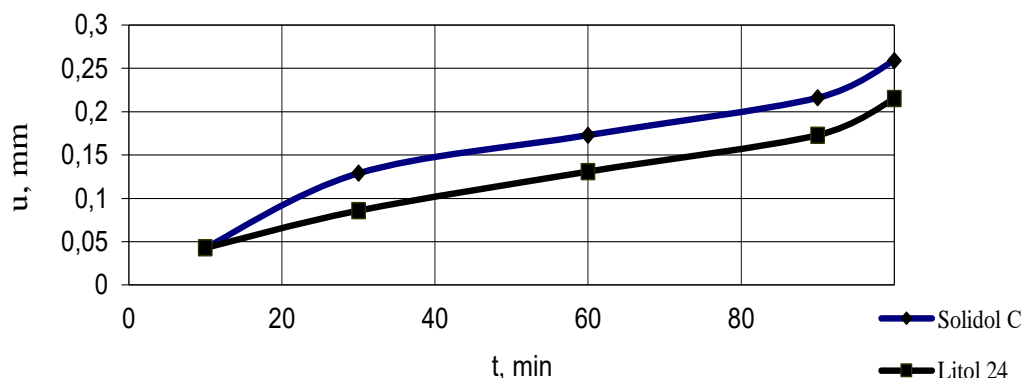
Fig. 5. Results of tribological tests of lubricants

It was found that Litol-24 oil has the best wear resistance. The nonlinear period of running-in for this oil is practically absent that, obviously, under the given conditions of tests is connected with more stable in time deformation properties.

Conclusions

1. One of the main methods of testing the deformation properties of plastic lubricants is to determine the number of penetrations. The essence of this method is to measure the depth of indentation of the conical indenter in the surface of the lubricant sample. The main disadvantages of this method are the following:

- the number of penetration is determined at one time point of the indenter indentation process, when measurements at other time points will be obtained data on the deformation of lubricants opposite to those obtained at a holding time of 5 s;

- the number of penetration of oil is determined by the depth of indentation of the indenter; more informative for such a process is the ultimate pressure, which actually reflects the phenomenon of resistance to indenter indentation in the material.

2. A more informative characteristic of the deformation properties of plastic materials is proposed - a function of dynamic hardness, which shows the dependence of the pressure of resistance to indenter indentation on the time of deformation.

3. To establish the analytical dependence for dynamic hardness, the mechanics of contact interaction of a rigid indenter in the form of a ball with plastic lubricant, which has the property of creep, is considered. Solved direct and inverse problems and recommendations for their use.

4. For uniform distribution of pressure under a spherical indenter the technique of construction of function of dynamic hardness of plastic materials is defined and on the basis of tests results of construction of dynamic hardness are received.

5. Tests on contact creep of plastic lubricants are carried out, functions of dynamic hardness are received and the analysis of influence of character of change of dynamic hardness on wear processes in the presence of lubricants is carried out.

6. The offered characteristic of dynamic hardness and a method of its definition allows to estimate and compare deformation and tribological properties of various plastic materials at certification control, operation and creation of new types of oils..

References

1. Fan, X., Xia, Y. & Wang, L. Tribological properties of conductive lubricating greases. Friction 2, 343–353 (2014). https://doi.org/10.1007/s40544-014-0062-2

2. Li, X., Guo, F., Poll, G. et al. Grease film evolution in rolling elastohydrodynamic lubrication contacts. Friction 9, 179–190 (2021). https://doi.org/10.1007/s40544-020-0381-4

3. Han, Y., Wang, J., Wang, S. et al. Response of grease film at low speeds under pure rolling reciprocating motion. Friction 8, 115–135 (2020). https://doi.org/10.1007/s40544-018-0250-6

4.   Li, G., Zhang, C., Luo, J. et al. Film-Forming Characteristics of Grease in Point Contact Under Swaying Motions. Tribol Lett 35, 149 (2009). https://doi.org/10.1007/s11249-009-9455-1

5.   Delgado, M.A., Valencia, C., Sánchez, M.C. et al. Thermorheological behaviour of a lithium lubricating grease . Tribol Lett 23, 47–54 (2006). https://doi.org/10.1007/s11249-006-9109-5

6. Lijesh, K.P., Khonsari, M.M. On the Assessment of Mechanical Degradation of Grease Using Entropy Generation Rate. Tribol Lett 67, 50 (2019). https://doi.org/10.1007/s11249-019-1165-8

7. Xia, Y., Wen, Z. & Feng, X. Tribological Properties of a Lithium-Calcium Grease. Chem Technol Fuels Oils 51, 10–16 (2015). https://doi.org/10.1007/s10553-015-0569-x

8. Zaichenko, V., Kolybel'skii, D.S., Popov, P.S. et al. Composition, Properties, and Structure of Low-Temperature Lubricating Greases Based on Polymeric Thickener. Chem Technol Fuels Oils 54, 531–540 (2018). https://doi.org/10.1007/s10553-018-0956-1

9. Ren, G., Zhang, P., Ye, X. et al. Comparative study on corrosion resistance and lubrication function of lithium complex grease and polyurea grease. Friction 9, 75–91 (2021). https://doi.org/10.1007/s40544-019-0325-z

10. Ge, X., Xia, Y., Shu, Z. et al. Erratum to: Conductive grease synthesized using nanometer ATO as an additive. Friction 3, 352 (2015). https://doi.org/10.1007/s40544-015-0085-3

11. Wang, Z., Shen, X., Chen, X. et al. Experimental investigation of EHD grease lubrication in finite line contacts. Friction 7, 237–245 (2019). https://doi.org/10.1007/s40544-018-0208-8

12. Huang, L., Guo, D., Wen, S. et al. Effects of Slide/Roll Ratio on the Behaviours of Grease Reservoir and Film Thickness of Point Contact. Tribol Lett 54, 263–271 (2014). https://doi.org/10.1007/s11249-014-0301-8

Диха О.В., Старий А.Л., Дитинюк В.О., Диха М.О. Визначення динамічної твердості консистентних мастил як характеристики деформаційних властивостей у трибоконтакті

Ефективність роботи пластичного мастила визначається тривалістю її збереження на поверхні. Оцінювання ефективності пластичних мастил залежить від їхніх механічних властивостей. Пропонується як одну з базових характеристик механічних властивостей пластичних мастил застосовувати залежність твердості від часу при втисненні сферичного індентора. Метод визначення функції твердості мастила ґрунтується на представленій в цій роботі механіці контактної взаємодії твердої кульки та площини, що має властивість повзучості за теорією течії. Одним з основних методів випробувань деформаційних властивостей пластичних мастильних матеріалів є визначення числа пенетрації. Число пенетрації мастила визначається глибиною вдавлювання індентора; більш інформативним для такого процесу є граничний тиск (твердість), який реально відображає явище опору вдавлювання індентора в матеріал. Для рівномірного розподілу тиску під сферичним індентором визначена методика побудови функції динамічної твердості пластичних матеріалів і на основі випробувань отимані результати побудови динамічної твердості. Проведені випробування на контактну повзучість пластичних мастил, отримані функції динамічної твердості і проведений аналіз впливу характеру зміни динамічної твердості на процеси зношування в присутності мастильних матеріалів. Для аналізу впливу деформаційних властивостей на трибологічні властивості мастил були проведені порівняльні випробування двох вказаних вище типів мастил на чотирикульковому приладі тертя. Встановлено, що мастило Литол-24 має кращі зносостійкі показники. Нелінійний період припрацювання для цього мастила практично відсутній, що, очевидно, за даних умов випробувань пов`язано з більш стабільними в часі деформаційними властивостями.

Ключьові слова: консистентне мастило, повзучість, число пенетрації, динамічна твердість, випробування, зношування

Study of the kinetics of wear of steels from the point of view of the provisions of the adhesive-hydrodynamic theory of wear

M.M. Poberezhnyi[1*], P.V. Kaplun[1], S.O. Kolenov[2]

[1]Khmelnytskyi National University, Ukraine
[2] Taras Shevchenko National University of Kyiv, Ukraine
*E-mail: antanta2015@gmail.com

Abstract

The article is devoted to the study of wear resistance of the surface layer of steels 40X and ШХ15, when rubbed in oil I-20. A comparison of the surface layer of samples of raw and nitrided steels, before and after the tests. The study of the fine microstructure of the samples with the help of the LDFP microscope, allowed us to conclude that the samples that were subjected to ionic nitriding, improved roughness. In turn, increased the area of linear contact, reduced contact load. The graphic dependence of roughness indicators is constructed. After testing, we can conclude that nitrided steel has a long service life, namely high hardness, resistance to abrasion, durability and corrosion resistance. The mechanism for obtaining increased resources needs further study.

Key words: test, operation, friction, 40X, ШХ15, ionic nitriding, sample, roughness, I-20

Purpose

Study of the kinetics of wear of steels from the point of view of the provisions of the adhesive-hydrodynamic theory of wear

Introduction

Quantitative comparison of performance characteristics of raw and nitrided steels. The studies were carried out with samples of 40X and ШХ15 steels. Rolling friction tests in I-20 oil were carried out for steels without and after heat treatment. The data are presented in tables.

Table 1

The nature of wear and durability of samples of steel 40X without heat treatment and nitrided, when tested for rolling friction in oil I - 20.

Test time, hour	The number of cycles, N·10⁶	Load per ball 150 H			
		Raw steel		Nitrided steel	
		Wear U, μm	Hardness H100, μm	Wear U, μm	Hardness H100, μm
0	0	0	5480	0	7460
10	5.4	5 − 6	5720	4 − 5	7500
25	13.5	–	–	–	–
50	27	10 − 12	–	9 − 12	7460
75	40.5	15 − 20	5550	14 − 19	–
100	54	26 − 30	5520	22 − 25	7280
150	81	–	–	–	–
200	108	40 − 45	5430	30 − 32	7100

Continuation of Table 1

250	135	–	–	–	–
300	162	55 − 60	5420	58 − 65	6840
350	189	370 hours			–
400	216	U = 58–62 μm,		65 − 70	6550
450	243	N·106 = 199.8, H100= 5520		–	–
500	270			70 − 75	5850
550	297			–	–
600	324			75 − 80	5400
650	351			–	–
700	378			80−85	4850
				The rest	

Table 2

Physical, mechanical and tribological characteristics of samples with different coatings and their durability during rolling friction tests in oil I-20.

Sample number	Steel grade	Type of heat treatment	Surface hardness	Load per ball 150 H		
				Test time, min	Wear U, μm	The number of cycles, $N \cdot 10^6$
1	ШХ 15	Without heat treatment	H_{100} 3340	80	46	0.7
2	ШХ 15	Tempered	HRC 60–61	–	–	–
3	ШХ 15	Tempered + nitrided	H_{100}= 5880	60	18	0.54
				Load per ball 300 H		
1	ШХ 15	Without heat treatment	H_{100} 3340	–	–	–
2	ШХ 15	Tempered	HRC 60–61	46	14	25.1
3	ШХ 15	Tempered + nitrided	H_{100}= 5880	34	38	18.4

Friction track of a sample made of 40X steel without heat treatment

12 hours of work

Friction track of a sample made of 40X steel, tempered and nitrided

183 hours of work

Fig. 1. Comparison of the friction paths of 40X steel samples without heat treatment and after nitriding, during friction in I-20 oil.

The studies of rolling friction in oil I-20 made it possible to determine the characteristics of strength, ductility and wear resistance of samples of steels 40X and ШХ15. The studies were carried out on samples without heat treatment, tempered and subjected to ion nitriding. The studies were carried out using a setup for testing contact endurance and wear resistance at linear contact. After the tests, it can be concluded that nitrided steel has a longer service life, namely, high hardness, resistance to seizure, endurance and corrosion resistance.

Study of the fine microstructure of samples using a LDFP microscope

Most carbon non-polar materials, when wetting the surfaces of machine parts, form epitropic liquid crystal structures on them in the nano- and micrometer range. Since their structure and properties are largely determined by the roughness of the working surface, it is necessary to have the most complete information about the three-dimensional state of the original surface. The nano-geometric surface of the samples needs appropriate control, which must be carried out by a non-contact method with high profile sensitivity and a sufficiently large field of view. Contact profilographs-profilometers of the Caliber M201 or M-283 type do not meet these requirements due to surface damage and low information content. Therefore, a laser scanning non-contact differential-phase microscope-profilograph-profilometer (LSDPMP) was used for the study. It was experimentally established that it is the 3D state of the working surfaces that characterizes their tribological properties, and not the roughness parameters (Ra, Rz, Rmax, Sm, tp, etc.), calculated only from the profilogram.

It has been experimentally established that for the same roughness parameter, in particular Ra, created by different technological methods, the surfaces have fundamentally different tribological properties depending on their 3D state.

In addition to roughness, the microscope allows you to determine the volume of worn material in cubic nanometers, which significantly increases the accuracy of determining the amount of wear.
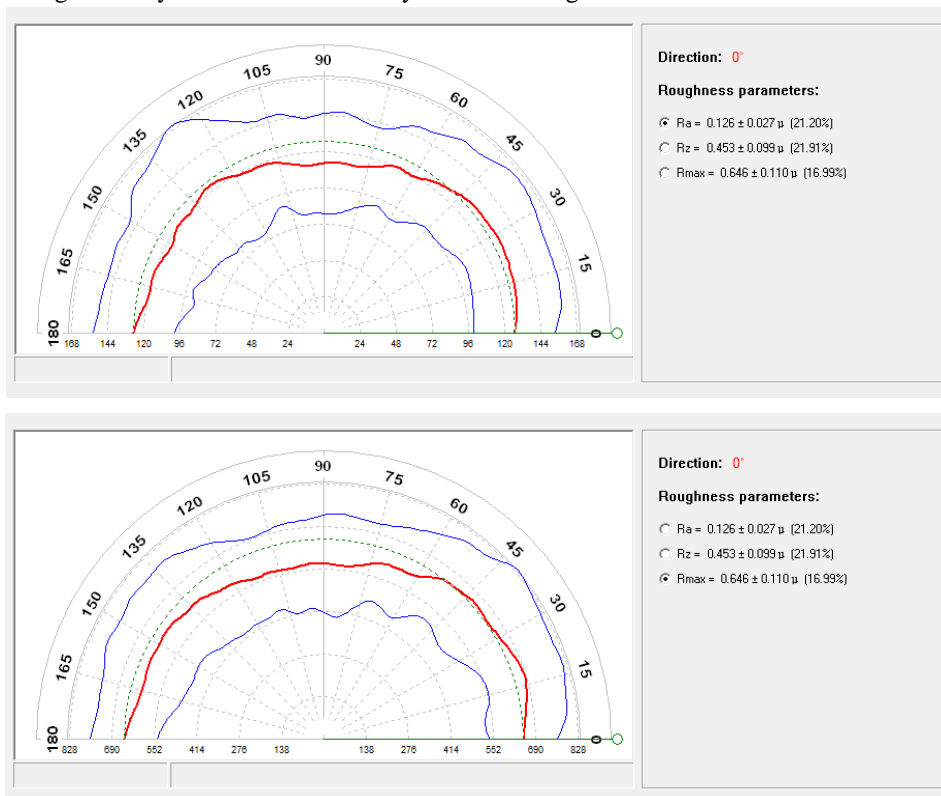
Fig. 2. Graph of displaying the dependence of the values of the roughness parameters on the azimuth angle in the XY plane

On the graph, the red line shows the angular dependence of the average value of the selected roughness parameter, and the blue lines show the boundaries of the deviation of this parameter from its average value within the studied area of the surface.

Results

After testing the wear resistance during rolling friction in I-20 oil, the surface of the samples was examined using an LDFP microscope, the results are presented in tables 3, 4.

Table 3

Parameters of the investigated roughness along the raceway.

No	Steel grade	Type of heat treatment	Roughness parameters, microns						
			Ra	Rz	Rmax	Rv	Rp	Rpk	Sm
1	40X	Without heat treatment, raw	0.125	0.525	0.694	0.346	0.348	0.137	48.255
2	40X	Temper + nitrided	0.096	0.472	0.585	0.299	0.286	0.110	25.392
3	ШХ15	Temper + nitrided	0.074	0.356	0.443	0.214	0.229	0.087	27.188
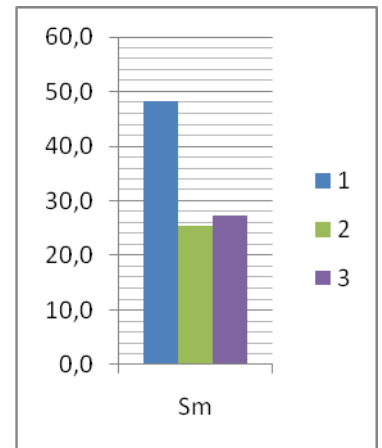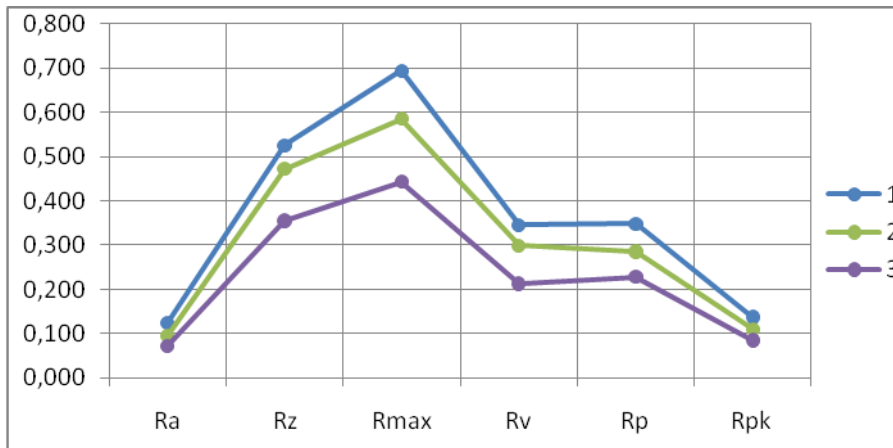
Table 4

Parameters of the investigated roughness along the lateral surface

No	Steel grade	Type of heat treatment	Roughness parameters, microns						
			Ra	Rz	Rmax	Rv	Rp	Rpk	Sm
1	40X	Without heat treatment, raw	0.161	0.652	0.855	0.410	0.445	0.187	48.078
2	40X	Temper + nitrided	0.036	0.177	0.217	0.113	0.103	0.038	27.596
3	ШХ15	Temper + nitrided	0.079	0.360	0.426	0.213	0.213	0.088	33.931
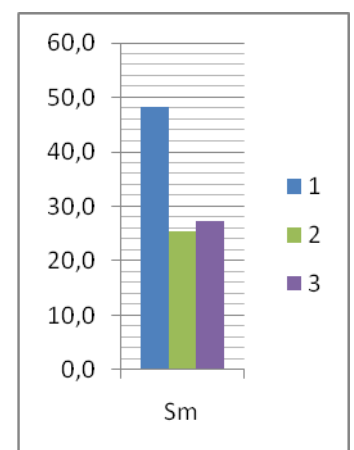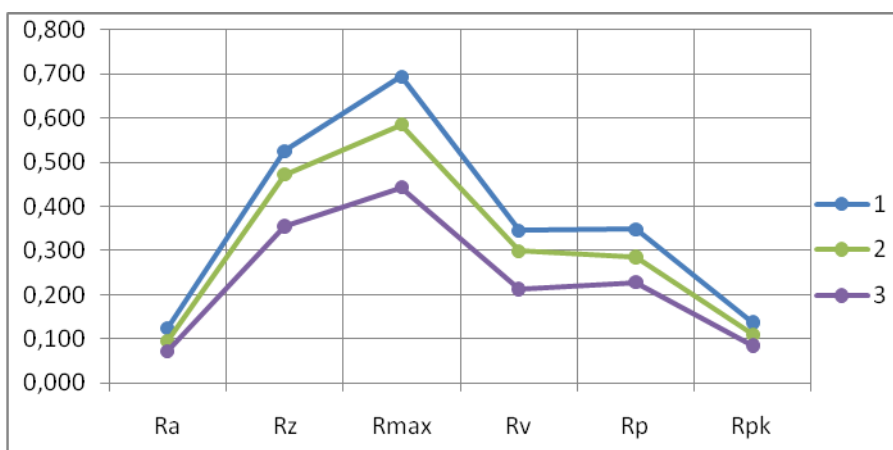
Conclusion

Samples of steel 40X and ШХ-15 were used for the experiment. The experiments carried out confirmed that the surface roughness of the boundary layer after ion nitriding improved, namely, the step of irregularities, the difference between tops and troughs of the relief decreases, the area of irregularities decreases, which in turn leads to an increase in the surface contact area, a decrease in the contact load.

References

1. Kaplun, P.V. Influence of Hydrogen on the Ion Nit riding of Steels (2018) Materials Science, 53 (6), pp. 818-822 DOI: 10.1007/s11003-018-0141-z

2. P. V. Kaplun, V. A. Honchar, T. V. Donchenko. Contact Durability of Steels After Ion Nit riding in Hydrogen-Free Media Materials Science, November 2019, Volume 55, Issue 3, pp 424–429 DOI:10.31891/2079-1372-2018-90-4-80-84

3. P.V. Kaplun, E.B. Soroka, A.V. Snozik/ The Impact of Hydrogen-Free Ion Nit riding on Physico mechanical and Performance Characteristics of Hard Alloys T5K10 and T15K6. 2018, Sverkhtverdye Materially, 2018, Vol. 40, No. 6, pp. 26–35 DOI: 10.3103/S1063457618060035

4. P.V.Kaplun, B.A. Lyashenko, O.Y. Rudyk, V.A. Gonchar / Life of Boride Coatings on Steels Under Cyclic Contact Load. Strength of Materials. 2021. Vol. 53. № 2. pp 291–296.DOI: 10.1007/s11223-021-00288-w

5 Molebny V.V., Kamerman G.W., Ilchenko L.M., Kolenov S.O., Goncharov V.O., Smirnov E.M., "Three-beam scanning laser radar profilometer", Proc. SPIE, 1998, Vol. 3380, P. 280-283.

6 Yano T., Kawabuchi M., Fukumoto A., Watanabe A. TeO2 acousto-optic Bragg light deflector without midband degeneracy // Appl. Phys. Lett. (USA), vol.26, no.12, p.689-91 (1975).

Побережний М.М. Каплун П.В. Каленов С.О. Дослідження кінетики зношування сталей з точки зору положень адгезійно-гідродинамічної теорії зношування

Стаття присвячена дослідженню зносостійкості поверхневого шару сталей 40Х і ШХ15, при терті кочення в мастилі I-20. Проведено порівняння поверхневого шару зразків сирих та азотованих сталей, до та після випробувань. Проведене дослідження тонкої мікроструктури зразків за допомого мікроскопу ЛДФП, дозволило зробити висновок, що у зразках які були піддані іонному азотуванню, покращились показники шорсткості, що в свою чергу збільшило площу лінійного контакту, зменшилось контактне навантаження. Побудована графічна залежність показників шорсткості. Після проведених випробувань можна зробити висновок що азотована сталь має великий ресурс роботи, а саме велику твердість, стійкість проти спрацювання, краща витривалість та корозостійкість. Виявлено доцільність проведення подальших досліджень з визначення впливу ХТО на механізми зношування поверхонь та шляхів підвищення їх зносостійкості.

Ключові слова: випробування, спрацювання, тертя, 40Х, ШХ15, іонне азотування, зразок, шорсткість, I-20.

Substantiation of conditions of effective working capacity of tribocouples of the details made of polymeric composite materials with high-modulus fillers

V.V. Aulin*, A.V. Hrynkiv, S.V. Lysenko, O.M. Livitskyi

Central Ukrainian National Technical University, Ukraine
*E-mail: AulinVV@gmail.com

Abstract

This work is devoted to the study of the conditions of effective performance of triad couplings of parts made of polymeric composite materials. The stress state of the material is associated with the characteristics of the accumulation of dislocations, the energy of activation of their movement. The average stress, friction stress is determined. Based on this, expressions for estimating critical stresses and loads on tribocouple parts are obtained. The distribution of the force on the tribocoupling of parts is determined taking into account the quality characteristics of the friction surfaces, modulus of elasticity and Poisson's constant of the components of the polymer composite material. This problem is considered for tribocouples of parts of various kinds.

Expressions for calculation of nominal pressures at different types of contact of material of details of tribocoupling are received, and also the equations on which it is possible to estimate in them values of nominal critical pressure are resulted.

The conditions for efficient operation of tribocoupling of parts made of polymer composite materials are clarified. It is determined that a significant increase in the nominal critical pressure on the tribocoupling is possible with the use of high-modulus fillers, the modulus of elasticity of which is greater than the modulus of elasticity of the polymer matrix.

Key words: polymer composite material, macroheterophase material, high modulus filler, tribocoupling of parts, matrix, filler, stress field, elastic contact, critical pressure, nominal pressure

Introduction

The efficiency of using tribocouples of parts made of macroheterophase polymer composite materials depends on the content of the filler, its size, shape, nature and tribological properties of the structural components of the composite material and the strength of the bond between them.

Today there is no single theory of reliability and efficiency of tribotechnical polymer composites and methods of substantiation of their optimal composition and structure. Existing methods for predicting the composition and structure of composites cover some cases due to practical application, but they do not take into account different types of contacts, the presence of an elastic component, which is achieved during the correct running of parts and critical pressure on the triad. There is also no criterion by which it is possible to assess a degree of efficiency of the triad couplings of systems and units of machines, parts of which are made of polymeric composite materials with high-modulus fillers.

Literature review

The use of tribocoupling of parts made of polymeric composite materials (PCM) has shown their effectiveness in increasing the durability of systems and units of machines [1-3]. However, there is a problem of optimizing the composition of polymer composites from the content of fillers, the distribution of stress fields in the polymer matrix, the geometric shape and concentration of the filler and the development of methods for

evaluating the efficiency and reliability of such tribocouples [4,5].

Specific features of the work of PCM with a macroheterogeneous structure necessitate the analysis of the stress-strain state (SSS), which occurs under load conditions during operation [6-8] by friction forces. There is a need to take into account different types of triangular parts and different types of contacts of their work surfaces. The same amount of deformation of the components of PCM can lead to brittle destruction of one component, to viscous – the second component and tired – the third component [7]. The strength characteristics of each of the components of the PCM are decisive. Research on SSS of surface layers reinforced with PCM [8] revealed the need to take into account the interaction of neighboring contour and actual contacts in the process of sliding friction. In the scientific literature, this issue is insufficiently studied and not all types of wear in the conjugation of machine parts are considered [9,10]. PCM chipping and exfoliation processes should also be considered. Note that in the implementation of such performance properties of materials as their wear resistance, the task is complicated by the significant dependence of stresses on the volume ratio of components, their size, shape, as well as design features of conjugate parts and properties of working (technological) environment.

The authors of [11-14] the main cause of destructive processes in the surface layers of PCM is SSS, which occurs as a result of contact stresses and deformations under the influence of loads on the tribocoupling of parts. This leads to a detailed study of the features in the surface layers of the materials of the tribocouples of parts. The study of the peculiarities of PCM in the process of functioning of three-part couplings allows to approach unsolved problems from a single position. The use of physical and mathematical models [7,8] is appropriate, and VAT estimates are carried out by load distribution in different types of contact by polarization-optical and other methods [9]. Attempts to compare the wear resistance and SSS of the surface layers of PCM made in [11]. According to research conducted in [15], there is a need for relaxation of local maximum stresses in the surface layers of tribocouple parts. It was found that with increasing volumetric content and filler size, the intensity of wear of parts decreases. However, the influence of these factors on the value of the maximum tangential stresses in the PCM is not sufficiently clarified [4,16].

The connection between the wear process of PCM and their mechanical properties is given in [6, 17]. The results of wear resistance studies of PCM with homogeneous and heterogeneous structure show that in the first case it is lower than in the second due to faster equalization of contact pressure. The phenomenon of spontaneous installation and maintenance of the stationary mode of wear of PCM is also revealed. This is due to the existence of feedback. Based on the ideal conditions of sliding contact, in [5] with the help of friction surface models, tribotechnical characteristics of PCM with different structure and different composition were calculated.

The current results of research [4-6] do not allow to fully assess the effectiveness of the triad coupling of parts and the nature and amount of wear. There is a need to connect them with the types of contacts and the conditions of contact.

It was found that in the operation of tribocouples of parts, elastic and plastic deformation of their materials are the main processes that initiate the emergence and development of physical, chemical and mechanical processes in the surface layers of PCM [17]. It is shown that in the PCM the main part of the load is received by the filler. Reinforcing fillers prevent the movement of dislocations in the matrix, which is subject to plastic deformation, limiting it [3]. Strengthening of PCM is carried out by increasing the content of the filler and reducing the distance between its particles. In [9] it was found that depending on the structural state of the PCM, the magnitude of the accumulated plastic deformation is not the same, which causes a different course of relaxation processes. The type and dispersion of filler particles (carbides, borides, oxides, intermetallics) in the polymer matrix, which are barriers to plastic deformation, significantly affect the inhibition of the relaxation process, but it is not known how the degree of dispersion of the filler affects the properties of PCM, filler – for stress relaxation, wear process and efficiency of triboconjugation of parts in general.

Purpose

The aim of this work is to identify the conditions for the effective operation of various truboconjugations of parts made of macroheterophase polymer composite materials with high modulus filler, taking into account different types of contact.

Results

Using different combinations of PCM, regarding the variation of high-modulus fillers in the polymer matrix, it is possible from a macroscopic point of view to ensure the predominant presence on the friction surfaces of parts of one or another type of contacts. Analytical methods for estimating the optimal structure of such PCM have not yet been developed. To determine the allowable force in heavy-duty tribocouples of parts made of macroheterophase PCM, one of the efficiency indicators can be the critical pressure, the value of which is estimated at the beginning of plastic deformation, brittle fracture or setting of friction surfaces. This uses the fact that in macroheterophase PCM the nature of deformation and fracture is similar to the nature of deformation and fracture of single-phase materials.

It is quite clear. that in tribocouples of parts made of materials of macroheterophase structure, the contacts of the two surfaces of polymeric materials are the least effective. These materials should be used in reinforced

form and provide such structures and composition that the share of space occupied by the contacts of two plastic materials was minimal, and with high-modulus fillers – maximum.

The quantitative efficiency of different types of contacts can be assessed by assuming that the main mechanism of setting of PCM materials is the formation of a common degree on the surface of physical contact. In this case, the stress created by the accumulation of dislocations in the area of the sources of dislocations, which is located beyond the contact boundary at a distance l, is:

$$\sigma_l = \sigma_f + \frac{1}{2}\left(\sigma - \sigma_f\right)\left(l_s / l_d\right), \tag{1}$$

where σ_f – friction stress; l_s – length of the sliding strip; l_d – distance to the cluster of dislocations.

If with increasing current voltage the value σ reaches the value σ_l at which the source of dislocations begins to work, we can assume that $\sigma_l = \overline{\sigma}$, $\sigma = \sigma_{cr}$, where $\overline{\sigma}$ is the average voltage; σ_{cr} – critical value of voltage. In this case, the value of the critical voltage is equal to:

$$\sigma_{cr} = 2\overline{\sigma}\left(\frac{l_d}{l_s}\right)^{1/2} + \sigma_f\left(1 - 2\left(\frac{l_d}{l_s}\right)\right)^{1/2}, \tag{2}$$

where $\sigma_f < \overline{\sigma}$; $l_d << l_s$.

The value of the average voltage can be determined from the equation:

$$\overline{\sigma} = \left(\frac{3b_d \ddot{e}k_b T}{V}\right)^{1/2} \exp\left(U_0 / 3k_b T\right), \tag{3}$$

where b_d – constant, characterizing the degree of deformation, 0.2%, of this material; $\dot{\varepsilon}$ – the rate of relative deformation of the material; V – activation volume; k_b – became Boltzmann; T – absolute temperature; U_0 – dislocation motion activation energy.

Similar to equation (3), the amount of friction stress is determined:

$$\sigma_f = \left(\frac{3b_d^f \ddot{e}k_b T}{V^f}\right)^{1/2} \exp\left(U_0^f / 3k_b T\right). \tag{4}$$

Given expressions (3) and (4) in equation (2), we obtain:

$$\sigma_{\kappa p} = 2\left(\frac{l_d}{l_s}\right)^{1/2}\left(\frac{3b_d \ddot{e}k_b T}{V}\right)^{1/2} \exp\left(U_0 / 3k_b T\right) + \left(1 - 2\left(\frac{l_d}{l_s}\right)\right)^{1/2}\left(\frac{3b_d^f \ddot{e}k_b T}{V^f}\right)^{1/2} \exp\left(U_0^f / 3k_b T\right), \tag{5}$$

Taking the critical load P_{cr} proportional σ_{cr}, we have:

$$P_{cr} = C_u \sigma_{cr} = C_u \left\{ 2\left(\frac{l_d}{l_s}\right)^{1/2}\left(\frac{3b_d \ddot{e}k_b T}{V}\right)^{1/2} \exp\left(U_0 / 3k_b T\right) + \left(1 - 2\left(\frac{l_d}{l_s}\right)\right)^{1/2}\left(\frac{3b_d^f \ddot{e}k_b T}{V^f}\right)^{1/2} \exp\left(U_0^f / 3k_b T\right) \right\}, \tag{6}$$

where C_u – is the coefficient that takes into account the shape and size of the contact irregularities of the working surfaces of the parts.

The lack of data on the values of C_u, l_d, b_d, b_d^f, U_0, U_0^f does not allow to determine the specific value of the critical load P_{cr} for a given triad of parts. From equation (16) it follows that the value P_{cr} of is greater the greater the energy of motion of dislocations U_0 and U_0^f.

Analysis of the influence of the structure and phase composition of PCM on the quality parameters of friction surfaces showed that when contacting tribocouples of parts made of macroheterophase composites, it is possible to provide the required share of friction surface area. In this case, you should use the laws of contact established for tribocoupling of the first kind, when single-phase material is in contact with single-phase. At the same time, the presence on the friction surface of areas with different composition of contact materials leads to a redistribution of contact pressures between contacts of different types. This causes a change in the critical load on the triad coupling of parts, and hence the coefficient of friction and wear resistance.

It is found that while ensuring the process of minimal wear and stabilization of the friction force, it is necessary to create such conditions when in the process of operation of tribocouples of parts on their friction surfaces an elastic contact is realized. Note that in the simplified calculation of the triad of parts with PCM in the first approximation, the following is taken into account:

– materials of tribocouples of the corresponding details consist of matrices M_1 and M_2 and fillers H_{1i} and H_{2j};

– the number of fillers in the material of the first part is i, and in the second – j;

– all parts of the total friction surface are real in triad conjugation;

– the structure of the PKM and the mutual orientation of the details of the triad coupling ensure the

independence of the fraction of the area occupied by one type of contact from their displacement along the direction of friction;

– the relative volume content of the filler in the surface layer of the parts is constant, the effect of their self-lubrication is absent, and secondary structures are not formed.

In the case of flat surfaces, with a nominal contour area of contact, the proportion of the area occupied by a particular type of contact is found by the expressions:

$$
\left.
\begin{aligned}
\alpha_{M_1-M_2} &= \left(1 - \sum_{i=1}^{n} \alpha_{1i}\right)\left(1 - \sum_{j=1}^{m} \alpha_{2j}\right); \\
\alpha_{M_1-M_{2j}} &= \left(1 - \sum_{i=1}^{n} \alpha_{1i}\right)\alpha_{2j}; \\
\alpha_{M_2-M_{ij}} &= \left(1 - \sum_{j=1}^{m} \alpha_{2j}\right)\alpha_{2j}; \\
\alpha_{H_{1i}-H_{2j}} &= \alpha_{1i}\alpha_{2j}; \quad i = \overline{1,n}; \quad j = \overline{1,m}.
\end{aligned}
\right\}
\tag{7}
$$

We assume that the nominal area of the entire friction surface is equal to A_a. The area occupied by contacts of the corresponding type (their nominal area) can be determined by multiplying the components of the system of equations (7) by A_a.

Since the friction surfaces of the parts conjugations are pressed by the force N, the different types of contacts account for the forces: $N_{M_1-M_2}$, $N_{M_1-H_{2j}}$, $N_{M_2-H_2 j}$, $N_{H_{1i}-H_{2j}}$. The equilibrium condition of the friction surfaces in the General case has the form:

$$
N_{M_1-M_2} + \sum_{j=1}^{m} N_{M_2-H_{2j}} + \sum_{i=1}^{n} M_{M_2-H_{1i}} + \sum_{j=1}^{m}\sum_{i=1}^{n} N_{H_{1i}-H_{2j}} = N .
\tag{8}
$$

Equation (8) makes it possible to obtain the equilibrium condition for any particular case of tribocontact with PCM material. For example, if both triad coupling parts are made of matrix single-phase materials M_1 and M_2, respectively, then $N_{M_1-M_2} = N$. In the case of contact of single-phase material M_1 with multiphase $M_2 + H_{2j}$, the equilibrium condition will look like:

$$
N_{M_1-M_2} + \sum_{j=1}^{m} N_{M_1-H_{2j}} = N .
\tag{9}
$$

When estimating the forces $N_{M_1-M_2}$, $N_{M_1-H_{2j}}$, $N_{M_2-H_{2j}}$ and $N_{H_{1i}-H_{2j}}$, assume that the micro-irregularities on the friction surfaces are deformed elastically and are located on a rigid base. There is no mutual influence of conjugate surfaces of parts, as the contact of nominally flat surfaces is considered. Convergence of friction surfaces under the action of force N in this case can be determined from the equation:

$$
a = \left\{ \frac{3N_c k_{fp}\left(R_{\max_{1c}} + R_{\max_{2c}}\right)^{\gamma_c-\gamma_c}\left[\left(E_{1c}\left(1-\mu_{2c}^2\right)\right)+E_{2c}\left(1-\mu_{1c}^2\right)\right]\left(\rho_{1c}+\rho_{2c}\right)}{4q_c\rho_{1c}\rho_{2c}E_{1c}E_{2c}\alpha_c b_c\left(v_c-\gamma_c\right)\beta\left(\frac{5}{2};v_c-\gamma_c\right)A_a} \right\}^{\frac{2}{3+2\left(v_c-\gamma_c\right)}} ,
\tag{10}
$$

where N_c – the force acting on the contacts; $R_{\max_{1c}}$, $R_{\max_{2c}}$ – the maximum height of the irregularities in the contact areas of the surfaces of the first and second parts of the tribocoupling; b_c, v_c – parameters of the reference curve of the equivalent surface; ρ_{1c}, ρ_{2c}, E_{1c}, E_{2c}, μ_{1c}, μ_{2c} – respectively, the radii of curvature of the vertices of micro-inequalities, the modulus of elasticity of Jung and the Poisson's ratios of the materials of the first and second parts of the tribocouple; γ_c, k_{fp} – coefficients that depend on the shape of the protrusions; $\beta\left(\frac{5}{2};v_c-\gamma_c\right)$ – beta function; q_c – the number of protrusions per unit area of the equivalent surface; α_c – the proportion of the friction surface area in the corresponding types of contacts of expression (7) c; A_a – nominal area of friction. Note that the number of equations of the form (10) is equal to the number of types of contacts in this triad of parts.

Using the equilibrium condition (8) and expression (10), we can trace the influence of the phase composition of the PCM on the amount of pressure that develops in the contacts of each type under the total force N. For clarity, it is convenient

– single-phase material M_1 is in contact with the second, (or the same M_1) single-phase M_2;

– single-phase material M_1 is in contact with multiphase $M_2 + H_{2j}$;

– multiphase material $M_1 + H_{1i}$ is in contact with multiphase $M_2 + H_{2j}$.

During the operation of tribocouples of parts of the first kind, the external force N is balanced by the forces on the contacts M_1 - M_2, ie $N_{M_1-M_2} = N$. Dividing this equality by the nominal area of friction A_a, we obtain that in this case the pressure $P_{M_1-M_2}$ is equal to the nominal pressure P_a. To eliminate the adhesion of materials in the tribocouple of this kind, it is necessary to reduce the force N until P_a is below the critical pressure $P_{cr_{M_1-M_2}}$ determined for the contact of the matrix M_1 with the matrix M_2 or experimentally by equation $P_{cr} = C_u \sigma_{cr}$.

During the operation of the tribocoupling of the second kind, the pressure in the contacts of different types in the general case should be different. To estimate it, it is necessary to use the equilibrium condition (9) and the equation of the form (10).

Solving the system of equations of the form (10), giving values $N_{M_1-H_{2j}}$ through $N_{M_1-M_2}$ and substituting them in equation (9), we can calculate the forces at the contacts of types M_1 - M_2 and M_1 - H_{2j}. Analytically, a system consisting of expressions (9) and $(j + 1)$ expressions of type (10) cannot be solved. However, using the appropriate experimental data, it is easy to do with application packages on a PC.

If the tribocoupling of parts of the second kind and the composite consists of a matrix of M_2 and j fillers, then solving the system of equations (9) and $(j + 1)$ equations of type (4), find the forces at the contacts M_1 - M_2 and M_1 - H_{2j} by the formulas:

$$N_{M_1-M_2} = \frac{N}{1 + \dfrac{1+x}{x\left(1 - \sum\limits_{j=1}^{m} \alpha_{2j}\right)} \sum\limits_{j=1}^{m} \dfrac{\alpha_{2j} z_j}{(1+z_j)}} ; \tag{11}$$

$$N_{M_1-H_{2j}} = \frac{N\alpha_{2j}(1+x)z_j}{\left(1 - \sum\limits_{j=1}^{m} \alpha_{2j}\right)x(1+z_j) + (1+x)(1+z_j)\sum\limits_{j=1}^{m} \dfrac{\alpha_{2j} z_j}{(1+z_j)}} , \tag{12}$$

where $x = \dfrac{E_{M_2}}{E_{M_1}}$; $z_j = \dfrac{E_{H_{2j}}}{E_{M_1}}$. \hfill (13)

If PCM $M_2 + H_{2j}$ consists of two phases, $j = 1$; $\alpha_{2j} = \alpha_{1i}$, the equation of the form (10) has the form:

$$a = \left\{ \frac{3N_{M_1-M_2} k_\phi (2R_{max})^{v-\gamma} \left[E_{M_2}\left(1-\mu_{M_1}^2\right) + E_{M_2}\left(1-\mu_{M_2}^2\right)\right]}{2q\rho E_{M_1} E_{M_2}(1-\alpha_{21})b(v-\gamma)\beta\left(\frac{5}{2}; v-\gamma\right)A_a} \right\}^{\frac{2}{3+2(v-\gamma)}} , \tag{14}$$

or

$$a = \left\{ \frac{3N_{M_1-H_{21}} k_\phi (2R_{max})^{v-\gamma} \left[E_{H_{21}}\left(1-\mu_{M_1}^2\right) + E_{M_2}\left(1-\mu_{H_{21}}^2\right)\right]}{2q\rho E_{M_1} E_{H_{21}}\alpha_{21}b(v-\gamma)\beta\left(\frac{5}{2}; v-\gamma\right)A_a} \right\}^{\frac{2}{3+2(v-\gamma)}} . \tag{15}$$

For two-phase PCM, based on formulas (12) and (13), we have:

$$N_{M_1-H_{21}} = \frac{N_{M_1-M_2}\left[E_{M_2}\left(1-\mu_{M_1}^2\right) + E_{M_1}\left(1-\mu_{M_2}^2\right)\right]E_{H_{21}}\alpha_{21}}{\left[E_{H_{21}}\left(1-\mu_{M_1}^2\right) + E_{M_1}\left(1-\mu_{H_{21}}^2\right)\right]E_{M_2}(1-\alpha_{21})} . \tag{16}$$

Solving equations (16) and (9), we find:

$$N_{M_1-M_2} = \frac{N(1-\alpha_{21})E_{M_2}\left[E_{H_{21}}\left(1-\mu_{M_1}^2\right) + E_{M_1}\left(1-\mu_{H_{2j}}^2\right)\right]}{\left[E_{M_2}\left(1-\mu_{M_1}^2\right) + + E_M\left(1-\mu_{M_2}^2\right)\right]E_{H_{21}}\alpha_{21} + \left[E_{H_{21}}\left(1-\mu_{M_1}^2\right) + E_{M_1}\left(1-\mu_{H_{21}}^2\right)\right]E_{M_2}(1-\alpha_{21})} ; \tag{17}$$

$$N_{M_1-H_{21}} = \frac{N\alpha_{21}E_{M_2}\left[E_{M_2}\left(1-\mu_{M_1}^2\right)+E_{M_1}\left(1-\mu_{M_2}^2\right)\right]}{\left[E_{M_2}\left(1-\mu_{M_1}^2\right)++E_M\left(1-\mu_{M_2}^2\right)\right]E_{H_{21}}\alpha_{21}+\left[E_{H_{21}}\left(1-\mu_{M_1}^2\right)+E_{M_1}\left(1-\mu_{H_{21}}^2\right)\right]E_{M_2}\left(1-\alpha_{21}\right)}. \quad (18)$$

To calculate the nominal pressures in the considered types of contact, we accept: $\frac{N}{A_a} = P_a$; $E_{M_2} = xE_{M_1}$;

$E_{H_{11}} = Z_1 E_{M_1}$; $\mu_{H_{11}} = \mu_{M_1} = \mu_{M_2}$. Taking into account equation (7), we have the following formulas:

$$P_{M_1-M_2} = P_a \frac{x(1+Z_1)}{x(1+Z_1)(1-\alpha_{21})+(1+x)Z_1\alpha_{21}} = \xi_1 P_a; \quad (19)$$

$$P_{M_1-H_{21}} = P_a \frac{Z_1(1+x)}{x(1+Z_1)(1-\alpha_{21})+(1+x)Z_1\alpha_{21}} = \xi_2 P_a. \quad (20)$$

Analysis of expressions (19) and (20) shows that the triad coupling of parts with PCM will work effectively under the condition: $P_{M_1-M_2} < P_{cr_{M_1-M_2}}$ and $P_{M_1-H_{21}} < P_{cr_{M_1-H_{21}}}$, for the matrix M_1 and filler H_{21}.

Given the conditions for the existence of contacts of type M_1 - M_2 and M_1 - H_{21}, equation (19) should be used at $0 \leq \alpha_{21} < 1$, and equation (20) – at $0 < \alpha_{21} \leq 1$.

The use of PCM in the details of tribocouples of the second kind is appropriate in the following cases: $x = Z_1$; $Z_l > x$. In the first case, the nominal pressures in the contacts of different types do not depend on the content of the filler and are equal to the nominal pressure P_a, the limit value of which should be below $P_{cr_{M_1-M_2}}$ and $P_{cr_{M_1-H_{2I}}}$. For this filler, the force N on the tribocouple cannot be increased, because the pressure $P_{M_1-M_2}$ will exceed the allowable pressure. It is determined that the use of high-modulus filler is appropriate if you can change the coefficient of friction in the contact of the filler from one of the matrices, which will be lower than the coefficient of friction in the contact M_1 - M_2.

In the second case, when $Z_1 > x$, the filler can be introduced only in the matrix that has in contact with the filler less critical pressure P_{cr}. If such a matrix is M_2. Then, when introducing a filler with $Z_1 > x$ into this matrix, the value $\xi_1 < 1$ and the voltage at the most dangerous contacts M_1 - M_2 can be reduced several times, which will increase the nominal force N acting on the tribocouples of parts.

If in one of the details of the tribocoupling of the second kind to enter j – fillers, the feasibility of this procedure is determined by the same conditions as when introducing one filler ($x = Z_i$ i $Z_j > x$). However, so that the pressure on them does not exceed the critical value when increasing N, you need to control a larger number of types of contacts.

In order to simplify the previous expressions, we accept: $E_{M_2} = xE_{M_1}$; $E_{H_{2j}} = z_i E_{M_1}$; $E_{H_{1i}} = y_i E_{M_1}$; $\mu_{M_1} = \mu_{M_2} = \mu_{H_{2j}} = \mu_{H_{1i}}$ and solving together equations (8) and (10), we express the forces on the contacts of different types through a set of data: N; x; Z_j; Y_j; α_{1j}; α_{2j}. Then we have:

$$\left.\begin{aligned} N_{M_1-M_2} &= N\frac{x\left(1-\sum_{i=1}^{n}\alpha_{1i}\right)\left(1-\sum_{j=1}^{m}\alpha_{2j}\right)}{\xi}; \\ N_{M_2-H_{1i}} &= N\frac{(1+x)y_i\alpha_{1i}\left(1-\sum_{j=1}^{m}\alpha_{2j}\right)}{(1+y_i)\xi}; \\ N_{M_1+H_{2j}} &= N\frac{(1+x)z_j\left(1-\sum_{i=1}^{n}\alpha_{1i}\right)\alpha_{2j}}{(1-Z_j)\xi}; \\ N_{H_{1i}-H_{2j}} &= \frac{y_i z_j(1+x)\alpha_{1i}\alpha_{2j}}{(y+z_j)\xi}, \end{aligned}\right\} \quad (21)$$

$$\xi = x\left(1-\sum_{i=1}^{n}\alpha_{1i}\right)\left(1-\sum_{j=1}^{m}\alpha_{2j}\right)+(1+x)\left\{\left(1-\sum_{i=1}^{n}\alpha_{1i}\right)\sum_{j=1}^{m}\frac{\alpha_{2j}z_j}{(1+z_j)}+\left(1-\sum_{j=1}^{m}\alpha_{2j}\right)\sum_{i=1}^{n}\frac{\alpha_{1i}y_j}{(1+y_i)}+\sum_{j=1}^{m}\alpha_{2j}z_j\left[\sum_{i=1}^{n}\frac{\alpha_{1i}y_i}{(y_i+z_j)}\right]\right\}. (22)$$

Dividing equation (19) by the area of the surface occupied by contacts of different types, and accepting $\frac{N}{A_a} = P_a$, we obtain expressions for calculating the pressure at the corresponding contacts:

$$P_{M_1-M_2} = P_a \frac{x}{Q}; \quad P_{M_1-H_{2j}} = P_a \frac{(1+x)z_j}{(1+z_j)Q};$$

$$P_{M_2-H_{1i}} = P_a \frac{(1+x)y_i}{(1+y_i)Q}; \quad P_{H_{1i}-H_{2j}} = P_a \frac{(1+x)y_iz_j}{(y_i+z_j)Q}.$$

(23)

Experimental studies have shown that the tribocoupling of parts will be able to work if the pressure on the contacts of different types of this type does not exceed the critical value for its constituent materials tribocoupling of parts.

Using equations (19), (20) and (23), we can quantify the dependence of the critical load on the tribocoupling of parts on the composition and tribological properties of structural components. As a criterion for the effectiveness of the filler in PCM, we take the ratio of the nominal critical pressure $P_{a\,cr}$ in the triad of parts made of PCM to the nominal critical pressure $P_{cr_{M-M}}$ of the triad of parts made of the same matrix material.

Assuming that in equations (19) and (20) $P_{M_1-M_2} = \delta P_{cr_{M-M}}$, a $P_{cr_{M_1-H_{21}}} = \chi P_{cr_{M-M}}$, the value of the nominal critical pressure for tribocoupling of parts of the second kind can be found by equations:

$$P_{acr} = \frac{\delta P_{cr_{M-M}}}{\xi_1}; \quad P_{acr} = \frac{\chi P_{cr_{M-M}}}{\xi_2}.$$

(24)

The calculation of $P_{a\,cr}$ tribocouples of parts must be performed on both equations. The smaller of the two obtained values of $P_{a\,cr}$ and will represent the limit value of $P_{a\,cr}$ on the triad, one of the parts of which is made of PCM.

We present equation (24) in the form:

$$\frac{P_{acr}}{P_{cr_{M-M}}} = \frac{\delta}{\xi_1};$$

(25)

$$\frac{P_{acr}}{P_{cr_{M-M}}} = \frac{\chi}{\xi_2}.$$

(26)

A smaller value $\frac{P_{cr}}{P_{cr_{M-M}}}$ of the ratio can be taken as the value of the criterion of the effectiveness of the filler for a given critical load.

It was found that the introduction of a high-modulus filler in a polymer matrix with a smaller modulus of elasticity $P_{M_1-H_{2j}} = 5P_{cr_{M_1-M_2}}$ can significantly increase the value of $P_{a\,cr}$ tribocoupling of parts, but not higher $P_{cr_{M_1-H_{21}}}$. In tribocouples of parts of the third kind, when two PCM are in contact with the macroheterophase structure, the criterion of filler efficiency $\frac{P_{acr}}{P_{cr_{M-M}}}$ is selected by the minimum value of the ratio $\frac{P_{acr}}{P_{cr_{M-M}}}$ calculated for the contacts *M-M*, *M-H* and *H-H*. If a matrix and a filler with different modulus of elasticity are used in triad couplings of parts with such a combination of contact types, the contacts made of materials with a smaller modulus of elasticity will be underloaded and the criterion value $\frac{P_{acr}}{P_{cr_{M-M}}}$ will be lower. When $E_H = 10E_M$ and $P_{M_1-H_{2j}} = 5P_{cr_{M_1-M_2}}$, the criterion $\left[\frac{P_{acr}}{P_{cr_{M-M}}}\right]_{\alpha_H=0,8} \approx 4$. This value, although lower $\frac{P_{acr}}{P_{cr_{M-M}}}$, with the same modulus of elasticity of the matrix and filler, but higher than in layered PCM with other combinations of contact types.

Conclusions

1. The field of stresses in tribocouples of parts made of polymer-composite materials is considered, taking into account the properties of friction surfaces. It is revealed that the critical pressure in the tribocouples of parts is determined primarily by the energy of motion of dislocations in the surface layers of their materials.

2. It was found that to ensure the process of minimal wear in the triad of parts of polymer-composite

materials should create conditions when in the process of their operation are realized elastic contacts. For the case of flat conjugate surfaces of details the basic requirements are formulated, expressions for a share of the areas occupied by this or that contact of the details made of polymeric composite materials are received.

3. Efforts on different types of contacts of tribocouples of details taking into account the modulus of elasticity and Poisson's constant of matrix materials and fillers, share of the areas occupied by this or that type of contact are considered, and also nominal pressures in them are defined.

4. It is shown that the efficiency of tribocouples made of polymer-composite materials should be evaluated by the critical pressures at the contact surfaces of parts.

5. It is determined that for the manufacture of both antifriction and friction polymer composite materials it is more effective to use fillers whose modulus of elasticity is greater than the matrix. In order to increase the strength of the parts, it is advisable to use tribocoupling of parts of the third kind, and in terms of saving filler – the second kind.

References

1. Aulin V.V., Derkach O.D., Makarenko D.O., Hrynkiv A.V. (2018) Vplyv rezhymiv ekspluatatsii na znoshuvannia detalei, vyhotovlenykh z polimerno-kompozytnoho materialu [Problems of tribology. №4] – S.65-69.

2. Aulin V.V., Derkach O.D., Hrynkiv A.V., Makarenko D.O. (2021) Vyznachennia robochoi temperatury kompozytnykh elementiv rukhomykh ziednan v zoni tertia [Naukovyi visnyk Tavriiskoho derzhavnoho ahrotekhnolohichnoho universytetu: elektronne naukove fakhove vydannia - Vyp. 11, tom 1, stattia21].

3. Aulin V.V., Hrynkiv A.V., Smal V.V., Lysenko S.V. ta in. (2021). Basic approaches and requirements for the design of tribological polymer composite materials with high-modulus fillers [Problems of Tribology, V. 26, No 4/102-2021] P.51-60.

4. Aulin V., Derkach O., Makarenko D., Hrynkiv A. ta in. (2019). Analysis of tribological efficiency of movable junctions "polymeric-composite materials – steel" [Eastern-European Journal of Enterprise Technologies. Vol. 4 (12-100)] - P. 6-15.

5. Aulin V.V., Derkach O.D., Kabat O.S., Makarenko D.O., Hrynkiv A.V., Krutous D.I. (2020). Application of polymer composites in the design of agricultural machines for tillage [Problems of Tribology, V. 25, No 2/96-2020] - P.49-58

6. Aulin V., Kobets A., Derkach O., Makarenko D., Hrynkiv A. ta in. (2020). Design of mated parts using polymeric materials with enhanced tribotechnical characteristics [Eastern-European Journal of Enterprise Technologies. Vol.5 (12-107)] - P. 49-57.

7. Aulin V.V. (2006). Pole napruzhen v kompozytsiinomu materiali ta kompozytsiinomu pokrytti v umovakh tertia kovzannia [Zb. nauk. prats LNAU. Seriia: Tekhnichni nauky. №.65(88)] S.13-20.

8. Aulin V.V. (2008). Vyznachennia obiemnoho vmistu napovniuvacha v antyfryktsiinomu kompozytsiinomu pokrytti [Mashynoznavstvo. №7(85)] S. 49-53.

9. Aulin V.V. (2006). Vplyv kharakterystyk komponentiv kontaktuiuchykh kompozytsiinykh materialiv i pokryttiv na parametry ta vlastyvosti zony tertia [Problems of tribology. №4 (42)] S. 110-112.

10. Bondarenko V.P. (1987). Tribotehnicheskie kompozityi s vyisokomodulnyimi napolnitelyami. [K.: Nauk. dumka] 232 s.

11. Aulin V.V. (2015). Trybofizychni osnovy pidvyshchennia znosostiikosti detalei ta robochykh orhaniv silskohospodarskoi tekhniky [dys. ... d-ra tekhn. nauk: 05.02.04] 360 s.

12. Aulin V.V., Brutskyi O.P. (2015). Pro dotsilnist vykorystannia polimernykh kompozytsii z nanonapovniuvachiv pry vidnovliuvanni ta vyhotovlenni resursovyznachalnykh detalei SHT. [Problemy konstruiuvannia, vyrobnytstva ta ekspluatatsii s.-h. tekhniky: materialy. Kirovohrad: KNTU] S.138-140.

13. Aulin V.V., Brutskyi O.P., Lysenko S.V. (2015). Doslidzhennia zakonomirnostei protsesiv tertia ta znoshuvannia v metalopolimernykh trybosystemakh. [Trybolohiia, enerho- ta resursozberezhennia: zb. tez. Mykolaiv: Vyd-vo ChDU im. Petra Mohyly] S.3-4.

14. Aulin V.V., Derkach O.D., Makarenko D.O., Hrynkiv A.V. (2018). Vplyv rezhymiv ekspluatatsii na znoshuvannia detalei, vyhotovlenykh z polimerno-kompozytnoho materialu [Problemy trybolohii. №4] S.65-69.

15. Sorokov S. (2003). Klasternyi pidkhid do rozrakhunku fizychnykh kharakterystyk kompozytnykh materialiv [Lviv: In-t fizyky kondens. system NANU] 23 s.

16. Aulin V.V., Kuzyk O.V. (2014). Dynamichne materialoznavstvo zon tertia detalei silskohospodarskoi tekhniky [Visnyk ZhNAEU: nauk.-teor. zbir. № 2(45), t.4, ch.II] S. 102-110.

17. Aulin V., Derkach O., Makarenko D., Hrynkiv A. et al. (2020). Krutous D., Muranov E. Development of a system for diagnosing bearing assemblies with polymer parts during operation [Technology audit and production reserves. № 5/1(55)] pp.18-20.

Аулін В.В., Гриньків А.В., Лисенко С.В., Лівіцький О.М. Обгрунтування умов ефективної працездатності трибоспряжень деталей, виготовлених з полімерних композитних матеріалів з високомодульними наповнювачами

Дана робота присвячена дослідженню умов ефективної працездатності трибоспряжень деталей, виготовлених з полімерних композитних матеріалів. Напружений стан матеріалу пов'язано з характеристиками скупчення дислокацій, енергією активації їх руху. Визначено усереднене напруження, напруження тертя. На основі цього отримано вирази для оцінки критичних напружень та навантаження на трибоспряження деталей. Визначено розподіл зусилля на трибоспряження деталей з врахуванням характеристик якості поверхонь тертя, модулів пружності та сталої Пуассона компонентів полімерного композитного матеріалу. Цю задачу розглянуто для трибоспряжень деталей різного роду.

Отримано вирази для розрахунку номінальних тисків у різних типів контакту матеріалу деталей трибоспряження, а також наведені рівняння, за якими можливо оцінити в них значення номінального критичного тиску.

З'ясовано умови ефективного функціонування трибоспряження деталей з полімерокомпозитних матеріалів. Визначено, що значне підвищення номінального критичного тиску на трибоспряження можливе використанням високомодульних наповнювачів, модуль пружності матеріалу яких більший за модуль пружності полімерної матриці.

Ключові слова: полімерний композитний матеріал, макрогетерофазний матеріал, високомодульний наповнювач, трибоспряження деталей, матриця, наповнювач, поле напружень, пружний контакт, критичний тиск, номінальний тиск